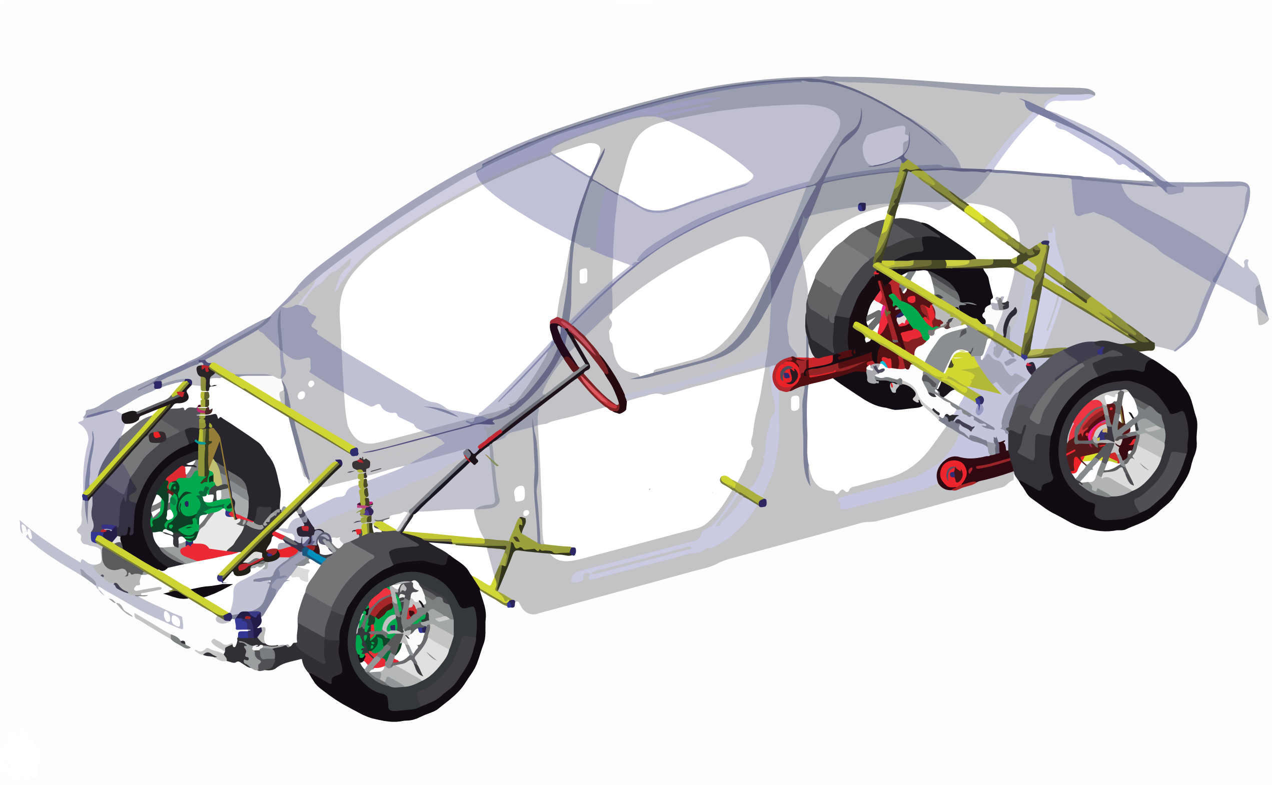

Influence of Body Stiffness on Vehicle Dynamics Characteristics in Passenger Cars

Master's thesis in Automotive Engineering

OSKAR DANIELSSON
ALEJANDRO GONZÁLEZ COCAÑA

Department of Applied Mechanics
Division of Vehicle Engineering and Autonomous Systems
Vehicle Dynamics group
CHALMERS UNIVERSITY OF TECHNOLOGY
Göteborg, Sweden 2015

Master's thesis 2015:68

MASTER'S THESIS IN AUTOMOTIVE ENGINEERING

Influence of Body Stiffness on Vehicle Dynamics Characteristics in Passenger Cars

OSKAR DANIELSSON
ALEJANDRO GONZÁLEZ COCAÑA

Department of Applied Mechanics

Division of Vehicle Engineering and Autonomous Systems
Vehicle Dynamics group

CHALMERS UNIVERSITY OF TECHNOLOGY

Göteborg, Sweden 2015

Influence of Body Stiffness on Vehicle Dynamics Characteristics in Passenger Cars
OSKAR DANIELSSON
ALEJANDRO GONZÁLEZ COCAÑA

Master's thesis 2015:68
ISSN 1652-8557
Department of Applied Mechanics
Division of Vehicle Engineering and Autonomous Systems
Vehicle Dynamics group
Chalmers University of Technology
SE-412 96 Göteborg
Sweden
Telephone: +46 (0)31-772 1000

Cover:
Volvo S60 model reinforced with bars for the multibody dynamics simulation tool MSC Adams

Chalmers Reproservice
Göteborg, Sweden 2015

Influence of Body Stiffness on Vehicle Dynamics Characteristics in Passenger Cars
Master's thesis in Automotive Engineering
OSKAR DANIELSSON
ALEJANDRO GONZÁLEZ COCAÑA
Department of Applied Mechanics
Division of Vehicle Engineering and Autonomous Systems
Vehicle Dynamics group
Chalmers University of Technology

Abstract

Automotive industry is a highly competitive market where details play a key role. Detecting, understanding and improving these details are needed steps in order to create sustainable cars capable of giving people a premium driving experience. Body stiffness is one of this important specifications of a passenger car which affects not only weight thus fuel consumption but also handling, steering and ride characteristics of the vehicle. By using a method developed to perform an extensive number of simulations and suitable for the analysis of the interesting points in the design space, it has been proved that not only torsional but lateral and local stiffness can play a role in giving the customer a premium feeling by affecting key metrics in the vehicle dynamics behavior of a passenger car. Furthermore it has been proved that the effect of the body in the vehicle dynamics of a car can be measured and targeted by using test maneuvers and metrics for handling and ride.

Keywords: vehicle dynamics, body stiffness, handling, steering, ride, multibody dynamics

Preface

Fast lead time play an important role during vehicle development. In order to increase vehicle perform and at the same time reduce lead time, testing is moving towards CAE simulations. Due to this movement an increased model accuracy is needed to be able to replace physical vehicle testing which usually takes place late in the design process with virtual testing. Previous work has shown that subjective physical measurements does not match the CAE results, therefore a deeper analysis of the influence of the body stiffness properties in the vehicle dynamics characteristic is needed.

Acknowledgements

We would like to thank Volvo Cars for the opportunity to perform a Masters Thesis connected to a real world application and for the possibility to use collected data to verify our results. We would also like to acknowledge the importance of all the support we have gotten throughout the project both at Volvo Vehicle Dynamics CAE department and at Chalmers VEAS Division. A special thanks to: Bengt Jacobson, Mathias Lidberg, Matthijs Klomp, Mohsen Bayani Khaknejad & Johan Hultqvist for the continuous supervision, feedback and useful discussions, Stavros Angelis for the support with IPG CarMaker, Kenneth Ekström for his precise physical subjective vehicle analysis, Richard Dekker for his help with K&C analysis, Axel Jonson & Daniel Hedendahl for their help with Sympathy For Data and thanks to Åsa Eriksson and the Vehicle Dynamics CAE department at VCC for their help, support and nice work environment.

Nomenclature

CM	CarMaker
CAE	Computer Aided Engineering
VCC	Volvo Car Corporation
FEA	Finite element analysis
BIW	Body in white
CoG	Center of gravity
MNF	Modal neutral file
SPMM	Suspension Parameter Measurement Machine
K&C	Kinematics and compliance
HPG	Hällered Proving Ground
TCL	Tool Command Language
TCP	Transmission Control Protocol
CSV	Comma-separated values
DOF	Degrees Of Freedom
LLT	Lateral load transfer
LLTD	Lateral load transfer distribution
FLLTD	Front lateral load transfer distribution
VFD	Vertical force distribution
FVFD	Front vertical force distribution
RBE2	Rigid Body Element
US	Understeer

Contents

Abstract i

Preface iii

Acknowledgements iii

Nomenclature v

Contents vii

1 Introduction 1
1.1 Statement of the problem 1
1.2 Research questions 1
1.3 Literature review 1
1.4 Scope and prerequisites 2
1.5 Significance of the study 2
1.6 Report layout 2

2 Theory 3
2.1 Body stiffness 3
2.1.1 Torsional stiffness 3
2.1.2 Bending stiffness 4
2.1.3 Lateral stiffness 5
2.1.4 Local stiffness 6
2.2 Vehicle dynamics characteristic: handling, steering and ride 6
2.2.1 Handling 7
2.2.2 Steering 7
2.2.3 Ride 7
2.3 Lateral load transfer model 7
2.4 Steady state bicycle model 10
2.4.1 Lateral compliance 11
2.4.2 Torsional stiffness 11
2.4.2.1 Axle cornering stiffness 11
2.4.2.2 Roll steer 12
2.4.3 Understeer gradient 12
2.5 Design of experiment 14
2.6 Statistical analysis 15
2.6.1 Graphical visualization and correlation of large data sets 15
2.6.1.1 Box-Whiskers 15
2.6.1.2 Student chart 15
2.7 Flexible Bodies 15
2.8 Tire models 16
2.8.1 IPGTire (RealTime Tire) 16
2.8.2 Pacejka 5.2 (Magic Formula) 16
2.8.3 MF-Tire/MF-Swift 6.1 (RealTime Tire) 17
2.8.4 TameTire 17

3 Method 18
3.1 Overview 18
3.2 Component to subsystem relation 19
3.2.1 MSC Adams Model 19
3.2.1.1 Suspension 19
3.2.1.2 Body 20
3.2.2 Parameterization of MSC Adams model 20
3.2.2.1 Suspension 20

3.2.2.2 Body stiffness . . . 20
3.2.3 Validation of the model . . . 21
3.2.4 Simulations . . . 22
3.2.5 Design of experiment Adams . . . 23
3.2.5.1 Post processing in modeFrontier . . . 23
3.2.6 FEM Model . . . 24
3.2.7 Parameterization of FEM model . . . 24
3.2.8 Validation of FEM model . . . 25
3.2.9 Load Cases FEM . . . 27
3.2.10 Design of experiment FEM . . . 27
3.2.10.1 Post processing in modeFrontier . . . 29
3.3 Subsystem to vehicle relation . . . 29
3.3.1 CarMaker Model . . . 30
3.3.1.1 Global body stiffness model . . . 30
3.3.1.2 Local stiffness model . . . 30
3.3.2 Parameterization of CarMaker model . . . 31
3.3.2.1 Suspension parametrization . . . 31
3.3.2.2 Suspension components . . . 32
3.3.2.3 Body stiffness parametrization . . . 32
3.3.3 Validation of the model . . . 34
3.3.4 Simulations and load cases . . . 35
3.3.4.1 Brake in turn . . . 35
3.3.4.2 Constant radius . . . 35
3.3.4.3 Constant radius with bump . . . 35
3.3.4.4 Constant radius with angled bump . . . 36
3.3.4.5 Frequency response . . . 36
3.3.4.6 High g swept steer . . . 36
3.3.4.7 Low g swept steer . . . 36
3.3.4.8 On center . . . 36
3.3.4.9 Primary ride . . . 36
3.3.4.10 Sine with dwell . . . 36
3.3.4.11 Step steer throttle release in turn . . . 36
3.3.4.12 Throttle release in turn . . . 37
3.3.4.13 Yaw stability . . . 37
3.3.4.14 Yaw stability - rough road . . . 37
3.3.5 Design of experiment . . . 37
3.3.5.1 Sympathy for Data post processing node in modeFrontier flow . . . 38
3.3.5.2 Post processing in modeFrontier . . . 39
3.4 Physical Testing . . . 39
3.4.1 K&C measurements . . . 39
3.4.2 Torsional Stiffness measurements . . . 40
3.4.3 Objective Testing . . . 40
3.4.4 Subjective Testing . . . 40

4 Results **42**
4.1 Component to subsystem . . . 42
4.2 Subsystem to vehicle . . . 43
4.2.1 Rigid body . . . 44
4.2.2 Reinforced body . . . 45
4.3 Correlation with Physical Testing . . . 47
4.3.1 K&C . . . 47
4.3.2 Torsional stiffness . . . 51
4.3.3 Full vehicle maneuvers . . . 52

5 Analysis and Discussion **53**
5.1 Validation of models . . . 53

5.1.1 Adams model: component to subsystem . . . 53
5.1.2 FEM model: component to subsystem . . . 54
5.1.3 CarMaker model: subsystem to vehicle . . . 54
5.2 Component to Subsystem . . . 54
5.3 Subsystem to Vehicle . . . 55
5.3.1 Rigid body compared to the baseline . . . 55
5.3.1.1 New maneuvers . . . 56
5.3.2 Reinforced body compared to the baseline . . . 57
5.3.2.1 New maneuvers . . . 57
5.3.3 Relation between how a reinforced or rigid body influence vehicle behaviour . . . 57
5.3.4 Largest factors influencing handling, steering and ride characteristics . . . 58
5.4 Component to Vehicle . . . 58

6 Conclusions **60**

7 Future work **61**

References **62**

1 Introduction

Automotive industry is a highly competitive market where details play a key role. Detecting, understanding and improving these details are needed steps in order to create innovative car technology capable of giving the customer a premium driving experience. Furthermore the requirements of lighter cars may lead to more flexible bodies compromising the dynamic behaviour of the vehicle.

In order to get a better understanding of the problem, this thesis will analyze how the vehicle dynamics characteristic are affected by the local and global car body stiffness properties of a car. The influence of these parameters in the vehicle handling, steering and ride attributes will be scrutinized through CAE analysis tools and compared to results from physical tests.

1.1 Statement of the problem

Physical subjective measurements performed at Volvo Cars have shown that changes in body stiffness properties do affect vehicle dynamics characteristics in passenger cars. But objective metrics calculated based on data from full vehicle simulations does not show the effect on vehicle dynamics behaviour which is seen from the subjective measurements. The correlation between subjective experiments and CAE analyses does not match. Therefore a deeper analysis of the influence of the body stiffness properties in the vehicle dynamics characteristic is needed.

1.2 Research questions

The purpose of this study is to investigate the influence of body stiffness on vehicle dynamic characteristics in passenger cars for different maneuvers using CAE tools in order to investigate the following research questions:

- How are vehicle dynamic characteristics affected by body stiffness?
- Which are the significant maneuvers where body stiffness plays a large role in vehicle dynamics characteristics?
- Which are the areas of the body where a variation in body stiffness improves handling, steering and ride performance?
- How can CAE simulation tools be used to model and evaluate design changes in body stiffness that influence vehicle dynamics?

1.3 Literature review

Previous studies have been carried out to investigate the effects of various body stiffeners on vehicle dynamics characteristics. They have found gains in both objective and subjective physical tests [3] & [14]. However the effect of increased torsional stiffness on overall vehicle performance is not completely known [4]. CAE assessments of body stiffness have been performed but they are not showing any big differences in the metrics used to objectively assess the handling, steering and ride characteristics of a vehicle [4]. Nevertheless during subjective vehicle assessments it is found that the stiffer car performs better.

Studies performed by Volvo Cars Corporation have shown an influence from body stiffness on subjective measurements taken during physical tests. However the CAE analysis performed are not able to capture the influence from body stiffness on vehicle dynamics characteristics seen in the subjective assessments where the car was described as more solid and premium.

According to Milliken [15], excessive chassis flexibility induces problems in the field of lateral load transfer, suspension kinematics and it results in unwanted vibrations. For a race vehicle, Milliken [15] states that the chassis torsional stiffness can be approximately designed to be 3-5 times the total suspension roll stiffness. This cannot be directly transposed to a passenger car but it gives an approximation of the influence of the body stiffness in the vehicle dynamics characteristics. Typical values for torsional stiffness in a passenger car are in the range of 17000 to 40000 Nm/deg, with a roll stiffness of 1000-2500 Nm/deg per axle. Meaning a chassis/roll stiffness ratio of 6,8-40 [7].

Regarding the vehicle dynamics properties, the overall response of the vehicle is improved with a stiffer chassis due to the better synchronization between front and rear according to subjective tests and objective measurements [14]. Up to 14% of improvement in the phase lags of the vehicle for steering input frequencies (0,5 Hz) through increasing the global torsional stiffness of the car is found. Regarding local stiffness, it is found that increasing the local stiffness in the front lower arm also shows an improvement in the overall vehicle response [3].

1.4 Scope and prerequisites

The scope of this project will be limited to influence of body stiffness in the vehicle dynamics characteristics (handling, steering and ride). Body stiffness is also an important factor in crash worthiness and NVH but these areas are out of the scope of this report and they are not further considered in this analysis. Suspension component stiffness as well as connections of the suspension parts to the body stays out of the investigations made in this project.

Physical tests will be analyzed in order to correlate the CAE results with physical subjective and objective measurements; however the design of the physical test will be carried out by VCC. Furthermore the scope of this project will not include subjective assessments using driving simulator.

1.5 Significance of the study

The results of this study will have an impact on the prerequisites of body stiffness regarding vehicle dynamics characteristics demanded by the company Volvo Cars. Moreover the developed optimization method can be used for VCC after the project is completed for other Vehicle Dynamics CAE analysis.

1.6 Report layout

This report is divided into six main chapters: Theory, Method, Results, Analysis, Conclusions and Future work. The Theory section covers the main aspects needed to fully understand the study. Method, results and analysis are following the same structure. They are divided into the following relation levels based on the method used for the CAE analysis: component-subsytem, subsystem-vehicle and component-vehicle. These connections will be further explained in the Section 3.1 together with Figure 3.13, which summarizes the process of the project. These chapters also include a last level of analysis, Physical Testing, which is used for validating the different models. Finally Conclusions and Future Work chapters summarize the outcomes of the project.

2 Theory

This chapter presents the basic theory behind the project in terms of body stiffness, vehicle dynamics characteristics, modal reduction and tire models. The section also includes the explanation of a simple vehicle dynamics model made to understand the expected outcome when using more complex models in the next steps of the study. Design of experiment and statistical analysis basics are also covered in this chapter.

2.1 Body stiffness

This section describes the main load cases and stiffness measurements within the body of a passenger vehicle. Regarding global stiffness load cases, torsional stiffness is the main parameter described but also bending stiffness and lateral stiffness are explained in the following paragraphs. Local stiffness load case is also covered in this chapter.

2.1.1 Torsional stiffness

The torsional stiffness of the car body is one of the key parameters of the vehicle design. It describes the resistance to twist that the body has when a torsion load is applied to the BIW. Figure 2.1 shows a schematic drawing of this load case. Torsional stiffness is calculated then following Eq. 2.1 for the torsion angle, Eq. 2.2 tor the torsion moment and Eq. 2.3 for the torsional stiffness value.

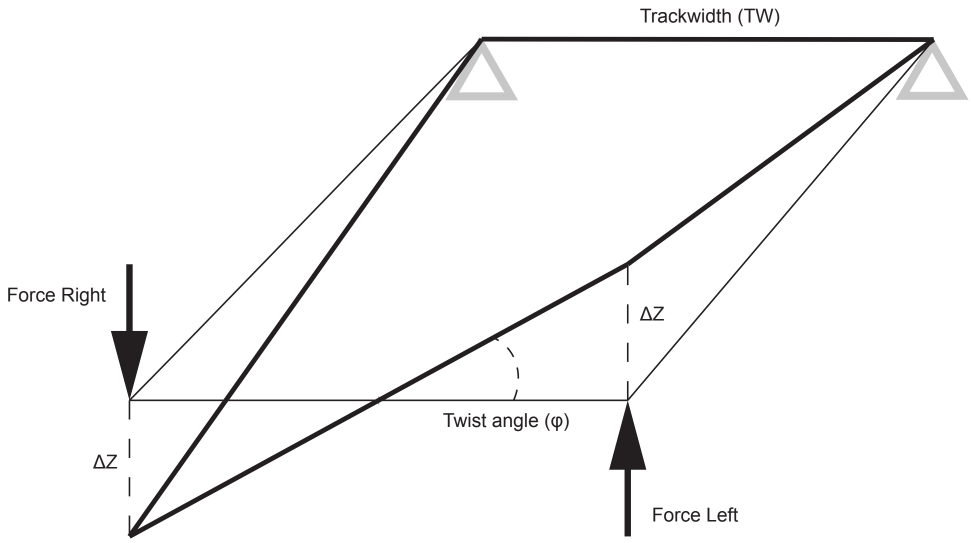

Figure 2.1: *Torsional stiffness load case scheme*

$$\phi_{front} = \arctan\left(\frac{\Delta z}{0,5 \cdot TW_{front}}\right) \tag{2.1}$$

$$T_{front} = \frac{1}{2} \cdot TW_{front} \cdot (F_{left} + F_{right}) \tag{2.2}$$

$$K_{body}[Nm/deg] = \frac{T_{front}}{\phi} \tag{2.3}$$

It is known that body torsional stiffness plays a significant role when designing a car, specially a race car body. Suspension kinematics and compliance, and handling, steering and ride behaviour of the vehicle are thus affected by a variation in torsional stiffness. This parameter will determine some of the tuneability capacity of the chassis. For instance, excessive chassis flexibility will cause problems in tuning lateral load transfer distribution with roll stiffness distribution. One can see this effect as modeling the vehicle with three torsional springs in series: one representing the front suspension, one representing the body and the last one representing the rear suspension. If the body spring stiffness is low, the spring that represents body stiffness will alter the effect that roll stiffness distribution has on lateral load transfer distribution (see Equation 2.4 to Equation 2.7, describing the equivalent relation between two spring in series). Meaning that it will be hard to control the resistance to roll moment between front and rear axle [15], making the axles independent of each other. This yields to the inability of modifying the car behaviour while modifying the suspension characteristics i.e. modifying the roll stiffness distribution in the model explained in section 2.3.

$$\frac{1}{k_{eq}} = \frac{1}{k_1} + \frac{1}{k_2} \tag{2.4}$$

$$k_1 << k_2 \tag{2.5}$$

$$\frac{1}{k_1} >> \frac{1}{k_2} \tag{2.6}$$

$$\frac{1}{k_{eq}} \approx \frac{1}{k_1} \tag{2.7}$$

A driving situation where torsional stiffness is one of the main body parameters affecting body twisting is when hitting a bump at an angle. In the same way the changes in the torsional stiffness will be shown if the bump is only hit by one of the wheels. These load cases causes the body to twist around its x-axis altering the vertical tire forces affecting vehicle behaviour.

The values for torsional stiffness of vehicle bodies are highly affected by the test method; how the body is clamped and where the displacements are measured (Figure 3.10 displays the exact method used in this study). The torsional stiffness method used for calculating the static torsional stiffness is further described by Stijn Wolterink in [21]. FEM simulations are done following the same procedure in order to estimate the value of torsional stiffness for the body-in-white, vehicle body's sheet metal parts without any other sub-assemblies, doors, fenders, etc. An estimation range can be set between $17kNm/deg$ to $40kNm/deg$ for most common car manufacturers and vehicle segments. For the multibody dynamic simulations the modal information of the BIW should be captured. More information about the modal flexibility method will be explained in Setion 2.7. Regarding this load case, as stated in [11] the contribution of the dynamic modes to the static stiffness is reduced to around the 40 first modes. For the dynamic simulations this number is considered precise enough for the low frequency simulations conducted in this study. An advanced modal analysis is required for higher frequency studies such as related with noise, vibrations and harshness. This dynamic testing method is as well an alternative for static analysis in order to avoid, for instance, the influence of clamping conditions. Nevertheless for the purpose of this study a static analysis has been done comparing the different vehicle bodies under the same conditions.

2.1.2 Bending stiffness

Bending stiffness refers to a difference in pitch angle between front and rear part of the body. The vehicle body bends when it is accelerated and load transfer occurs. This situation appears during accelerations and decelerations of the car. These effects are the so-called dive and squat behaviour. The pitch angle recovering after hitting a speed bump can be seen as another situation where bending stiffness plays a role. While designing vehicle bodies it is believed that a high value of torsional stiffness will yield as well to an adequate bending stiffness value of the body [15]. However it is interesting to analyze if an improvement in bending stiffness will generate changes in vehicle dynamics behaviour of a passenger car.

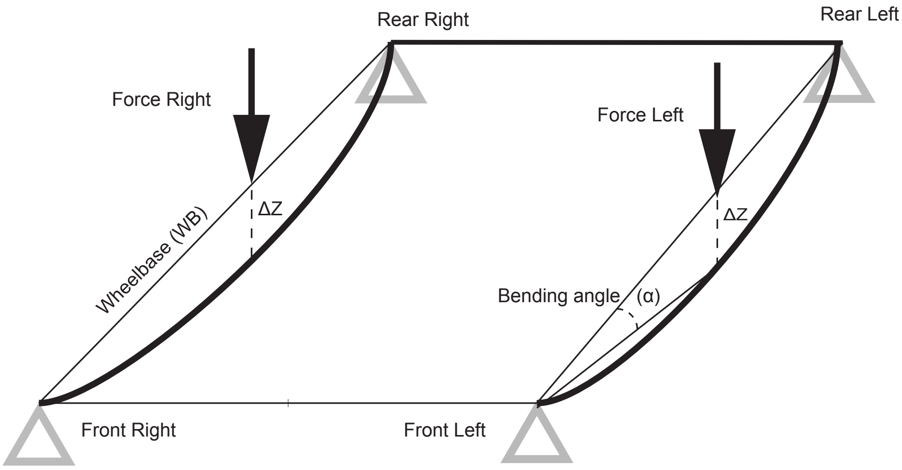

Figure 2.2: *Bending stiffness load case scheme*

One common method of measuring static bending stiffness is the three point bending test. A schematic view of this load case can be seen in Figure 2.2. The formulas used for calculating the bending stiffness are Eq. 2.8 for the bending angle, Eq. 2.9 for the bending moment and Eq. 2.10 for bending stiffness.

$$\alpha_{front} = \arctan\left(\frac{\Delta z}{0,5 \cdot WB_L}\right) \tag{2.8}$$

$$T_L = \frac{1}{2} \cdot WB_L \cdot R_{FL} \tag{2.9}$$

$$K_{body}[Nm/deg] = \frac{T_L}{\alpha} \tag{2.10}$$

As for torsional stiffness, the values of this parameter are highly dependent on the test method used (Figure 3.11 shows in more detail the clamping points and force application points used in this study). In CAE bending stiffness can be measured with FEM models mimicking the static test. For dynamics simulations a modal flexibility analysis is needed in order to capture the dynamics behavior of the structure in the same case as for torsional stiffness. However the number of flexible modes needed for a reasonable accuracy is a key parameter of a dynamic study. According to J. Helsen [11] about 40 flexible modes gives an error less than 10% in the static stiffness measurements. Furthermore the frequency of the vehicle dynamics simulations performed will determine the number of necessary modes. In general this frequency will be low, reducing the demands of a detail modal model for the BIW. Whilst it will still capture the bending dynamic information.

2.1.3 Lateral stiffness

Lateral stiffness refers to the load case where a force is applied in lateral direction at front and rear axle. A scheme of this load case is showed in Figure 2.3. This can be seen as the centrifugal forces acting through the wheels whilst cornering. Yaw behaviour of the vehicle is affected since the lateral stiffness distribution between front and rear axle will have an impact on the yaw performance of the car.

Lateral stiffness of the BIW is not one of the most common parameters measured for body design but it is believed that its importance for vehicle dynamics should not be disregarded. In this study, the lateral stiffness is captured through K&C analyses, where loads are applied in front and rear wheels while the vehicle is clamped at the sills as shown in Figure 3.15. The case described in Figure 2.3 reflects the global lateral stiffness. However

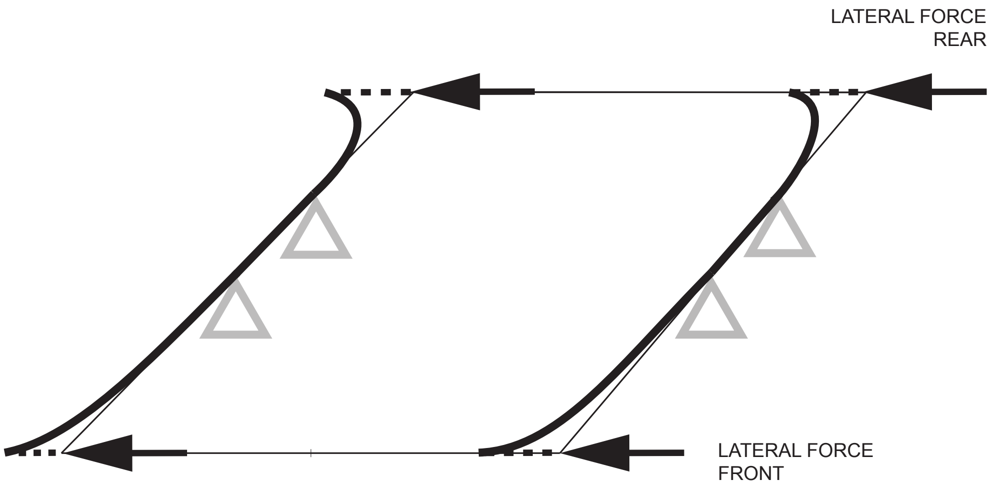

Figure 2.3: *Lateral stiffness load case*

this load case is indeed affected by the local lateral stiffness values of both front and rear axle. Thus in this study global lateral stiffness has been taken into account by modelling local lateral stiffness independently for front and axles. An estimation of this parameter for passenger cars using the explained method is $0,7kN/mm$ for both front and rear axles in lateral stiffness.

2.1.4 Local stiffness

Local stiffness is referring to the stiffness of the suspension attachment points on the body. In order to take local stiffness values into account for Camber and Toe, Kinematics and Compliance tests are used. In these tests a force or a torque is applied at the center of the wheel and the wheel center displacements and rotations are measured in six DOF. So, there are 6 forces and moments with 6 displacements and rotation responses each, leading to 36 stiffness coefficients describing the local stiffness. These forces and moments are reduced then to 5: force in x and y and moment in x, y, z. Force in z is not accounted for, due to that the influence of body local stiffness is believed to be small for this load case. This leads to a total number of 30 stiffness coefficients describing local body stiffness. The most important are camber stiffness and toe stiffness, together with the previously described local lateral stiffness. Camber stiffness is estimated with a torque applied around the longitudinal axis of the vehicle (x-axis). An estimation of this parameter for passenger cars is $0,2deg/kN$. Toe stiffness is estimated similarly as Camber stiffness but with a torque applied around the vertical axis of the car (z-axis).

2.2 Vehicle dynamics characteristic: handling, steering and ride

Characterizing the vehicle dynamics behaviour is not a trivial task. It involves many parameters and aspects of the car, each of them having high level of complexity. Furthermore it is a key indicator not only for vehicle dynamics characteristics but also for active safety. A repeatable way of evaluating vehicle dynamics is needed in order to be able to identify the influence of small design changes. Hence standard maneuvers and metrics are used. In this study the vehicle behaviour is divided in three different attribute groups, where performance is measured by executing different maneuvers. These attribute groups are handling, steering and ride.

For each of these three groups a set of maneuvers are performed in order to evaluate different attributes. From these maneuvers a set of scalar continuous metrics are calculated for each attribute with the help of a post processing tool. The calculated metrics are then used to assess vehicle performance in handling, steering and ride.

2.2.1 Handling

The complete handling behaviour of a car is characterized using several maneuvers which try to evaluate the handling characteristics of the vehicle. These maneuvers are generally included in the most common International Standards (ISO) or National Standards (Svensk Standard). Braking in turn (ISO 7975:2006), Transient response test with one period of sinusoidal input (ISO/TR 8725), Straight-ahead braking (ISO 14512:1999) or Steady-state circular driving behaviour (ISO 4138:2012) are some of the tests used to measure the handling performance of the vehicle. Nevertheless these tests should be analyzed together in order to draw a picture of the actual vehicle performance. Cornering stability together with transitional stability and straight ahead stability are the characteristics evaluated within these maneuvers.

These tests are performed in the same way in the test track, where the car is controlled by steering robots, and in the CAE multi-body dynamics simulations. Common parameters measured in these tests are lateral acceleration, longitudinal velocity, yaw velocity or vehicle roll angle. Repeatability of these tests is highly influenced by track condition, tyres or suspension setups. One should be aware of these factors while comparing CAE results and test data. Even thought the car is controlled by a robot and the measurement equipment is the same for all test runs, discrepancy in the simulations and tests can appear due to the previous mentioned sources of error.

2.2.2 Steering

Steering characteristics of passenger vehicles include the study of cornering controllability, straight ahead controllability and first impression behaviour. The maneuvers used for measuring these parameters include low to high lateral acceleration tests, for example Random input (ISO 7401:2011) or Continuous sinusoidal input (ISO 7401:2011).

In the same way as for the handling maneuvers, these tests are performed in the test track using the appropriate transducers and using the standard equipment for controlling the steering wheel and pedals. The same source of errors mentioned for Handling can appear for Steering metrics.

2.2.3 Ride

Ride maneuvers can be divided between Primary Ride and Secondary Ride. They measure the control, comfort and balance of the vehicle in different amplitude roads and frequencies. Events containing frequencies above $50Hz$ are considered as noise, vibration and harshness therefore out of the scope of vehicle dynamics. Primary ride includes frequencies up to $10Hz$ and secondary ride from $4Hz$ up to $50Hz$. Primary and secondary ride frequencies have an overlapping area between $4Hz$ and $10Hz$. The tire model has a high impact in this measurement, specially for higher frequencies. Because of that this study is only considering Primary Ride characteristics for the analysis of body stiffness on Ride characteristics. Pitch balance, roll motion or roll balance are some of the metrics calculated from these maneuvers. The roads used for ride measurements are classified according to the amplitude (small and large), roughness (smooth and rough) and impacts level (from 10mm to 30mm).

2.3 Lateral load transfer model

In order to estimate the effect from torsional stiffness on a passenger car, a simple steady state model studying the effect on lateral load transfer is used. Lateral load transfer is one of the key factors for tuning vehicle over/understeer behaviour and in order to control lateral load transfer distribution between front and rear axle a sufficiently stiff body is needed.

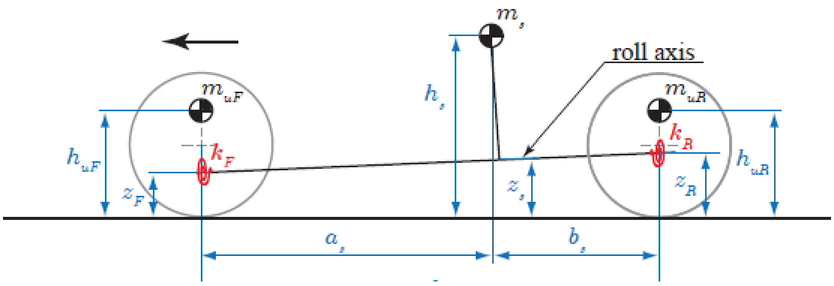

Figure 2.4: *Three mass lateral load transfer distribution model for a rigid body [16]*

A vehicle asserted to a lateral acceleration a_y will have a total load transfer dependent on mass m, centre of gravity height h_G and front/rear track width t, see Equation 2.11. Hence the total lateral load transfer is only affected by vehicle design parameters and it can therefore not be altered or tuned with for example anti roll bar stiffness. However lateral load transfer distribution between front and rear axle can be varied by a change in roll stiffness on either front or rear axle. This change will shift load transfer from either front to rear axle or rear to front axle.

$$\text{Total lateral load transfer: } \Delta F_z = \frac{m \cdot a_y \cdot h_G}{t} \tag{2.11}$$

Milliken [15] presents a set of equations used to evaluate each individual vertical wheel load and therefore also lateral load transfer distribution. Milliken [15] introduces the following assumptions:

- A lateral load applied anywhere along the roll axis does not produce roll.
- Front and rear roll rates are measured independently.
- Tire deflection rates are included in roll rates.
- Solid axle roll is not included.
- Center of gravity and roll centers are positioned on the vehicle center line.

In Milliken's [15] two spring lateral load transfer distribution model seen in Figure 2.4, there are two main factors creating roll moment around the roll center axis and therefore contributing to body roll: sprung and unsprung mass. The largest factor is sprung mass which has a lever arm length dependent on the hight of body CG above the roll center axis (Equation 2.12). The second factor, unsprung mass which also has a lever arm around the roll center axis dependent on CG hight over roll center axis (Eq. 2.13 and Eq. 2.14). Here: $d_s = h_s - z_s$ represents the height of the sprung mass over the roll centre axis , m_s the sprung mass, m_{uF} & m_{uR} front & rear unsprung mass respectively and h_{uF} & h_{uR} front and rear unsprung mass CG height over respective roll centre height.

$$M_s = a_y \cdot d_s \cdot m_s \tag{2.12}$$

$$M_{uF} = a_y \cdot h_{uF} \cdot m_{uF} \tag{2.13}$$

$$M_{uR} = a_y \cdot h_{uR} \cdot m_{uR} \tag{2.14}$$

The two spring LLTD model displayed in Figure 2.4, includes the effects from front and rear roll stiffness k_F & k_R. The equations derived from Milliken's model [15] seen in Figure 2.4 describing lateral load transfer distribution can be seen below:

$$\text{Front LLT rigid body [16]: } \Delta F_{zF} = (\frac{k_F}{k_F + k_R} d_s \cdot m_s + \frac{b_s}{L} \cdot z_F \cdot m_s + h_{uF} \cdot m_{uF}) \cdot \frac{a_y}{t} \tag{2.15}$$

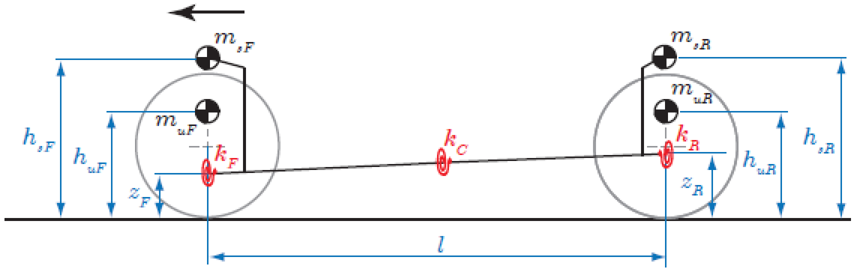

Figure 2.5: *Lateral load transfer distribution for a flexible body [16]*

$$\text{Rear LLT rigid body [16]: } \Delta F_{zR} = (\frac{k_R}{k_F + k_R} \cdot d_s \cdot m_s + \frac{a_s}{L} \cdot z_R \cdot m_s + h_{uR} \cdot m_{uR}) \cdot \frac{a_y}{t} \tag{2.16}$$

To study the effect on lateral load transfer distribution a front lateral load transfer proportion $\chi = \Delta F_{zF}/\Delta F_z$ and roll stiffness proportion $\lambda = k_F/(k_F + k_R)$ is defined as proposed by Sampo [16]. Where ΔF_{zF} represents the Equation 2.15 & 2.16 is rewritten with the previously stated proportions to equation 2.17, according to Sampo's work [16].

$$\text{LLTD [16]: } \chi = \lambda \frac{d_s \cdot m_s}{h_G \cdot m} + \frac{b_s \cdot z_F \cdot m_s}{L \cdot h_G \cdot m} + \frac{h_{uF} \cdot m_{uF}}{h_G \cdot m} \tag{2.17}$$

Equation 2.17 shows the factors affecting FLLTD. The first factor in Equation 2.17 represents the contribution from roll moment created by the sprung mass from the lever arm to the roll center axis and how much of that is distributed to the front axle. Whilst the second term describes the effect from lateral load and the third term the contribution to LLT from unsprung mass [16]. The second and third term contains design parameters and can hardly be tuned in a late design process. On the other hand the first term can be altered by varying the roll stiffness relation between front and rear axle, this is the most common way to vary load transfer between front/rear axle and through this alter the behaviour of the vehicle (over/understeer).

To also account for body torsional stiffness Sampo [16] adds a torsional spring with stiffness k_C between the front and rear axle as shown in Figure 2.5. The sprung mass is also divided into two parts. The derived equations presented by Sampo [16] for front and rear load transfer for a flexible body are presented in Equations 2.18 & 2.19. d_{sF} & d_{sR} represents the height of the front and rear sprung mass over the roll center axis for front and rear respectively.

$$\text{Front LLT flexible body [16]: } \Delta F_{zF} = \frac{a_y}{t_F} \cdot (\frac{k_F \cdot d_{sF} \cdot m_{sF}}{k_F \cdot \frac{k_R \cdot k_C}{k_R + k_C}} + \frac{\frac{k_F \cdot k_C}{k_F + k_C} \cdot d_{sR} \cdot m_{sR}}{\frac{k_F \cdot k_C}{k_F + k_C} + k_R} + z_F \cdot m_{sF} + h_{uF} \cdot m_{uF}) \tag{2.18}$$

$$\text{Rear LLT flexible body [16]: } \Delta F_{zR} = \frac{a_y}{t_R} \cdot (\frac{\frac{k_R \cdot k_C}{k_R + k_C} \cdot d_{sF} \cdot m_{sF}}{\frac{k_R \cdot k_C}{k_R + k_C} + k_R} + \frac{k_R \cdot d_{sR} \cdot m_{sR}}{k_R \cdot \frac{k_F \cdot k_C}{k_F + k_C}} + z_R \cdot m_{sR} + h_{uR} \cdot m_{uR}) \tag{2.19}$$

$$\text{Torsional stiffness to total roll stiffness relation: } \mu = \frac{k_C}{k_F + k_R} \tag{2.20}$$

If Eq. 2.20 is introduced together with $\chi = \Delta F_{zF}/\Delta F_z$ & $\lambda = k_F/(k_F + k_R)$; Eq. 2.18 and Eq. 2.19 can be rewritten to Eq. 2.21 according to Sampo's work [16].

LLTD for a flexible body [16]:

$$\chi = \frac{\lambda^2 - (\mu + 1) \cdot \lambda \cdot d_{sF} \cdot m_{sF}}{(\lambda^2 - \lambda - \mu) \cdot h_G \cdot m} - \frac{\mu \cdot \lambda \cdot d_{sR} \cdot m_{sR}}{(\lambda^2 - \lambda - \mu) \cdot h_G \cdot m} + \frac{z_F \cdot m_{sF}}{h_G \cdot m} + \frac{z_{uF} \cdot m_{uF}}{h_G \cdot m} \tag{2.21}$$

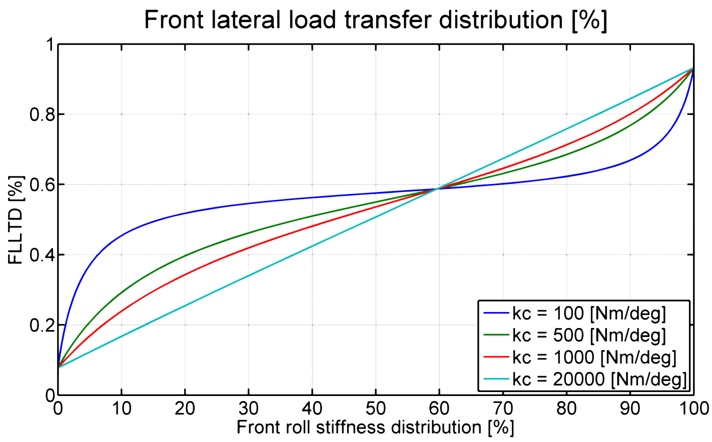

Figure 2.6: *Front lateral load transfer distribution model, for a flexible body*

Equation 2.21 contains four terms, two of them corresponding to non linear terms resulting in a non linear relationship between LLTD and roll stiffness distribution. However the relation is moving towards a linear relationship if $\mu \rightarrow Inf$. It can also be seen that there are three values of λ where a change in μ (relation between torsional stiffness and total roll stiffness) does not affect lateral load transfer distribution [16]. This is when either front or rear roll stiffness is zero; or when front to rear roll stiffness ratio is equal to front to rear roll moment ratio [16].

To analyze the characteristics of body stiffness changes in passenger cars Equation 2.21 is used together with characteristic values from a typical passenger car. The resulting relation between FLLTD and front roll stiffness distribution is shown in Figure 2.6.

Figure 2.6 shows the relationship between roll stiffness distribution and lateral load transfer distribution for a torsional stiffness of k_c = 100, 500, 1000 & 20000 $[Nm/deg]$. A typical passenger car has a torsional stiffness of 17 to 40 kNm/deg. It can be seen that a stiff body is more responsive to a change in roll stiffness distribution than a flexible body, the linearity between LLTD and SD is also gradually decreasing as torsional stiffness is decreasing. For a body where $k_C \rightarrow Inf$ the relation between LLTD and SD is linear, meaning that the roll moment created by the sprung mass is distributed according to roll stiffness distribution.

In order further analyze vehicle sensitivity to roll stiffness distribution, FLLTD/SD ratio vs body torsional stiffness is presented in Figure 2.7. FLLTD/SD is calculated as: $FLLTD/SD = \partial(FLLTD)/\partial(SD)$. It represents how much a change in roll stiffness distribution affects the LLTD. As can be seen in the plot the influence from body torsional stiffness decreases exponentially when the FLLTD/SD ratio gets close to 100%. Deakin [6] states as an example that a sufficient body stiffness is fulfilled when a FLLTD/SD ratio of 80% is reached. For the case with a normal passenger car this ratio is reached for a torsional stiffness of around 8000 $[Nm/deg]$. On the other hand Milliken [15] states that the body torsional stiffness should be 3-5 times larger than the total roll stiffness, for a typical passenger car: 7000-12000 $[Nm/deg]$.

These results show that the torsional stiffness of a passenger car is set very high according to the lower limits presented by Milliken [15] and Deakin [6]. Meaning that the torsional stiffness is set high enough to not affect lateral load transfer distribution.

2.4 Steady state bicycle model

When the vehicle body twists or bends the wheel forces and angles are altered leading to a changed vehicle behaviour dependent on body stiffness values. To get a fundamental understanding of the relative influence from these global stiffness values (torsional & lateral) on vehicle characteristics, the understeer gradient for varying body stiffness values during steady state cornering is investigated in this section. The model accounts

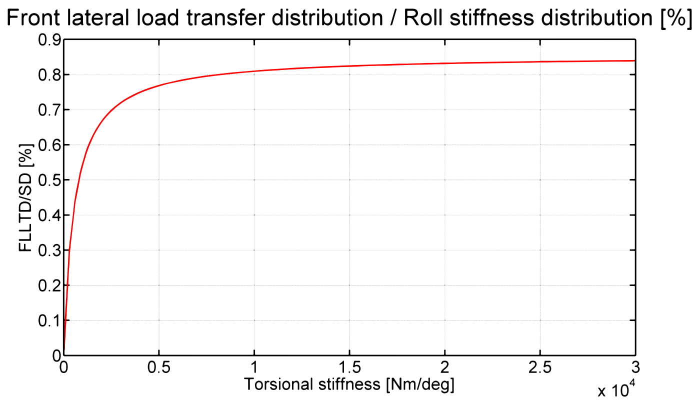

Figure 2.7: *Front lateral load transfer distribution / Roll stiffness distribution - ratio, for a flexible body*

for the influence of body stiffness on roll steer, effect from varying lateral load transfer from varying torsional stiffness on axle cornering stiffness and the influence from lateral compliance on front and rear wheel angles. The evaluation is based on a bicycle model with the following assumptions:

- Small steering and side slip angles.
- Aerodynamic forces are not considered.
- Longitudinal forces are not considered.
- The relation between cornering stiffness and tyre cornering force is considered to be linear.

2.4.1 Lateral compliance

In order to model the influence from lateral compliance, measurements relating lateral force to wheel angle rotations are used. The measurement values lc_F & lc_R describe how the wheel toe angles change for a given lateral force. Equations 2.22 & 2.23 represent the relation between wheel toe angle lcs_F and lateral compliance K&C measurement value lc_F, vehicle longitudinal speed v_x and corner radius R.

$$lcs_F = lc_F \cdot \frac{m \cdot {v_x}^2}{R} \cdot \frac{l_R}{L} \tag{2.22}$$

$$lcs_R = lc_R \frac{m \cdot {v_x}^2}{R} \cdot \frac{l_F}{L} \tag{2.23}$$

2.4.2 Torsional stiffness

Torsional stiffness has an affect on both vertical wheel forces and the kinematics behaviour of the suspension due to that the front and rear axle are permitted to have different roll angles. Both the influence from torsional stiffness on vertical forces and on roll steer is added to the simulation model and they are described in the two subsequent sections.

2.4.2.1 Axle cornering stiffness

Torsional stiffness has an influence on lateral load transfer distribution as explained in Section 2.3. The load transfer shifting between front and rear axle results in varying vertical wheel forces, which then are dependent on torsional stiffness. Conventional pneumatic tires do not behave according to Coulomb's model of friction, where the friction force is linearly dependent on the vertical force. The load sensitivity of the tire means that the coefficient of friction is reduced for an increasing vertical load. An increased vertical load will still lead to an increase in maximum lateral force but at a reduced rate. The influence from lateral load transfer distribution increases or decreases the difference in vertical load between right and left wheel within one axle during cornering, the influence from tire load sensitivity therefore increases or decreases the maximum axle lateral force that can be developed. The influence from torsional stiffness on lateral load transfer distribution can thus be seen to effect the axle cornering stiffness C describing lateral force F_y at a certain slip angle α. Equations 2.24 & 2.25 describe the non-linear influence from wheel lateral forces on front and rear cornering stiffness.

$$C_F = (c_0 \cdot F_{zFL} - c_1 \cdot F_{zFL}^2) + (c_0 \cdot F_{zFR} - c_1 \cdot F_{zFR}^2) \tag{2.24}$$

$$C_R = (c_0 \cdot F_{zRL} - c_1 \cdot F_{zRL}^2) + (c_0 \cdot F_{zRR} - c_1 \cdot F_{zRR}^2) \tag{2.25}$$

2.4.2.2 Roll steer

A flexible chassis will result in a vehicle that has different roll angles φ for front and rear axle (see Equations 2.26 & 2.27). This will in turn affect wheel angles according to the suspension kinematic characteristics. Suspension geometries for passenger cars usually incorporates a certain amount of roll steer (wheel toe angle change connected to vehicle roll motion) which will steer the front and rear wheels for a given front and respectively rear roll angle. A flexible chassis will permit different roll angles at front and rear axle, which leads to the existence of a relation between a change in wheel toe angle to a change in chassis torsional stiffness k_C during cornering. Equations 2.28 & 2.29 describe the relation between roll steer rs and axle roll angle φ, where rk $[rad/rad]$ is describing the ratio between toe angle and axle roll angle.

$$\varphi_F = a_y \cdot \frac{k_C \cdot (m_{sF} \cdot d_{sF} + m_{sR} \cdot d_{sR}) + k_R \cdot m_{sF} \cdot d_{sF}}{k_F \cdot k_R + k_R \cdot k_C + k_C \cdot k_F} \tag{2.26}$$

$$\varphi_R = a_y \cdot \frac{k_C \cdot (m_{sF} \cdot d_{sF} + m_{sR} \cdot d_{sR}) + k_F \cdot m_{sR} \cdot d_{sR}}{k_F \cdot k_R + k_R \cdot k_C + k_C \cdot k_F} \tag{2.27}$$

$$rs_F = rk_F \cdot \varphi_F \tag{2.28}$$

$$rs_R = rk_R \cdot \varphi_R \tag{2.29}$$

2.4.3 Understeer gradient

Equation 2.30 is derived from the simplified bicycle model equations presented in Appendix 7, the model is thoroughly described by Milliken [15]. Equation 2.30 describes the front wheel angle required for the vehicle to keep a certain cornering radius R and lateral velocity v_x. It accounts for the influence from lateral compliance on toe angle change lcs, torsional stiffness on roll angle and on toe angle change rs; and the influence from torsional stiffness on lateral load transfer distribution and thus cornering stiffness. The first term in the equation is the required front wheel angle for a rolling vehicle to take a turn with radius R, it is called the kinematic steer angle. The other terms in the equation is dependent on lateral acceleration and therefore has a non-linear relation to longitudinal speed. These terms together are called the dynamic steer angle.

$$\delta_F = \frac{L}{R} + \frac{m \cdot {v_x}^2}{R} \cdot \frac{C_R \cdot l_R - C_F \cdot l_F}{C_R \cdot C_F \cdot L} - lcs_F + lcs_R - rs_F + rs_R \tag{2.30}$$

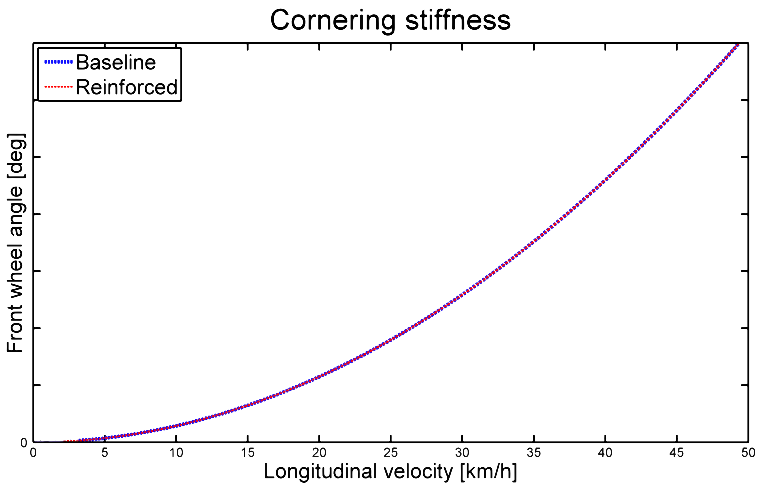

(a) *Cornering stiffness*

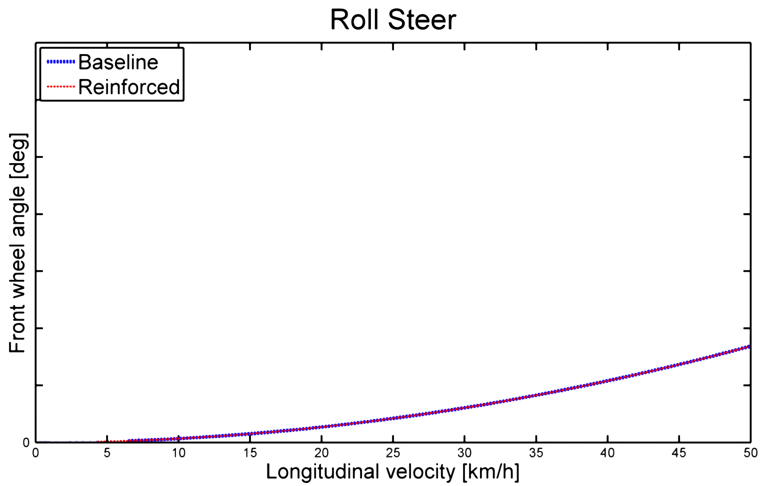

(b) *Roll steer*

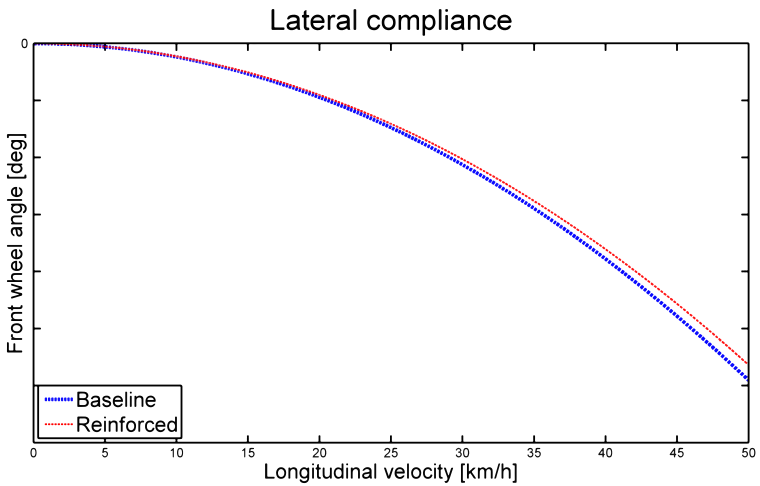

(c) *Lateral compliance*

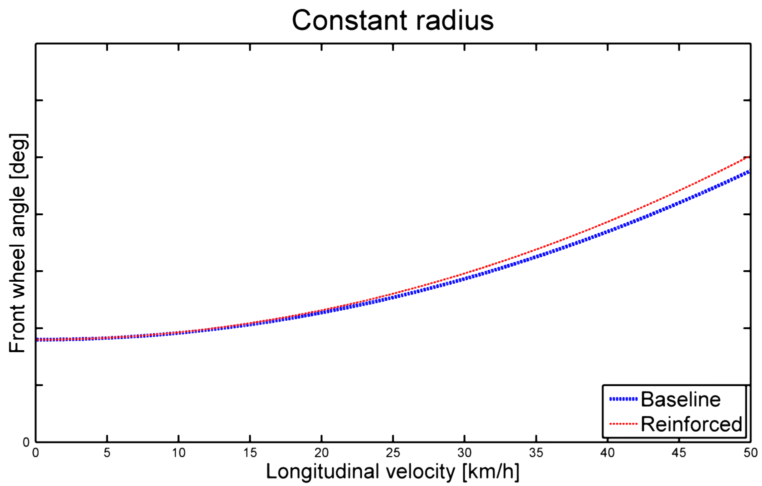

(d) *Constant radius*

Figure 2.8: *Influence from torsional and lateral stiffness on vehicle characteristics*

Figures 2.8a, 2.8b & 2.8c illustrate the influence from body stiffness (torsional & lateral) on respectively cornering stiffness, roll steer & lateral compliance (they have the same relative y-axis scale). These three figures display the individual effect from cornering stiffness, roll steer & lateral compliance on the front wheel angle required to run in a constant radius with increasing lateral velocity. Global torsional stiffness is the variable which changes in Figures 2.8a & 2.8b, respectively describing the effect from cornering stiffness and roll steer.

Whilst in Figure 2.8c which is describing the influence from lateral compliance, it is global lateral stiffness which is changing. The plots compare the baseline vehicle (Volvo S60) to the same vehicle fitted with various body reinforcements, see Section 3.2.2 for more information on where the reinforcements have been fitted. It can be seen from Figure 2.8c that the largest body stiffness factor influencing vehicle behaviour during steady state cornering is lateral compliance, whilst torsional stiffness is not affecting the vehicle behaviour.

Figure 2.8d show front wheel angel vs longitudinal velocity, it can be seen that the vehicle with a reinforced body is slightly more understeered than the baseline vehicle i.e. the front wheel angle has to be increased more in relation to the increased vehicle speed compared to the baseline vehicle. The understeer gradient for the vehicle with a reinforced body is approximately 8.0 % larger than for the baseline vehicle.

2.5 Design of experiment

The design of experiment technique was invented in 1920 by Ronald A. Fisher [9]. The goal of this technique is no other but maximizing the knowledge gained from experimental data while reducing the number of experiments. The traditional experimental approach suggests changing one parameter at a time and analyzing the change produced in the outputs. However this method is inefficient when one needs to perform a great number of experiments. Hence instead of changing one parameter at a time the DOE methods allows a proper analysis modifying more than one input in each experiment. In this project the multi-optimization tool modeFrontier will be used in order to design, control and automatize the experiment.

When it comes to DOE one need to consider some steps before proceeding with the further work. First and most important is a proper recognition and design of the problem. This task is crucial and it is not trivial for most of the cases. The experiment should be analyzed and decomposed in a suitable way for the purpose of the analysis. Once this step is fulfilled a proper selection of input factors and outputs is also needed, as well as the appropriate optimization conditions in case that those are needed for the study. Furthermore the design of experiment should be connected to the data analysis so that some characteristics and aspects are correct: the input domain is covered and the replication of scenario is taking into account all possible combination of inputs. Full-factorial DOE can be used in modeFrontier in order to cover all the possible input combinations and levels of interaction. However, another DOE options are available in order to reduce the number of experiments. These options investigate the levels of inputs required for determined level of outputs through a deterministic mathematical model allowing the space filling of the rest of the domain. Reduced factorial, Plackett-Burman, Cubic Face Centered are some of these models. A trade-off between the computational power available, number of inputs and experiment requirements should be done in order to decide the sampling method required.

In this study the DOE is used to perform a sensitivity analysis. Statistical tools are therefore of vital importance to evaluate the results and they will be explained in Section 2.6. A sensitivity analysis gives information about the influence of the inputs on the different outputs therefore a proper formulation of the problem is needed. The risk of selecting a non-optimal point of the design space is not present in the sensitivity analysis since the purpose of the study will not pick any optimal solution. However a proper scanning of the design space is needed in order to capture the impact that the changes in the inputs has on the different outputs. This will be covered in this study by using a full-factorial DOE when the simulation times and inputs combinations allow so. For the same reason, the performance of a sensitivity analysis, no optimization algorithms will be used. However the possibilities are open for carrying out this kind of analysis in future work. The optimization algorithms then should be evaluated together with the problem design in order to find the optimal solution in the design space. Providing a good starting point for the algorithm as well as identifying robust solutions are other key steps when the DOE is performed towards optimization purposes.

2.6 Statistical analysis

Interpretation and presentation of the collected data in the experiments is covered by using statistical analysis tools. The most important relations, plots and coefficients used in this study are presented in the next paragraphs.

2.6.1 Graphical visualization and correlation of large data sets

The software used for the graphical visualization and correlation of large data sets of results from the performed DOE is modeFrontier. This multi-objective optimization software contains a variety of tools used to perform statistical analysis. These tools are used to explore the design space and to analyze results. Data and data distributions can be visualized using scatter, bubble plots, histograms and cumulative plots. In this section the tools used for finding correlations and trends are explained.

2.6.1.1 Box-Whiskers

Summarizing information about data in an effective way is a key feature when the DOE contains a large number of inputs and outputs. Common statistical functions i.e. mean, confidence, interval, the quartiles and outliers are used for this purpose. Visualizing the distribution can be done by using the Box-Whiskers chart [9]. The box will highlight the middle half of the data points and quartiles together with endpoints. Outliers are marked in the chart as circles and defined as designs with a value greater or less than 1,5 of the standard deviation measured from the mean value [9].

2.6.1.2 Student chart

To calculate a value which represents the effects of an input factor (x) on an output variable (y), the value range is spliced in two parts by dividing them in low and high values of y. Then the mean of y in the lower and upper part of the variable set is calculated, the difference between these two values results in the “effect” [9]. The “effect” is a measure on how much the input variable is affecting the output variable and it is useful when analyzing the effects of multiple factors on a single output variable.

When creating a student chart in modeFrontier a Student test is performed. This assesses the probability of that the “effect” is capturing an existing trend by examining the overlap of the two “mean sets” [9]. A value called Significance which spans from 0 to 0.5 is created. A low value represents high probability and a high value represents low probability [9].

2.7 Flexible Bodies

One of the challenges while performing Multi-Body Dynamics simulations is capturing the deformation of the bodies. These deformations are needed in order to take into account how the stiffness/compliance of these parts are affecting the simulated models. In this study the dynamics simulations performed in Adams Car will capture this effect using the modal flexibility method.

The main assumption made to simulate these flexible bodies is that only small linear deformations are taking into account in a local frame of reference while that frame has a non-linear global motion. This means a finite element model where the infinite number of DOF of the real component are discretized to a finite number of nodes containing the information of the linear deformation of such nodes. That information is equivalent to a combination of mode shapes (eigenvectors) which are assigned to the flexible body. The relative amplitude of each mode is calculated during the time frame and then linear superposition is used to combine all the mode shapes and to calculate the deformation of the flexible body. In other words, the deformations in the modelled flexible bodies are a linear combination of deformation shapes. This information is contained in a modal neutral file (MNF). An MNF is created from a FEA software and it contains the location of nodes, nodal mass and inertia, mode shapes and generalized mass and stiffness for mode shapes [1].

The problem arises when selecting the mode shapes required to capture all the needed information of the model. Component Mode Synthesis is performed for creating the Adams Flexible Bodies based on the Craig-Bampton Method [2]. This method is used in order to perform the modal reduction of the FEA model information contained in the previously mentioned MNF files.

2.8 Tire models

An essential part in a good vehicle model is the tire model. Special attention to this matter has been given for the full vehicle simulations performed with the software IPG CarMaker. This tool supports four different models:

- IPGTire (RealTime Tire)
- Pacejka 5.2 (Magic Formula)
- MF-Tire/MF-Swift 6.1
- TameTire

The suspension kinematics and compliance model in CarMaker requires the forces/torques at the wheel centers, therefore the tire models are calculating the slips and forces/torques in the road contact point. Then, these forces are transfered to the wheel center points [13].

2.8.1 IPGTire (RealTime Tire)

The IPGTire model can be used when tire characteristic measurements (lateral force vs. slip angle, longitudinal force vs. longitudinal slip and self-aligning torque vs. slip angle) are available. One of its greatest advantages is the ease of creating the model with the measured tire characteristics. The CM tire file is created by collecting the tire measurements in a text file (TYDEX format) which is then converted to a binary file which can be read by CarMaker [13]. The TYDEX (Tyre Data Exchange) format offers the automotive industry a standardized way of storing and exchanging tire measurement data [13].

IPGTire calculates the lateral tire force from three different components: slip angle, inclination angle and a third component which arises from the distortion of the contact surface area (can be neglected for car tire) [13]. To account for the inclination angle (camber angle) of the tire the following formula is used: $a' = a + multiplyingfactor \times d$, where a' is the slip angle used to calculate the side force, a is tire slip angle, d tire inclination angle [13]. The multiplying factor is retrieved from the CM tire file and it is used to increase the tire lateral force linearly with increasing tire inclination angle [13].

2.8.2 Pacejka 5.2 (Magic Formula)

The Pacejka Magic Formula is based on trying to match tire characteristics with a mathematical formula (see Eq. 2.31, Eq. 2.32 and Eq. 2.33). This is possible due to that characteristic curves of tire behaviour have been found to have very similar shapes [13]. The Magic Formula can be used to parameterize lateral force vs. slip angle, longitudinal force vs. longitudinal slip and self-aligning torque vs. slip angle (for self-aligning torque the sine function have to be replaced with a cosinus function) [13]. This model was implemented in CarMaker and used during this study.

$$y(x) = D \times sin[C \times atan\{Bx - E(Bx - atan(Bx))\}] \tag{2.31}$$

$$Y(X) = y(x) + SV \tag{2.32}$$

$$x = X + SH \tag{2.33}$$

- The Pacejka parameters are stored in a text file which is read by CarMaker and the parameters can be directly modified in the text document. This allows for fast tuning of the model without having to perform any file format conversions [13].
- One of the drawbacks with this model is that it is unstable at low vehicle speeds [13], but IPG has included a "separate" model for low vehicle speeds and for stationary operation [13].

2.8.3 MF-Tire/MF-Swift 6.1 (RealTime Tire)

MF-Tire/MF-Swift is an extended version of the Magic Formula tire model. More information about this tire model can be found in [13].

2.8.4 TameTire

TameTire is a tire model developed by Michelin which is based on three different models: a mechanical model, a rubber compound model and a thermal model. The advantages with TameTire is that the model can account for a larger variety of conditions: thermal, tire pressure and transient effects are taken into account in this tire model [19].

3 Method

In order to perform the CAE study of the influence of body stiffness on vehicle dynamics characteristics a method connecting component, subsystem and vehicle characteristics is built. This is thus an important section of the report, where firstly an overview of the methodology is presented and then subsequently broken down into different relation levels. The same structure is utilized for explaining all the relation levels and for explaining the tools, models, parameters and simulations used to analyze that relation between the subsystems. How the models are correlated with real life is also an important point and in the end of this section the methodology utilized for the physical testing is also explained.

3.1 Overview

The study of body stiffness influence on vehicle dynamics characteristics was conducted from a comparison between a standard Volvo S60 and a Volvo S60 with body reinforcements. The car's body was modified with detachable steel bars allowing the body stiffness to increase or decrease in specific areas. Meaning that the same vehicle can be compared against a baseline but with an increment or decrement in body stiffness. The setup configuration for the rest of the car, including parameters for: dampers, springs, tires, anti-roll bars, aerodynamics settings, drive train etc., are kept constant in order to isolate the effect from body stiffness on vehicle dynamics characteristics.

The study was performed with both physical tests and CAE simulations. Objective and subjective physical tests were performed with the two car configurations: reinforced configuration, all the steel bars attached to the car; and baseline configuration, all of the reinforcements removed from the body. The rest of the setup parameters were kept constant. One more vehicle configuration was used in the CAE study, a rigid body. This configuration was used in order to maximize the difference between the baseline and the stiffer body. The difference seen in these results for a vehicle with a flexible body compared to a rigid body represents the error in full vehicle simulations for the case where a flexible body is assumed to be rigid.

The CAE analysis method used for correlating body stiffness and vehicle dynamics characteristics is divided in three different relations levels: component to sub-system, sub-system to vehicle and component to vehicle, as shown in Figure 3.1. The component level describes the local stiffness of the body i.e. how the different steel bars are increasing body local stiffness; the sub-system level corresponds to global stiffness and K&C values i.e. lateral compliance, toe compliance, camber compliance, bending stiffness or torsional stiffness; and the vehicle level assesses the dynamic behaviour of the car in terms of handling, steering and ride.

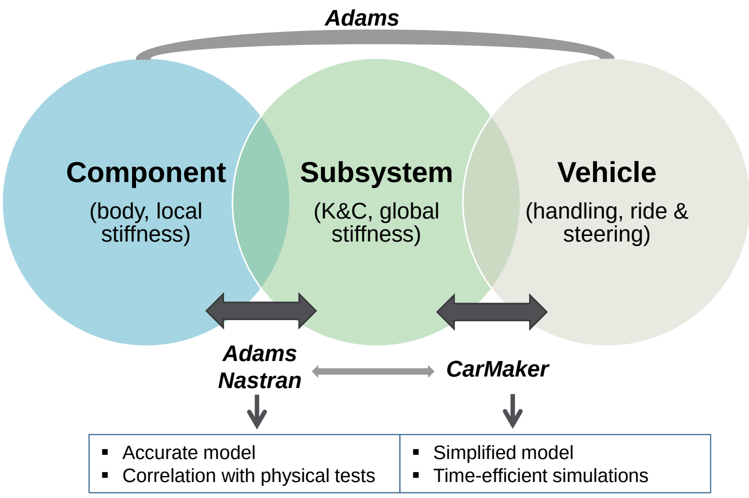

Figure 3.1: *CAE relation levels*

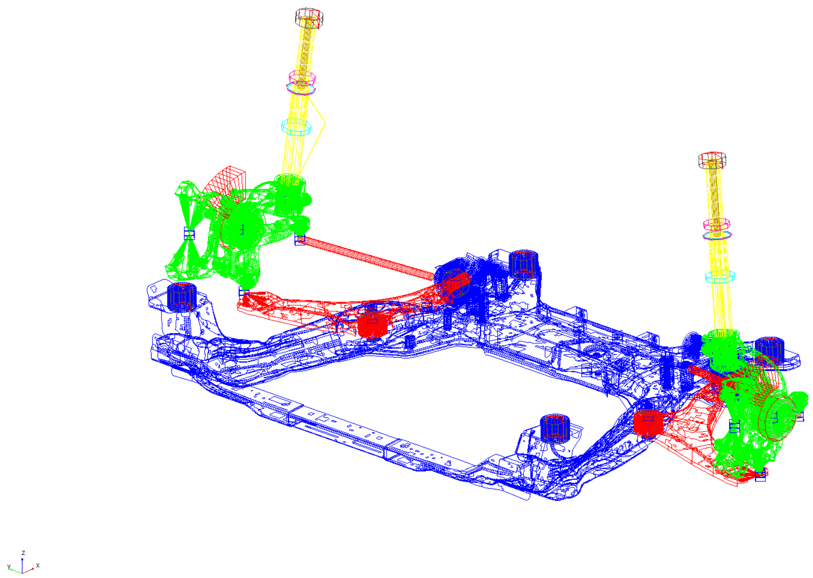

Figure 3.2: *Front suspension MSC Adams Model*

3.2 Component to subsystem relation

This section describes the Adams and Nastran models and how they were used to relate component to subsystem characteristics. For the case of the Adams model, how the different reinforcements in the subject car are affecting the compliance values. This relation is analyzed performing quasi-static multi-body simulations. For the Nastran model, how the bars are affecting the bending and torsional stiffness parameters. This influence is studied by performing a finite element analysis.

3.2.1 MSC Adams Model

This section describes how the model has been built for relating component to sub-system characteristics through the multi-body simulation software Adams Car and kinematics and compliance simulations. The suspension and the body are described as independent main assemblies of the model in Sections 3.2.1.1 and 3.2.1.2 respectively.

3.2.1.1 Suspension

The model of the Volvo S60 used in this study was provided by Volvo Car Corporation and its front and rear suspension are described in this section. This information is relevant for the performed analysis since the conclusions will be limited to the studied car, hence the influence from the chosen vehicle suspension geometry is present in the results.

The front suspension system in the Volvo S60 (Figure 3.2) is a McPherson strut suspension. The lower control arm and the subframe are modelled as flexible bodies including up to 34 and 112 modes respectively. The rear suspension is a multi-link suspension (Figure 3.3) where the spring link, toe link and camber link are modelled as flexible bodies with modal information for 30 modes. Rear subframe and trailing arm has modal information up to 60 modes.

The antiroll bars are modelled as multi-beam elements for both front and rear suspension. Regarding details for: dampers, bushings and bump stops, these have been modelled according to the ones mounted in the physical car tested on the track. However, as stated before in this report, during the CAE analysis suspension settings are not modified; only body stiffness is changed.

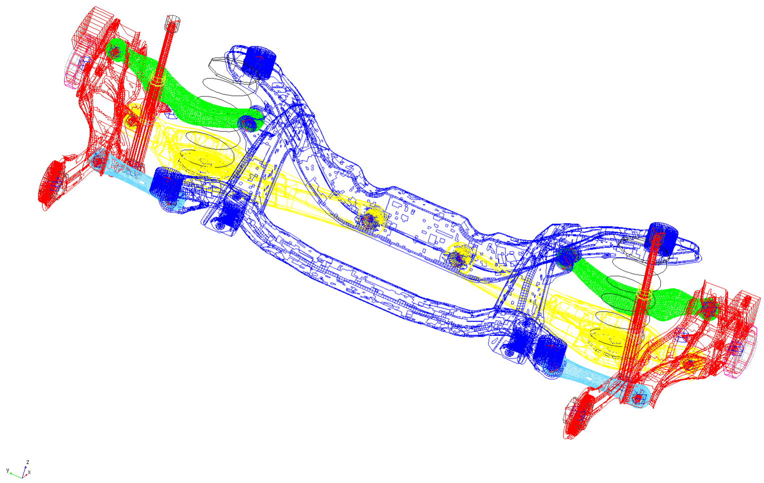

Figure 3.3: *Rear suspension MSC Adams Model*

3.2.1.2 Body

The body of the model corresponds to the baseline BIW of a Volvo S60. A flexible model is used to capture the deformations of the body while driving. Adams Car uses a MNF modal reduction representation of the body from an FEM model in order to simulate these effects. In this case the modal information for the S60 baseline body is containing 221 modes. According to the research presented in Section 2.1 the modal reduction frequency levels are believed to be enough for the frequencies used in the studied maneuvers. Which are the selected modes has also a crucial importance in the performance of the model. However this aspect has not been investigated in this study.

For the reinforced car model, the study has been performed by reinforcing the BIW with different bars, as it was done in the physical test car. The tube thickness of the bars is $2mm$ with an external diameter of $15mm$. However these reinforcements are modeled in Adams Car with rigid beams i.e. rigid connections, connecting the two desired points of the BIW. The modeling of these beams has been done this way so that the compliance values obtained in the SPMM rig correlates with the CAE simulations performed in Adams Car.

3.2.2 Parameterization of MSC Adams model

In this section the parameters used in the Adams model are described for the suspension and the body. These are the two relevant assemblies for the purpose of this study.

3.2.2.1 Suspension

The parametrization of the suspension components has been done according to the library of existing modeled parts at VCC for Adams Car. The values used for springs, bushing and bump stops in the CAE simulations matches those for the physical components fitted to the S60 tested at HPG.

3.2.2.2 Body stiffness

In order to analyze the effect from different reinforcements on the K&C values, combinations of different reinforcements attached to the car has been simulated using the Adams model. The model is composed of 17 steel bars connecting different points in the BIW. In the front part of the car the spring towers are connected with a transversal bar and two longitudinal bars are going down towards the crash box area. In the same zone, another transversal bar increases the stiffness of the front part of the BIW. On the underbody two main supports are built. One cross member in the front and a transversal bar in the rear. In the trunk: cross members, side and transversal beams are mounted in order to improve the stiffness in this area.

Table 3.1: Stiffener groups

Group	Reinforcements	Numbering
Front Longitudinal	2 longitudinal bars	H2-H3, V2-V3
Front Transversal	2 transversal bars	H1-V1, H4-V4
Underbody	1 cross section & 2 longitudinal bars	H6-V7, V6-H7, H5-V5, H8-V8
Rear Longitudinal	2 longitudinal bars	V14-V18, H14-H18
Rear Transversal	3 transversal bars	V10-H10, V12-H12, V17-H17
Rear Cross	1 cross section	V16-H15, H16-V15, V13-V14, H13-H14

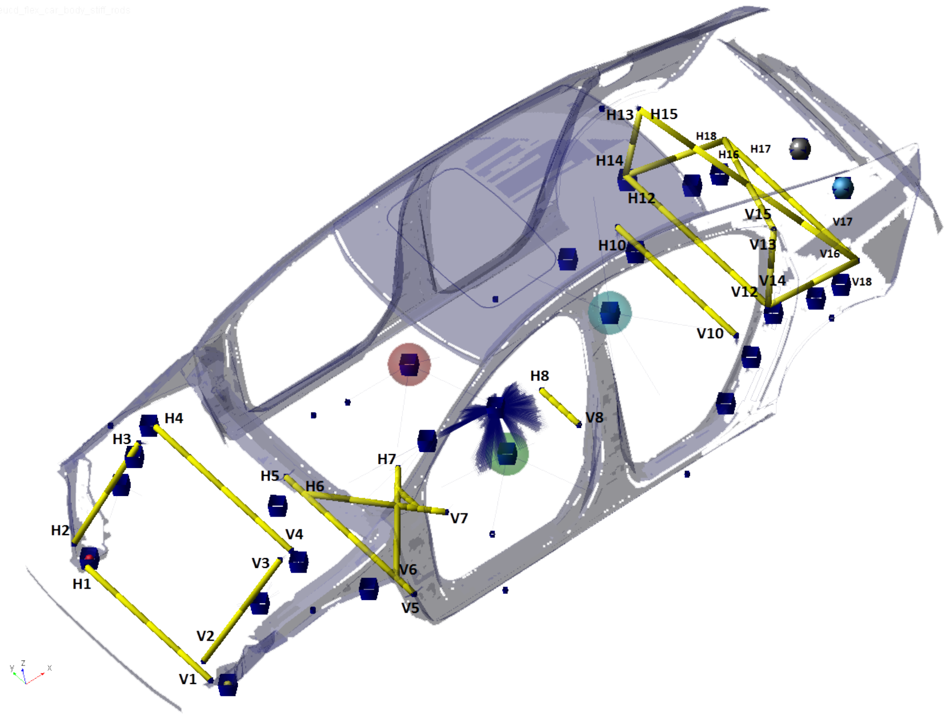

Figure 3.4: *Stiffeners in the Adams Car model*

As discussed in Section 2.5, a full factorial DOE is preferred in order to ensure that the design space is fully covered. Because of this reason 6 groups were created from the 17 steel bars. The number of groups were chosen based on the total simulation time, for this case 6 groups results in 64 simulations (full factorial DOE containing 6 groups with 2 levels: on/off). The groups are classified based on in which area of the car the bars are situated: front, rear or underbody; and the orientation of them: longitudinal, transversal or cross mounted. Table 3.1 contains the different groups and numbering of the bars in accordance with Figure 3.4.

3.2.3 Validation of the model

The Adams Car S60 model was verified in two vehicle configurations: with and without reinforcements. It was done by comparing Adams K&C simulations with real K&C measurements performed in the SPMM rig at HPG. The K&C simulations in Adams Car were done with the full vehicle, but independently for front a rear suspension. However in the SPMM rig at HPG the analysis was performed for both front and rear suspensions at the same time. This difference between the test methods was not expected to be a problem for the validation of the results in terms of kinematic metrics and lateral compliance. However due to the limitations in the Adams K&C test rig, it was expected that the absolute values for toe and camber compliances will not correlate well with those from the physical measurements. Because of that the validation of the model for these two metrics has been done in the delta difference between the car with the reinforcements on and with the reinforcements off, since the main purpose of this study is to investigate how the outputs are affected by a delta change of an input.

Table 3.2: Load case equivalences

SPMM rig test load case	Equivalent CAE load case
Longitudinal force X	Force X + Torque Y
Lateral force Y	Force Y + Torque X
Aligning Torque Z	Torque Z

Table 3.3: Adams load cases

[number] Load case	Adams mode	Load	Force/Torque application point
[1] Braking	Static load	Force	Tire contact patch
[2] Cornering	Static load	Force	Tire contact patch
[3] Force in x	Static load	Force	Wheel center
[4] Force in y	Static load	Force	Wheel center
[5] Parallel wheel travel	Parallel wheel travel	Wheel travel	Tire contact patch
[6] Single wheel travel	Single wheel travel	Wheel travel	Tire contact patch
[7] Torque around x	Static load	Torque	Tire contact patch
[8] Torque around y	Static load	Torque	Tire contact patch
[9] Torque around z	Static load	Torque	Tire contact patch

Furthermore, the validation of the Adams model was done by comparing physical measurements from real tests with the simulation results from Adams. However the load cases performed in Adams Car were not exactly the same as the tests performed in the SPMM rig at HPG. The CAE analysis for force load cases (lateral force and longitudinal force) was done applying the load in the wheel center while the tests in the real car were performed by applying the loads in the tire contact patch. The reason behind this discrepancy between simulations and real measurements is the need of using Adams simulations to create a CarMaker model for the next step of the analysis: the relation between sub-system and vehicle characteristics. The equivalence of the load cases is presented in Table 3.2 and was made taking into account the radius of the wheel and the fact that when a load in the contact patch is applied a torque in the center of the wheel appears. The main kinematics metrics validated are derived from the Vertical Bounce Test (Parallel wheel travel) and the Steering Geometry test (where both the front wheels are given a steering angle range). The lateral, toe and camber compliance metrics are calculated based on measurements gathered from the Longitudinal Compliance, Lateral Compliance and Aligning Torque tests.

3.2.4 Simulations

The simulations performed in MSC Adams consists of standard K&C tests presented in Table 3.3. The tests are performed independently for front and rear suspension i.e. in a two wheel rig which enables testing on one axle at a time. The tests are static load, parallel wheel travel and single wheel travel. These three tests are conducted to gather absolute values describing the following kinematic variables: wheelbase, track, wheel travel, camber, spin angle, toe, spring length, damper length, buffer length and stabilizer length; and also absolute values describing the following compliance variables: wheel base variation, track variation, wheel travel variation, camber variation, spin angle variation and toe angle variation. The input parameters for the K&C load cases are shown in Table 3.4.

Load case number 1, 2, 3, 4, 7 & 8 (Table 3.3) are compliance tests, which are performed once for front axle and once for rear axle. In these tests, translation and rotations are measured while a force or torque is applied in the point specified in Table 3.3.

The wheel travel analyses conducted describes how suspension characteristics are affected by vertical wheel motion. Test number 5, parallel wheel travel is a kinematics test were both wheels are moved vertically inside a pre-set bump/rebound range; tires are kept at the same height throughout the test. To fully capture the kinematics of the front axle the test is performed at 11 different wheel angle positions, this is not required for the rear axle due to that it is not steered. For all these configurations data describing wheel center motion is gathered. To get information about anti roll bar force, test number 6, single wheel travel is performed. In this test one wheel is translated vertically between the specified bump and rebound positions while the opposite

Table 3.4: Adams load case parameters

Parameter	Value
Number of steps	60 [mm]
Bump travel	74 [mm]
Rebound travel	-100 [mm]
Symmetric lateral force	10000 [N]
Symmetric longitudinal force	10000 [N]
Symmetric aligning torque	300000 [N]
Symmetric overturning moment	300000 [N]
Symmetric braking torque	300000 [N]
Symmetric steer travel	84 [mm]
Number of steer outputs	5
Single travel outputs	5

wheel is kept at a specified height.

3.2.5 Design of experiment Adams

The scheme displaying the process flow in the multi-objective optimization tool modeFrontier is shown in Figure 3.5. The experiment is connecting the Multi-body Dynamics Simulation tool MSC Adams Car, the postprocessing code in MatLab and the needed scripts to change the inputs and read the outputs.

The inputs are changed according to a full factorial DOE. As presented in Section 3.2.2, six groups and two levels (on/off) were used. ModeFrontier generates the full factorial combination of the input variables and sends the values for each simulation to the node “Command file ADAMS” as can be seen in Figure 3.5. This node is changing the command instructions for the Adams simulations i.e. activating or deactivating the six groups of reinforcements previously defined with a parameter in the Adams template file (containing model information). The next node in Figure 3.5 is a batch script “ADAMS K&C Simulations” which is opening Adams Car in batch mode, loading the Volvo S60 model with the correct configuration of stiffeners and executing the front and rear K&C analysis. The result files from the simulations are then stored and saved for postprocessing in the MatLab node, “Post-Processing Results K&C”. This node extracts the values required from the simulation results and it compiles them in a .skc file, which can be used as an input file in CarMaker (describing K&C characteristics). The last node, “Reading K&C Results to MF”, contains a script made in Python which reads the mentioned .skc files and extracts the needed values and calculates the metrics (value for the slope describing the compliance) for further statistical analysis in modeFrontier.

3.2.5.1 Post processing in modeFrontier

The last node (“Reading K&C Results to MF”) in the modeFrontier process flow seen in Figure 3.17 reads the compliance values i.e. the translations and rotations for each load case calculated by Adams and stored in text files by the Matlab scripts. It calculates the metric values (linear regressions based on translation and rotations of the wheel centre) and it outputs them into modeFrontier for further post processing when all simulation combinations stated by the DOE has been completed.

The metrics data stored for each simulation combination is further post processed within modeFrontier. This is done with the Overall Student Chart described in Section 2.6.1.2, which calculates the effect of an input factor on an output variable.

Post processing of modeFrontier data in Sympathy for Data

The output data from modeFrontier is then post processed in another tool which allows simpler analysis of data outputs, Sympathy for Data (more information about this tool will be given in Section 3.3.5.1, due to the fact that the project contains 60 output variables and subsequently 60 (number of metrics) times 6 (number

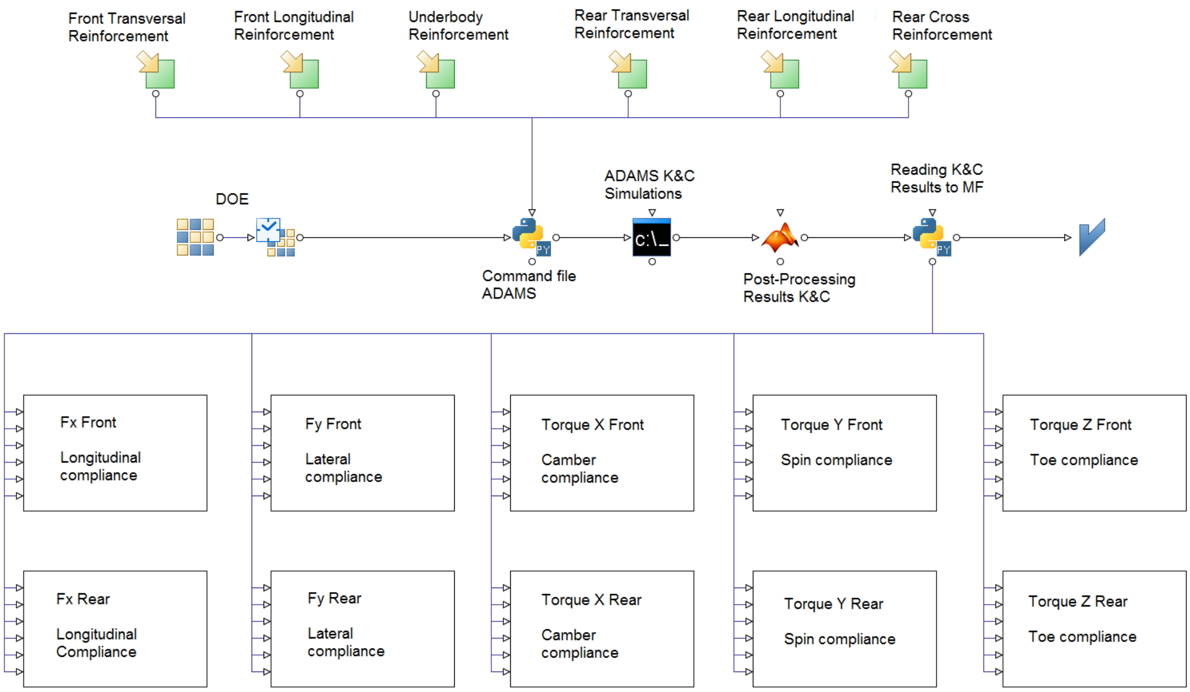

Figure 3.5: *ModeFrontier scheme for Adams simulations*

of stiffener groups) values of effects. This data has to be further post processed and sorted. This task was performed with a stand alone Sympathy for Data flow. The flow calculates the percentage change of each metrics with a flexible body as baseline.

3.2.6 FEM Model

The FEM model used for calculating the static stiffness has approximately 1 million elements and it represents the BIW of a Volvo S60. It has been reinforced in key areas in order to avoid local deformation while performing the static stiffness tests. Specifically the top mounts and force application area in the floor for the three point bending test have been reinforced, as seen in Figure 3.6. The reinforcement has been done by transforming the named areas into rigid body elements using RBE2 constraint (rigid body with independent DOF at one GRID and dependent DOF in the slave nodes around). The stiffeners which are decreasing the body compliance are modeled using CBAR elements, simple beam connections. They connect the different points in the BIW in the same way as for the physical test vehicle.

3.2.7 Parameterization of FEM model

The FEM model baseline has been built according to the Volvo S60 construction and hence parametrized according to a Volvo S60. Panels and materials are modelled in line with the real vehicle. In accordance with the Adams Car model body stiffness is increased or decreased by adding and removing bars which connects different points in the BIW. As explained in the previous Section 3.2.6, the reinforcements are modelled as rigid connections between the desired points. In total 10 supports are built as presented in Table 3.5 and Figures 3.7, 3.8 & 3.9. The supports are then grouped in the same manner as described in Section 3.2.2 for the Adams Model. In this case the reason of having the same groups yields in the intention of doing the same sensitivity analysis with the results form the FEM simulations as described for the Adams simulations. The input groups can then be related with torsional and bending stiffness; and the effect of each group can be analyzed together with the Adams results (Section 3.2.2).

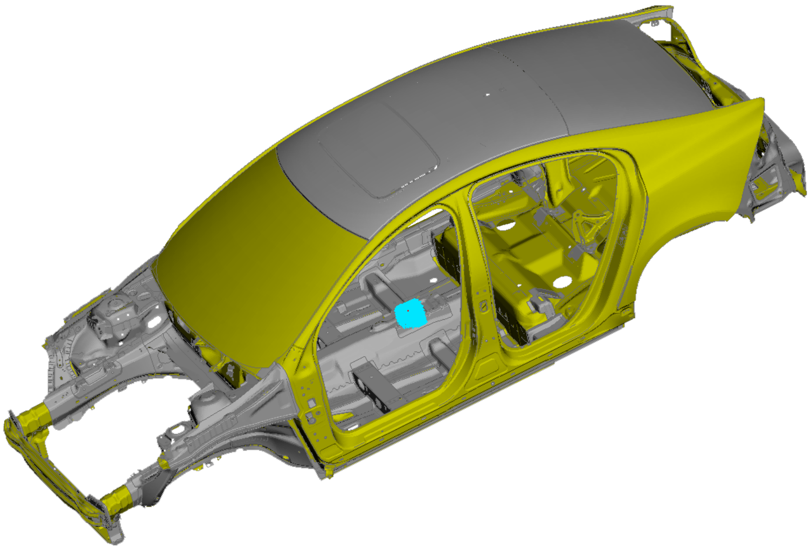

Figure 3.6: *BIW reinforcements for avoiding local deformation in bending stiffness test*

Table 3.5: Supports in FEM Model

Reinforcement	**Group**	**Figure**
Crashbox Front	Front Longitudinal	Figure 3.7
Spring Tower	Front Longitudinal	Figure 3.7
Top Mounts	Front Transversal	Figure 3.7
Trunk Cross	Rear Cross	Figure 3.8
Trunk Front	Rear Transversal	Figure 3.8
Trunk Rear Seat	Rear Transversal	Figure 3.8
Trunk Longitudinal	Rear Longitudinal	Figure 3.8
Tunnel Front Cross	Underbody	Figure 3.9
Tunnel Front Straight	Underbody	Figure 3.9
Tunnel Rear	Underbody	Figure 3.9

3.2.8 Validation of FEM model

The validation of the FEM model has been performed by comparing the static torsional stiffness simulation results with the physical torsional stiffness test results performed according to the test method presented in [21]. The physical test is done without demounting the body from the rest of the parts of the vehicle. However during the CAE analysis the torsional stiffness is measured directly in the BIW, without any influence of the rest of the parts of the car i.e. applying the forces directly to the desired points. The twist angle is then measured in the top-mounts and a value for torsional stiffness is calculated. The limitation of the test rig methods can yield to a small discrepancy in the results. However it is believed that the four-poster rig used for applying the torsion moment to a fully assembled vehicle results in a force application point in the correct location of the BIW yielding in approximately the same moment around the centreline as the moment applied in the CAE simulations.

The comparison has been performed for four different combinations, so a validation of the main stiffener groups can be done. As presented in Table 3.6, the first validation has been performed with all the stiffeners on. Second and third case has been done without the longitudinal bars for front and rear parts of the car respectively. Last case is done with only longitudinal bars in the front and underbody.

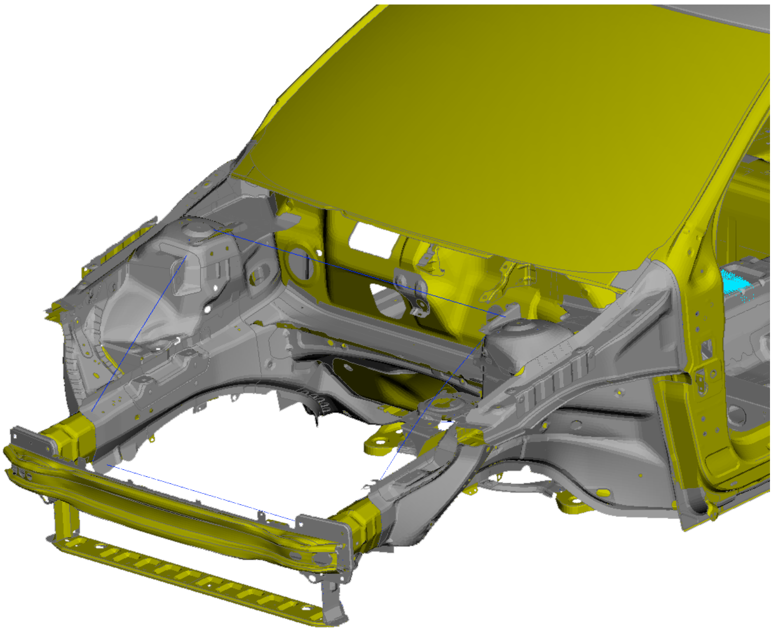

Figure 3.7: *BIW front reinforcements*

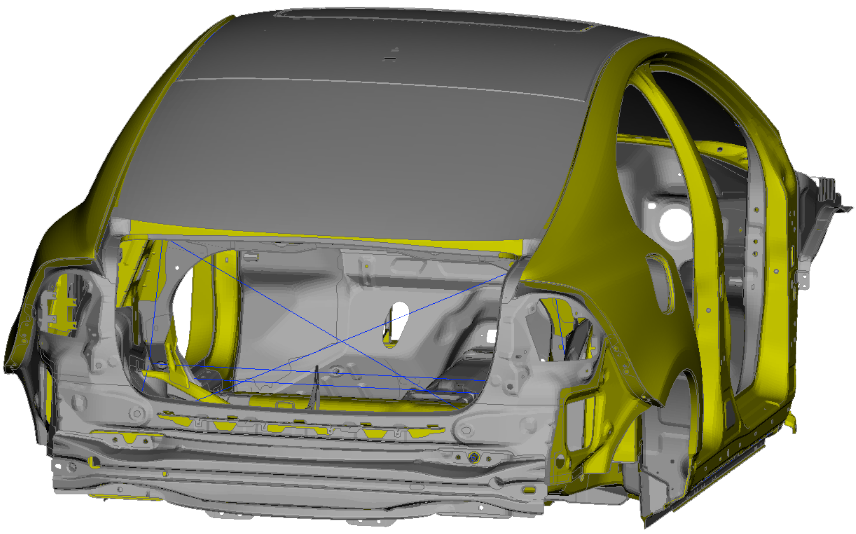

Figure 3.8: *BIW rear reinforcements*

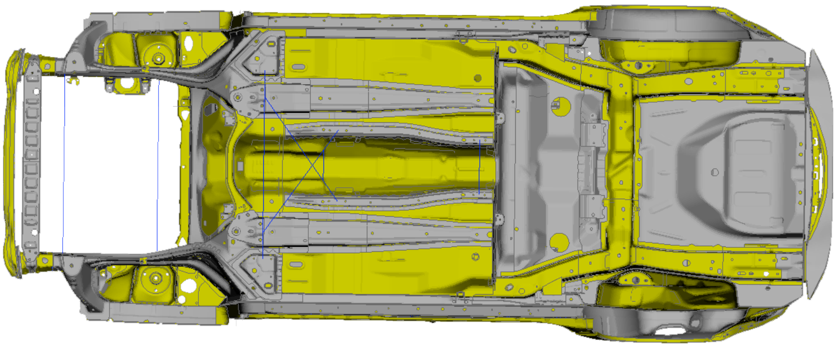

Figure 3.9: *BIW underbody reinforcements*

Table 3.6: Cases for validating the FEM model

Case	**Front trans.**	**Front long.**	**Rear trans.**	**Rear long.**	**Rear Cross**	**Underbody**
Case 1	ON	ON	ON	ON	ON	ON
Case 2	ON	OFF	ON	ON	ON	ON
Case 3	ON	ON	ON	OFF	ON	ON
Case 4	OFF	ON	OFF	OFF	OFF	ON

3.2.9 Load Cases FEM

Two load cases are used in the FEM simulations: bending stiffness and torsional stiffness. Both of them are performed using the software Nastran and by following the standards presented in this section.

Torsional stiffness test A value of global torsional stiffness required both for the CarMaker model and for the component to sub-system relation in terms of body stiffness is found by performing a torsional stiffness test of the BIW using FEA with the sofware Nastran. The body is constrained at the rear top mounts in the degrees of freedom shown in Figure 3.10. Torque is applied as a force couple (Fz=+-3.0kN) at the front spring towers. To prevent the body from bending, the front bumper beam is constrained in DOF 2 & 3. The torsional stiffness is defined as the applied torque divided by the twist angle of the body calculated from the z-deflections at the force application points. To get an accurate value of global torsional stiffness (unaffected by local stiffness/deformation) the constrained points and the points where the force is applied are modeled as stiff components i.e. the stiffness of the BIW is reinforced in those areas to prevent the local deformation.

Three point bending test The value for global bending stiffness used by the CarMaker model and used for the study of the influence of each bar in the BIW stiffness is calculated with the results from a three point bending test. FEA is used with the software Nastran in order to perform the analysis. In this test the body is constrained in the damper mounts according to the DOF shown in Figure 3.11 and a load of -3.0kN is applied at a stiffened part in the middle of the underbody.

3.2.10 Design of experiment FEM

The scheme for the process flow in the multi-objective optimization tool modeFrontier is shown in Figure 3.12. The design of experiment is similar to the process built for the Adams simulations previously mentioned in Section 3.2.5. In this case the scheme connects the FEM simulation tool MSC Nastran, an internal post-processing process in modeFrontier and the scripts made to change the inputs and read the outputs.

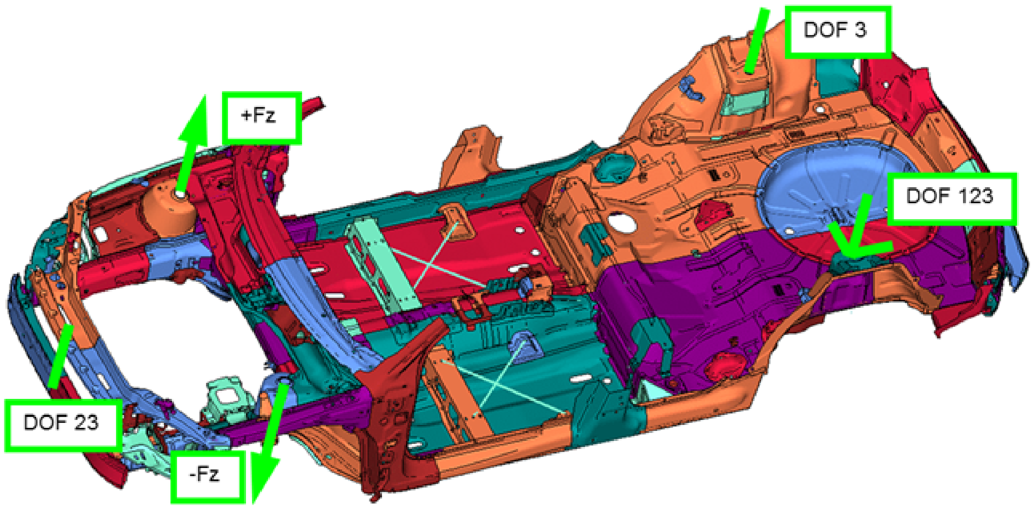

Figure 3.10: *Torsional stiffness test*

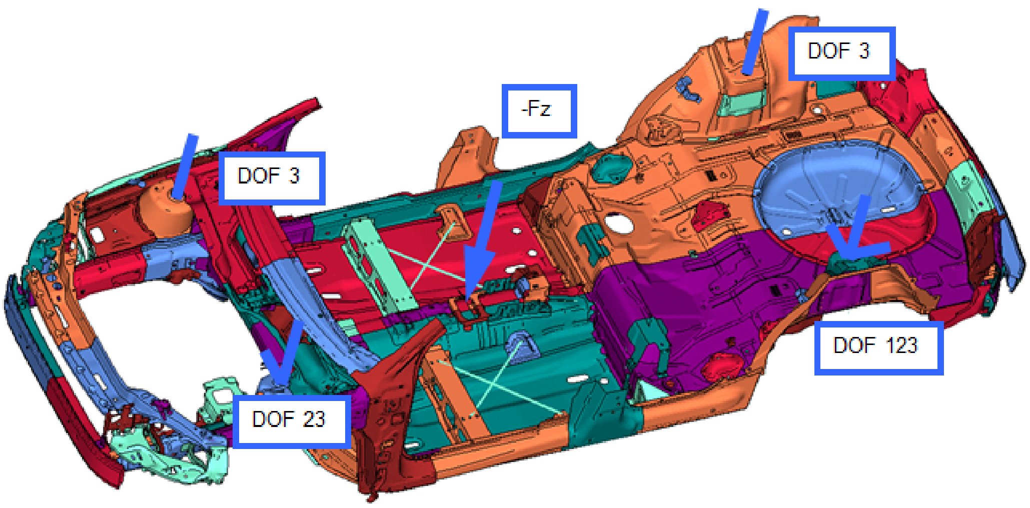

Figure 3.11: *Three point bending test*

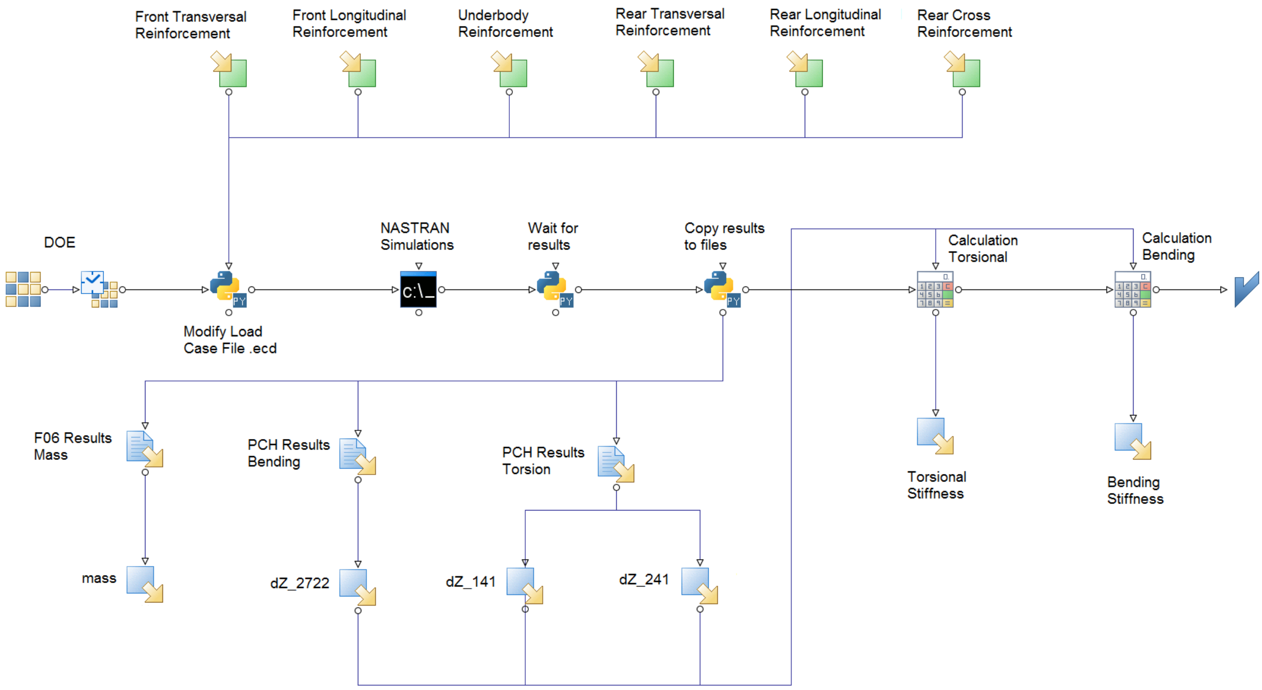

Figure 3.12: *DOE for FEM simulations*

The inputs are modified according to a full factorial DOE in order to cover the whole design space. The groups used are the same as for the Adams simulations explained in Section 3.2.7. The bars reinforcing the body are then activated or deactivated for each simulation dependent on which combination is going to be simulated. This is done by modifying a .ecd file which contains the load cases, boundary conditions and parts of the model. The "Modify Load Case File .ecd" script is then including or not including the required group of bars for the corresponding simulation. This action is made both for the torsional stiffness load case and for the bending stiffness load case. Next step in the flow is the call for Nastran in order to run the simulations. In order to save time, the analysis is done remotely on a cluster instead of locally, allowing the DOE to run in significantly less time. After the "Nastran Simulations" node a Python script ("Wait for results") runs in order to pause the process flow until the simulations are finished. Once the analysis is completed the results are copied to the modeFrontier environment where torsional stiffness and bending stiffness are calculated.

3.2.10.1 Post processing in modeFrontier

Once the metrics are calculated the data is stored for each combination and then post processed within modeFrontier. This is done with the Overall Student Chart described in Section 2.6.1.2, which calculates the effect of an input factor on an output variable. The same method was used for the Adams simulation results.

3.3 Subsystem to vehicle relation

This section describes the CarMaker model and how it was used to relate subsystem to vehicle dynamics characteristics i.e. the relation between compliance values & global body stiffness to handling, ride and steering characteristics.

3.3.1 CarMaker Model

This section describes how CarMaker models different subsystems in the vehicle with focus on body stiffness. The CarMaker model compared to the steady state bicycle model described in Section 2.4 allows transient maneuvers to be performed and is also including bending and local stiffness compared to only torsional and lateral stiffness which was included in the bicycle model. The methodology used for modelling global and local body stiffness in CarMaker is explained in the following paragraphs.

3.3.1.1 Global body stiffness model

Simulating a flexible body in CarMaker can be done by dividing the body into two parts (two rigid bodies: body A and B, corresponding with front and rear part of the vehicle as seen in Figure 3.13) and a connection joint between these two rigid bodies. This is an inbuilt function in the software CarMaker and more information about the model can be found in [12]. The joint has two degrees of freedom; torsion and vertical bending of the vehicle body, where both stiffness [Nm/deg] and damping [Nms/deg] can be varied [12]. One of the limitations of this model is that global lateral stiffness can not be taken into account in this joint. Instead, local lateral stiffness coefficients will be used; this is further explained in Section 3.3.2.3. When splitting the vehicle body into body A and body B the mass and inertias has to be defined for each body. For this CarMaker offers two alternatives, either split the mass and inertia equally in the two bodies (positions of the masses will be arranged so that total mass, inertia and CoG will remain in their original static locations for a vehicle placed on level ground), or the body properties for both bodies (mass, inertia and CoG) are defined independently of each other [12]. If the second option is chosen, the joint location can be altered in x, y & z direction [13]. The first option is selected in this study and the body parametrized with values from the Adams S60 model described in section 3.2.1. The position of the joint is based on the relative location of the two body masses [12].

The joint's spring and damper elements were parametrized with results from FEA simulations. This parametrization will be described in Section 3.3.2.3.

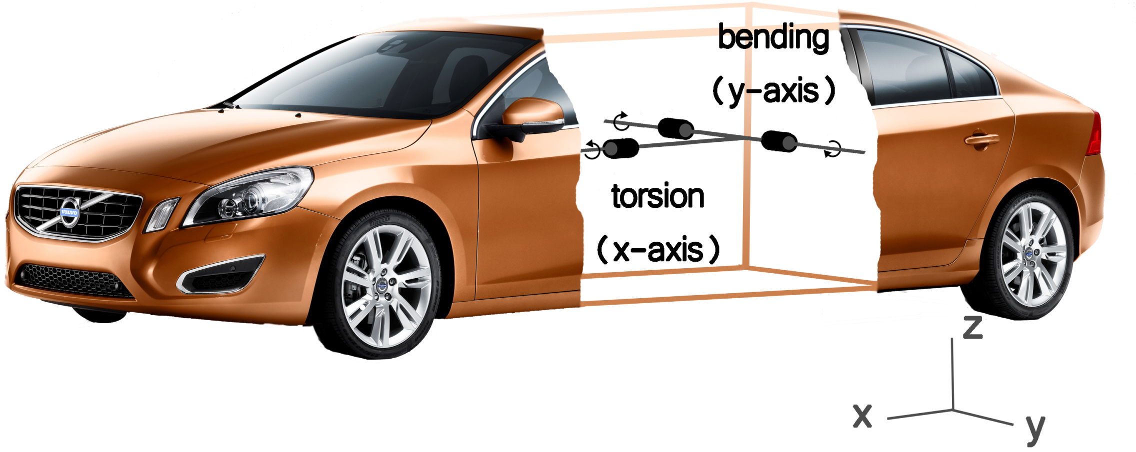

Figure 3.13: *CarMaker body stiffness model*

3.3.1.2 Local stiffness model

Kinematics & compliance values describes suspension geometry and deflections with respect to vertical wheel travel, steering angle and driving forces. The K&C values are used to model local stiffness of the body. Below follows a short description of how the CarMaker K&C model works.

Kinematics

To describe the wheel center movements with respect to a certain input (wheel travel or steering angle) CarMaker uses a kinematics and compliance model. The model offers two options, to use a linear model or a non-linear model. The linear model can be either a 1, 2 or 3 degrees of freedom model, where the degrees of freedom are represented by wheel travel, steering rack displacement or opposite wheel movement [13]. For front, either 2 or 3 degrees of freedom can be used. These two options are dependent on if the kinematics should rely on wheel travel and steering rack displacement or wheel travel, steering rack displacement and movement of the opposite wheel. For the rear either a 1 or 2 degrees of freedom kinematics model can be used, either if the kinematics should only be affected by wheel travel or by wheel travel and movement of opposite wheel. For the linear models the variation in the following variables: wheelbase, track, wheel travel, camber, spin angle, toe, spring length, damper length, buffer length and stabilizer length is described with one or more coefficients based on the number of degrees of freedom [13]. The coefficients are representing a linear relationship between input (for example wheel travel) and output (wheel translation and rotation).

For the non-linear model an external file contains all the kinematics data. In this case absolute values for all variables are collected for a number of steps for each chosen degree of freedom (wheel travel, steering rack displacement and opposite wheel movement). All absolute values are stored in a look up table which CarMaker uses when simulating. The non-linear kinematics model offers the best accuracy, therefore it was chosen in this study in favour of the linear models. For the front axle wheel travel and steering rack displacement were considered, while for the rear only wheel travel was considered. This is due to that effects from opposite wheel travel is only needed for a rigid or a semi-rigid axle.

The look up table contains 61 bounce levels for the front axle kinematics table. At each of these bounce levels 11 steps in steering motion are used. The rear axle kinematics table consists of only 61 bounce levels and no levels for steering, due to that the rear axle is a non steered axle. All kinematics values are produced with the MSC Adams model and MSC Adams K&C Simulations (the exact procedure of how to extract the values is presented in Section 3.3.2).

Compliance

Compliance is describing how the wheel center translates and rotates when forces and torques are applied at the wheel center. This is due to the flexibility in body, subframe and suspension components. Modelling compliance in CarMaker can be done in two different ways, with linear coefficients or with a look up table with absolute values [13]. For both cases the model can be dependent on both force/torque applied and on bounce level [13]. Load cases include: Fx (force in x), Fy (force in y), Tx (torque around x), Ty (torque around y) and Tz (torque around z). The affected variables are tx, ty, tz, rx, ry and rz; these variables represent respectively: wheel base variation, track variation, wheel travel variation, camber variation, spin angle variation and toe angle variation. The coefficients/absolute values describe how the wheel center translates and rotates for a certain force/torque at a certain bounce level. For both front and rear axle absolute values are used and only dependency between the previous mentioned variables and applied force/torque is considered (different compliance values at different values for wheel travel height is not taken into account). The model also neglects the effect that a force applied on one side has on the translations and rotations of the wheel center on the opposite side. The resolution in the applied force/torque was set to 61 steps.

3.3.2 Parameterization of CarMaker model

This section describes the parameters used in the Volvo S60 CarMaker model for suspension kinematics, compliance, global body stiffness and for suspension components. Special attention must be given to the body stiffness parametrization section, since it explains how the CarMaker model is capturing local and global body stiffness.

3.3.2.1 Suspension parametrization

This paragraph describes how K&C measurements were parametrized in the model built in CarMaker. It should be mentioned as well that the compliance values are used for taking into account lateral stiffness and local stiffness of the BIW and this will be explained in the Section 3.3.2.3, Body stiffness parametrization.

Kinematics and compliance look up tables

To be able to accurately describe suspension kinematics and compliance behavior in the CarMaker vehicle model, K&C simulations were performed with the S60 Adams model presented in Section 3.2.1 in order to find the parameters describing wheel center motion with respect to input forces/torques, vertical wheel travel and steering motion. These parameters were then used to parametrize the kinematics and compliance look up tables described in Sections 3.3.1.2 & 3.3.1.2.

In total 9 kinematics and compliance tests described in Section 3.2.4 were used in the Adams simulations. From the compliance tests performed, only: "Force in x", "Force in y", "Torque around x", "Torque around y" and "Torque around z" were used to parametrize the compliance model for front and rear axle due to that these load cases apply the force at the wheel center. This load application point is chosen based on the fact that the CarMaker vehicle model requires forces/torques around this point and the CarMaker tire model calculates forces/torques at the wheel center (see Section 2.8).

To investigate the suspension characteristics two kinematics tests were performed: parallel wheel travel and single wheel travel. Only parallel wheel travel was used to parametrize the kinematics model in CarMaker. The data gathered from this test contains the relation between wheel travel and: wheelbase, track width, wheel travel, camber angle, spin angle & toe angle. Spring length is also needed in the kinematics model, this variable is equal to the wheel travel with the assumption that the spring sits vertically above the wheel center (the value for spring stiffness is therefore changed to a value for wheel rate). Damper length is also extracted and anti roll bar movement is assumed to be the same as the vertical wheel center movement. Data describing spring, damper and anti roll bar movement in relation to vertical wheel travel is described, but to prevent the suspension from reaching its mechanical end positions bump stops are installed. These bump stops are progressive and they have higher stiffness than the springs. The relation between wheel travel and displacement of the bump stops is approximated with damper movement in the CarMaker model.

3.3.2.2 Suspension components

Characteristic values used to parametrize dampers and bump stops are picked from the S60 Adams model described in Section 3.2.1. Values for anti roll bar and spring stiffness are calculated from the K&C simulation results (see Section 3.2.4 for a description of MSC Adams K&C simulations).

3.3.2.3 Body stiffness parametrization

To model local and global stiffness the built CarMaker model uses compliance values together with stiffness values of the joint connecting the front and the rear part of the vehicle. The joint used to model body stiffness captures torsional and bending stiffness whilst the compliance values capture local stiffness of the front and rear axle together with lateral stiffness. In total eight parameters groups are used for modeling body stiffness in CarMaker. These groups are shown as eight different load-cases in Figure 3.14. Torsional and bending stiffness are modeled according to the two load cases described in the Section 3.2.9, and they are shown in Figure 3.14 as the blue and orange torque arrows around y-axis and x-axis in the middle of the body. Lateral stiffness is modeled with lateral compliance values corresponding to the grey and yellow forces in Figure 3.14, which are representing two lateral loads applied on the front and rear wheel center. Local stiffness is modeled with toe and camber compliance for both front and rear axle and it is represented in Figure 3.14 by two blue torques around z-axis and y-axis in the front axle and green and light brown torques around z-axis and y-axis in the rear axle.

Compliance groups

The CarMaker compliance model described in Section 3.3.1.2 includes five load cases: force in x, force in y, torque around x, torque around y and torque around z. These five load cases affect translation and rotation of the wheel center (translation in x, translation in y & translation in z) and rotation (rotation around x, rotation around y & rotation around z). The look up table consists of 61 levels for each variable (3 translations & 3 rotations), meaning 3660 values. Instead of changing individual values, coefficients which are multiplied

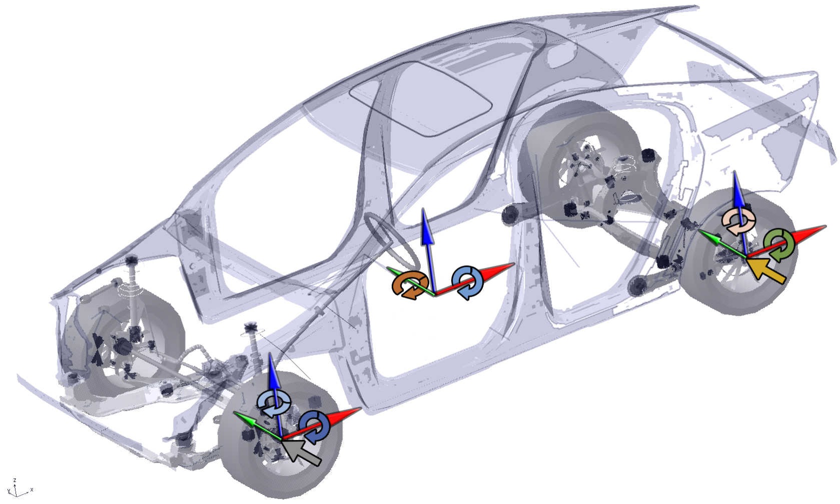

Figure 3.14: *CarMaker model load cases*

Table 3.7: Compliance groups

Load case	**Translations**	**Rotations**
Force in x	tx, ty, tz	rx, ry, rz
Force in y	tx, ty, tz	rx, ry, rz
Torque in x	tx, ty, tz	rx, ry, rz
Torque in y	tx, ty, tz	rx, ry, rz
Torque in z	tx, ty, tz	rx, ry, rz

with the individual values are used as parameters. These 60 parameters represents local stiffness of the front and rear axle together with lateral stiffness. This many parameters consequently leads to long simulation times if all combinations should be investigated (full factorial DOE). To reduce simulation time, groups which combine the coefficients describing compliance were created. These groups are based on the load cases used in the CarMaker compliance model (see Table 3.7). Each group consequently consists of six parameters, which describes compliance in three rotations and three translations. The 6 parameter values change together and they are based on what load case is applied to the vehicle body. Taking this into account it should be mentioned that even though the 6 DOF of the center of the wheel are parametrized together in the same load case, each force or torque application will affect in a greater way 1 of the 6 DOF. For instance, the lateral force load case (Force y) will affect the translation in y compliance value more than any other wheel-center motion value.

The groups are created to correlate load case to vehicle dynamic characteristics rather than wheel angles to vehicle dynamic characteristics due to that the body stiffness influence on vehicle characteristics is investigated. In total six compliance groups are used as it was described in the beginning of this section. Three groups are used for modeling body stiffness in the front part of the vehicle and another three are used for modeling the rear body stiffness, as it is shown in Figure 3.14. Summarizing, the six groups are used for modeling lateral and local stiffness in CarMaker based on compliance tests. These groups are Lateral Compliance Front and Lateral Compliance Rear for lateral stiffness. For local stiffness the groups are Toe Compliance Front, Toe Compliance Rear, Camber Compliance Front and Camber Compliance Rear. These groups will be named indistinctly as Compliance or Stiffness groups since the physical meaning is the same.

Finite Element Analysis

Finite Element Analysis is performed in order to capture torsional body stiffness and bending body stiffness. These parameters for stiffness are not completely taken into account in the K&C measurements since the body is clamped in the middle section when those tests are performed (see Figure 3.15). The borders between where K&C and respectively the FEA simulations will account for body stiffness are somewhat diffuse, for example the roof structure will not be clamped during the K&C tests while the underbody in the middle area is in fact, clamped. For this reason the values for torsional and bending stiffness are going to be considered as global values of the body properties and calculated based on standard procedures described in Section 3.2.9. Torsional stiffness tests and three point bending tests are performed in CAE in order to calculate values for both static properties. Furthermore only static stiffness tests are performed due to that handling, steering & primary ride events operates at a frequency below 20Hz; and the first body eigen mode is located around 40Hz.

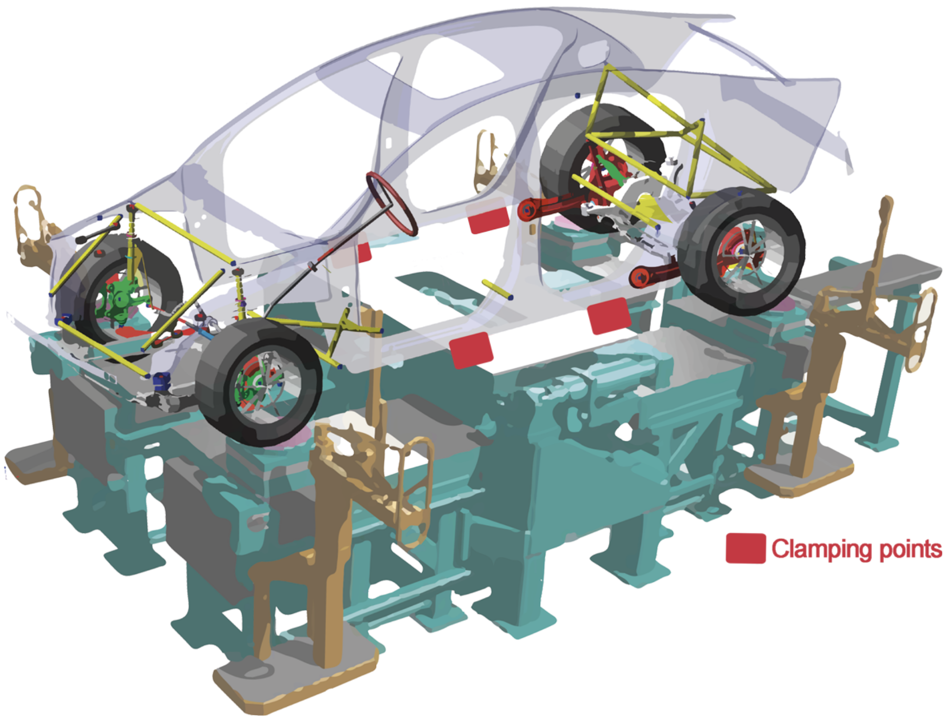

Figure 3.15: *SPMM rig clamping*

3.3.3 Validation of the model

The first part in building a CarMaker model is acquiring the data needed to parametrize the model. In this case the model was built with data from a MSC Adams S60 model described in Section 3.2.1, together with results from K&C simulations in MSC Adams performed with the S60 model. Consequently it is important that results from the S60 Adams model are validated.

It is important that the input data to the CarMaker model is accurate and corresponds to the physical vehicle with which it will be verified. The input data used in the kinematics and compliance models were therefore compared to data from physical K&C tests, to see if they produce the same absolute values and if the correlation between a flexible body to a reinforced body is the same in the CAE environment as in the physical tests environment.

To ensure that the vehicle model was implemented correctly and that it is producing reasonable and accurate results it was verified and validated as well. In order to verify the model, output metric values were checked for reasonable results for various input parameters in different driving maneuvers. The model was also validated with data from physical tests to ensure the accuracy of the model. This was done by performing a set of standard maneuvers with the simulation model and compare the results to data gathered from objective physical tests.

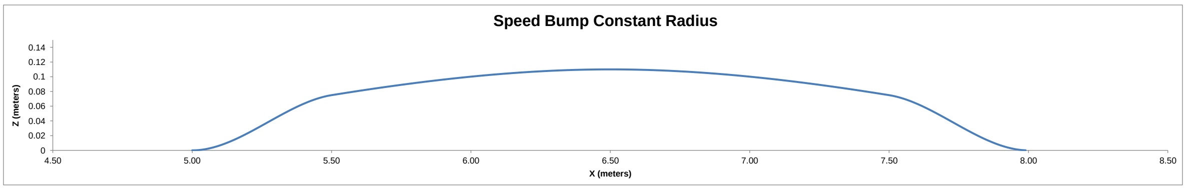

Figure 3.16: *Bump for maneuver Constant radius with bump*

3.3.4 Simulations and load cases

To objectively evaluate the vehicle dynamics characteristics of the vehicle, three categories are used: handling, steering and ride. Fourteen maneuvers within those characteristics were implemented and performed in IPG CarMaker. These maneuvers are:

- Brake in turn
- Constant radius
- Constant radius with bump
- Constant radius with angled bump
- Frequency response
- High g swept steer
- Low g swept steer
- On centre
- Primary ride
- Sine with dwell
- Step steer throttle release in turn
- Throttle release in turn
- Yaw stability
- Yaw stability - rough road

3.3.4.1 Brake in turn

Brake in turn is designed to evaluate vehicle directional response and change in steady state cornering characteristics when brakes are applied while turning. The test procedure is similar to ISO 7975:2006 "Brake in a turn". Side-slip and yaw rate delta values are used to evaluate abruptness and under/oversteer behaviour.

3.3.4.2 Constant radius

Constant radius evaluates steady-state characteristics of the vehicle, from normal turning up to maximum lateral acceleration. The test is performed similarly to "Steady-state circular driving behaviour" in ISO 4138:2012. Roll, pitch, lateral acceleration and under steer gradient is calculated in order to investigate steady state vehicle characteristics, progressivity, roll and pitch behaviour.

3.3.4.3 Constant radius with bump

Constant radius with bump is performed similarly to "Constant radius" but at constant speed and with a bump positioned transversally on the track. The transient condition occurring when hitting the bump is analyzed. The bump geometry is presented in Figure 3.16.

3.3.4.4 Constant radius with angled bump

Constant radius with angled bump is performed similarly to "Constant radius with bump" but with the bump positioned at an angle to the track. The transient condition occurring when hitting the angled bump is analyzed.

3.3.4.5 Frequency response

Frequency aims to asses vehicle turning performance in the linear range, both transient and steady state. The steering input is in the form of a sine wave were the frequency is linearly reduced. It is a open loop test and the procedure is similar to that of "Random input" in ISO 7401:2011. Phase lag and roll is used to asses response and roll behaviour.

3.3.4.6 High g swept steer

High g swept steer is a open loop maneuver performed in order to evaluate turning performance at steady state. The steering wheel angle is linearly ramped up to a pre-set value; the procedure is similar to that in "Pulse input" in ISO 7401:2011. Under steer gradient and steering wheel torque is used to evaluate torque feedback and response.

3.3.4.7 Low g swept steer

Low g swept steer is similar to "High g swept steer" but is conducted at a higher speed and lower level of lateral acceleration. Response and torque feedback is analysed with steering wheel angle and torque.

3.3.4.8 On center

On center evaluates steering performance for low lateral accelerations and steering input frequencies. It is an open loop maneuver with a continuous sinusoidal steering input. It is conducted at different velocities and lateral acceleration levels, in order to simulate straight ahead correction performance and performance on roads with linked right and left hand corners. The test procedure is similar to that of "Continuous sinusoidal input" in ISO 7401:2011. Yaw gain and steering wheel torque are evaluated.

3.3.4.9 Primary ride

Primary ride aims at investigating low frequency movement of the vehicle with aspect of road irregularities (small and large). Comfort, balance and vehicle control are investigated.

3.3.4.10 Sine with dwell

Sine with dwell is designed to test vehicle transient response behaviour. The test procedure is similar to "Sinusoidal" test in ISO 7401:2011. The maneuver is performed with a sine wave steering input with dwell. Time lags, lateral acceleration peaks and yaw gain are calculated.

3.3.4.11 Step steer throttle release in turn

Step steer throttle release in turn assesses vehicle behaviour when a step steer input and a braking input is applied simultaneously in a steady state turn. To evaluate the directional stability of the vehicle the difference in side-slip and yaw rate during the maneuver and at steady state is calculated.

Table 3.8: Body stiffness groups and load cases

Input Group	Load Case
Toe Compliance Rear	Torque Z
Lateral Compliance Rear	Force Y
Camber Compliance Rear	Torque X
Toe Compliance Front	Torque Z
Lateral Compliance Front	Force Y
Camber Compliance Front	Torque X
Torsional stiffness	Torsional kts
Bending stiffness	Three point bending test

3.3.4.12 Throttle release in turn

Throttle release in turn evaluates change in vehicle behaviour (directional stability) when throttle pedal is released during steady state cornering. The test procedure is similar to "Power-off reaction of a vehicle in a turn" in ISO 9816:2006. Change in side-slip and yaw rate from the steady-state condition is analyzed.

3.3.4.13 Yaw stability

Yaw stability is a test with a steering step input, similar to the "Step input" maneuver described in ISO 7401:2011. The vehicle is driven straight and a rapid steering input is applied up to a preselected steering wheel angle, where it is kept until the vehicle reaches steady state. The test assesses transient vehicle behaviour. Values on maximum side slip and yaw rate are calculated.

3.3.4.14 Yaw stability - rough road

Yaw stability with waves is performed similarly to "Yaw stability". It is not performed on a flat surface but at a surface containing small irregularities.

3.3.5 Design of experiment

The scheme for the Design of experiment for relating subsystem and vehicle characteristics in the multi-objective optimization tool modeFrontier is shown in Figure 3.17. The experiment is connecting the tool CarMaker, the post processing tool Sympathy for Data and the Python scripts needed for changing and reading the data.

The inputs of the workflow are changed according to a full factorial DOE. As presented in Section 3.3.2, eight groups and two levels (on/off) were used. The compiled information of each group and load case can be seen in Table 3.8. ModeFrontier generates the full factorial combination of the inputs and sends the values to the node "CarMaker Full Vehicle Simulations". This node is a Python script which has two missions. Firstly, it is the node responsible of changing the parameters in the CarMaker simulations. The test run is modified so the body stiffness is changed according to the input values for each modelled group. Secondly it executes the CarMaker software and starts the simulations through a TCP connection and a TCL script. When the simulations are done, the results are stored in the standard CarMaker format and they are read by Sympathy for Data in the "Sympathy for Data Post-Processing" batch node. Once the results are post processed, they are stored in a CSV file which is read by a Python script and sent out to the modeFrontier environment. The output metrics are grouped into maneuvers, but also into DNA for vehicle dynamics characteristics. This will allow for optimization of a specific group of vehicle dynamics properties in further work.

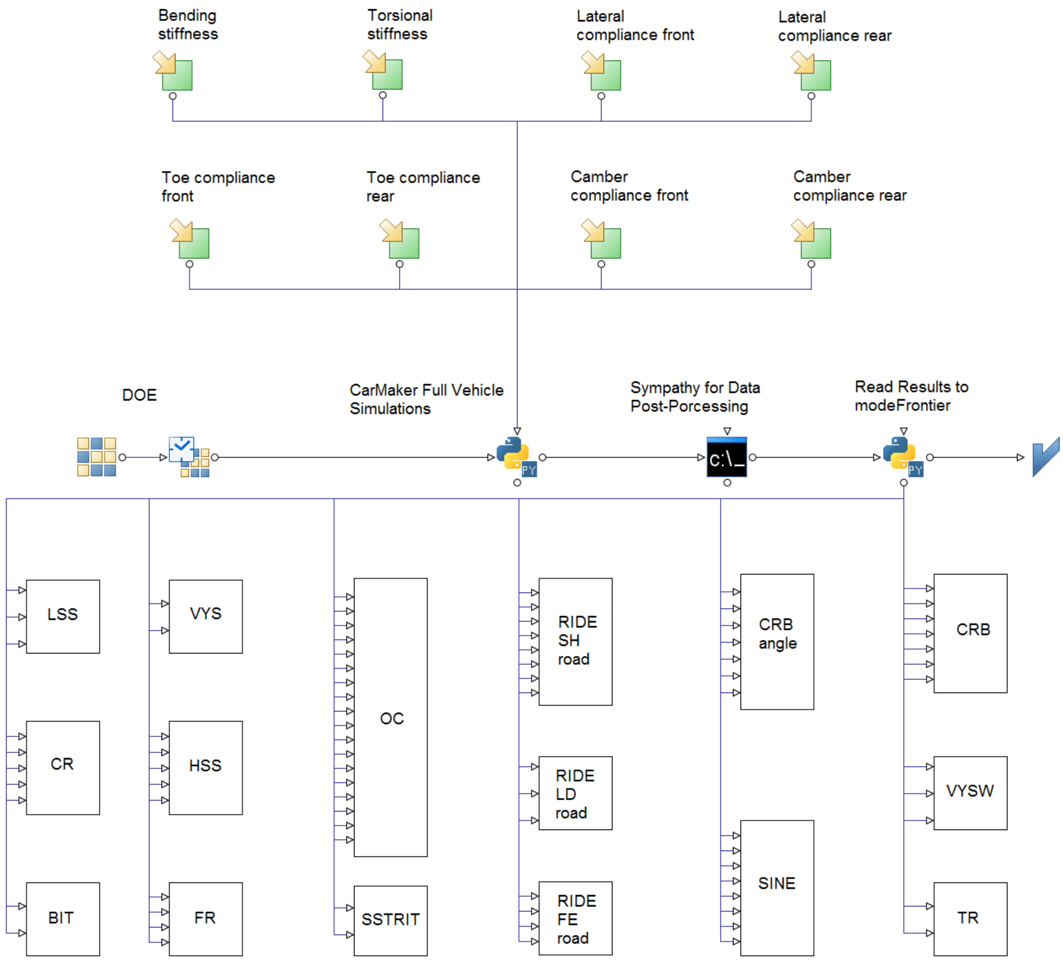

Figure 3.17: *ModeFrontier scheme for CarMaker simulations*

3.3.5.1 Sympathy for Data post processing node in modeFrontier flow

Sympathy for Data is used in the modeFrontier scheme to post process the raw data from CarMaker and output metrics used to access vehicle performance. To remotely run Sympathy for Data a batch node called "Sympathy for Data Post-Processing" was created (see Figure 3.18), this node contains a batch script which executes a python script, which in turn start Sympathy for Data work flows.

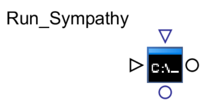

Figure 3.18: *Sympathy for Data node in modeFrontier*

Sympathy for Data is an open source program that offers good overview through the different parts of the data processing. An example flow showing the different steps is presented in Figure 3.19. The first step in the flow is to adapt the CarMaker data to a standard format. In order to do this a subflow called "Read Result Files" was created. The intention of this subflow is to change units & axis coordinate systems to adapt data from CM into a standard format in order for the post processing flows to understand and automatically read the data from CarMaker (see Appendix 7). In the second step "Make and select wanted channels" the channels needed for the metrics calculations were created. The third step "Find Event" finds the time window in which the maneuver was performed and removes all data outside of this window. Then the data is filtered, and finally the metrics are calculated and exported to a Excel sheet. Data channels used to calculate the required metrics are presented in Appendix 7.

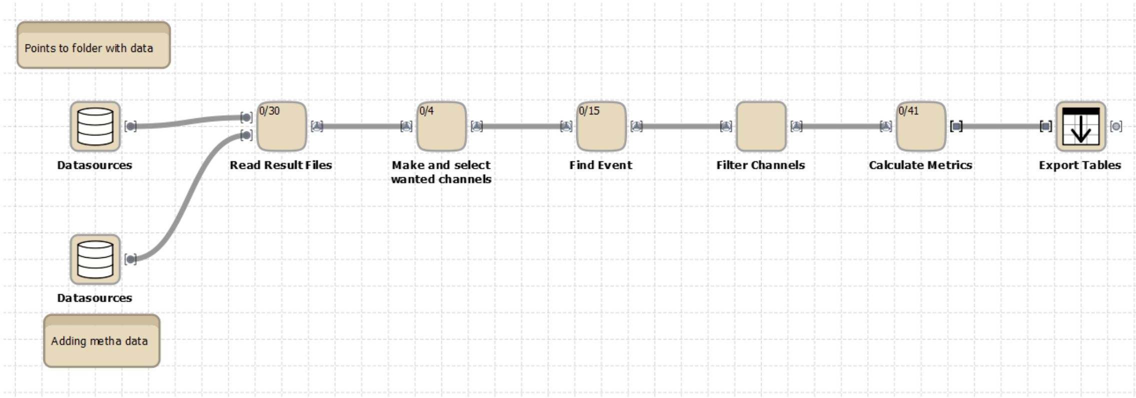

Figure 3.19: *Sympathy for Data - Example flow*

3.3.5.2 Post processing in modeFrontier

The last node in the modeFrontier process flow seen in Figure 3.17 reads the metrics values, which were calculated and stored in excel sheets in the previous node ("Sympathy for Data Post-Processing"). This node outputs these metrics values into modeFrontier. After completion of all combinations stated by the DOE, all metrics data stored for each combination was post processed within modeFrontier. This was done with the Overall Student Chart described in Section 2.6.1.2, which calculates the effect of an input factor on an output variable.

Post processing of modeFrontier data in Sympathy for Data

Due to that the modeFrontier project contains 83 output variables and subsequently 83 times 8 values of effects, this data has to be further post processed and sorted. The task was performed with a stand alone Sympathy for Data flow. The flow calculates the percentage change of each metrics with a flexible body as baseline. It also calculates the metric effect value normalized against each metric target range. This is done in order to give an idea of how the change in the metric will feel in the actual vehicle rather than representing a percentage change for all the measurements. The target range is independent for each metric and it represents the tolerance range of each metric value for a specific vehicle. These values are then sorted after either: mean metrics absolute change for all groups or absolute metrics change for each group. This is done in order visualize in an easier way the information in the data.

3.4 Physical Testing

Physical testing is utilized in this study mainly for model validation. K&C and torsional stiffness measurements validate the component - subsystem relation and objective testing correlates the subsystem to vehicle relation level. The methods used for performing the tests are explained briefly in this section.

3.4.1 K&C measurements

Physical kinematics and compliance tests were performed in order to accurately measure suspension and steering characteristics of the physical test vehicle. These tests were performed with the Suspension Parameter Measurement Machine (SPMM) from Anthony Best Dynamics Ltd, see Figure 3.20. The SPMM is a test

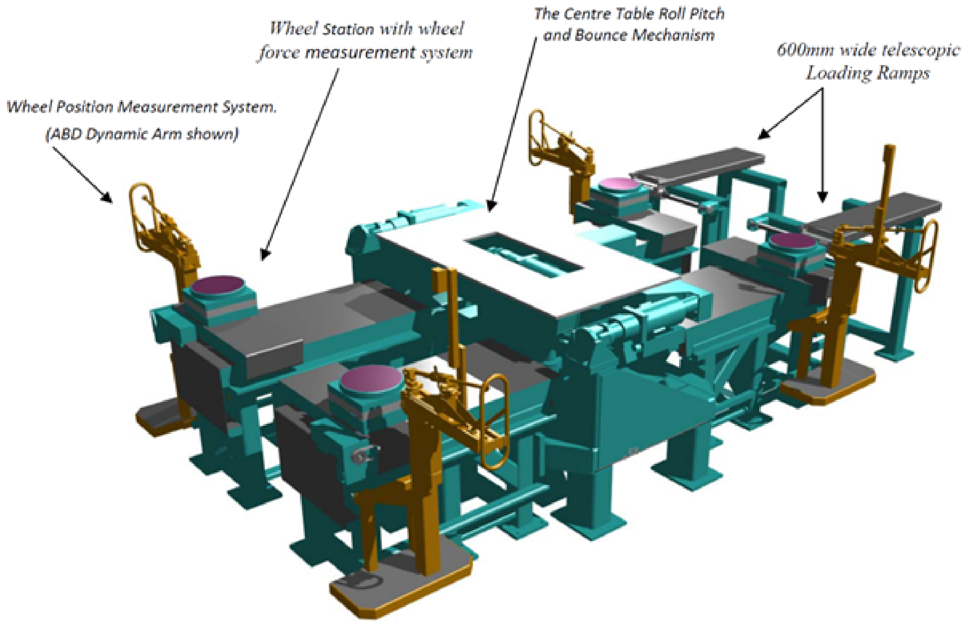

Figure 3.20: *SPMM rig [18]*

machine that uses electro mechanical actuators to move the body relative to the wheels allowing the performance of K&C analysis.

3.4.2 Torsional Stiffness measurements

Torsional stiffness measurements are performed in a test rig composed of four post, one for each wheel. The desired torque is applied to the body through wheel forces. The wheels are moved individually so the desired moment is generated by lifting the two diagonal wheels and lowering the other two. Then transducers and measurement equipment acquired the required data for the torsional stiffness calculation: forces values and angles.

3.4.3 Objective Testing

Objective testing is performed at HPG where the same steering, handling and ride maneuvers simulated in CAE are performed in a real track. Some of the equipment used in these tests can be seen in Figure 3.21. Steering robots control the steering wheel angle. These devices are also equipped with a torque sensor. An inertial platform measures acceleration, speed and position of the vehicle. Some of the maneuvers required controlled pedals for braking and accelerating. However for the rest of test procedures the driver performance is also evaluated and in case that the driver performance does not fulfill the maneuver standard requirements, the test is repeated in order to achieve an objective measurement. In case of ride maneuvers some more equipment is needed like accelerometers located in other positions of the car as well as string potentiometers. It should be mentioned that the objective testing minimizes the driver influence in the measurements but obviously real testing is highly affected by the ambient and track surface conditions. Data coming from these tests should be analyzed carefully.

3.4.4 Subjective Testing

Subjective testing is performed in order to get a feeling of the vehicle dynamics behavior of the car. The car is tested under different maneuvers and conditions and a report is fulfilled pointing out the changes between the different vehicle configurations. The subjective testing is carried out by professional test drivers and the comments are analyzed together with the rest of the data. It is intended to match the subjective results with

Figure 3.21: *Instrumentation for objective testing, courtesy of Volvo Cars*

the objective measurements and CAE analysis. Some example comments for previous subjective analysis for vehicles with different body stiffness are:

- The car feels more solid.
- It handles speed bumps more controlled.
- Premium feeling.
- Less harshness feeling.

The comments show that the vehicle performance is increasing when increasing the body stiffness. They suggest a more controlled and responsive car. And as stated in the Introduction chapter of this report, this is one of the starting points of the following study: subjective assessment shows an improvement in vehicle dynamics characteristics while CAE analysis does not show a significant change.

4 Results

This chapter presents the results obtained in the study. Component to subsystem results are presented first, coming from the Adams K&C simulations and the Nastran stiffness analysis. Later on the subsystem to vehicle results are presented meaning the full car simulations performed in CarMaker. The next results, component to vehicle, show the full vehicle simulations performed in Adams. Finally the correlation with physical testing is presented in order to evaluate the accuracy of the models and methodology used.

4.1 Component to subsystem

This section presents results from both the MSC Adams model and the FEM model and it contains results connecting component characteristics to subsystem characteristics. The Adams model described in Section 3.2.2 is used to capture the effect of lateral and local stiffness from adding stiffening bars to the BIW, the resulting groups seen in Figure 4.1 are: Lateral Stiffness - Front, Lateral Stiffness - Rear, Camber Stiffness - Front, Camber Stiffness - Rear, Toe Stiffness - Front & Toe Stiffness - Rear. In order to also capture the relation between stiffening bars and global torsional and bending stiffness values, results from the FEM model described in Section 3.2.6 are also included in Figure 4.1; these results are represented by two groups: Global Torsion Stiffness & Global Bending Stiffness. The groups connected to lateral and local stiffness displayed in Figure 4.1 were chosen based on effect of the bars on each compliance set of parameters. Compliance values used for selecting groups are attached in Appendix 2 & 3. A positive value in the percentage change means that the stiffness value is increasing when adding reinforcements to the BIW.

As it can be seen in Figure 4.1 all individual bars are colour coded according to within what group they are included: Front Longitudinal, Front Transversal, Rear Cross, Rear Longitudinal, Rear Transversal or Underbody. For further information on how the groups were created, see Section 3.2.2.2 & 3.2.7.

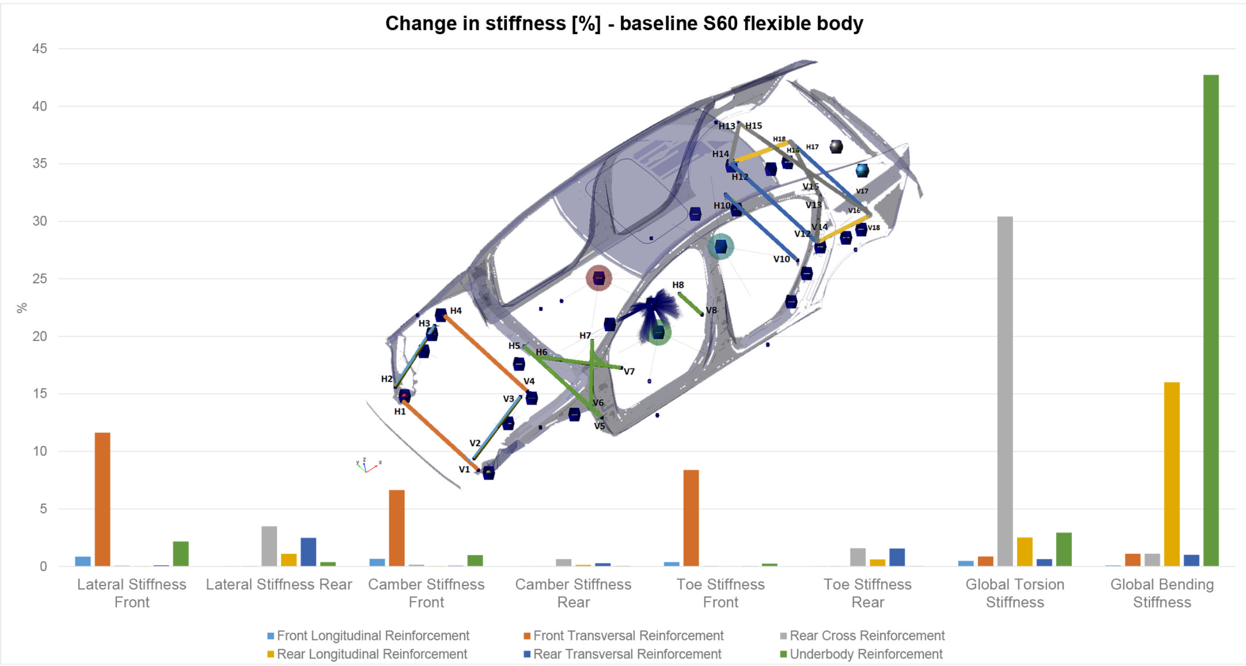

Figure 4.1: *Effect of stiffening bars*

The results in Figure 4.1 show how each stiffener affects compliance values, a table containing all absolute values is attached in Appendix 4. It can be seen that Front Transversal, Rear Cross, Underbody and Rear Longitudinal are the main groups of bars affecting the stiffness of the BIW. Global stiffness values are affected by the Rear Cross, Underbody and Rear Longitudinal bars. The bars located under the middle part of the car together with the Rear Longitudinal bars largely affect global bending stiffness whilst the Rear Cross is affecting global torsional stiffness. Regarding lateral and local stiffness values: they change to a lesser extent than the global stiffness values, with Front Transversal showing the largest effect on the lateral and local stiffness parameters. These results also show that bars from the groups Front Longitudinal, Rear Longitudinal and Rear Transversal barely has any effect on local or global compliance values.

4.2 Subsystem to vehicle

This section presents the results from the CarMaker model simulations described in Section 3.3.1. It relates subsystem characteristics to vehicle dynamics characteristics. This relation can be translated into the relation between K&C and global stiffness with handling, ride and steering characteristics. In order to make this connection simulation groups containing compliance values related to load cases were created. These compliance groups chosen for the evaluation of vehicle dynamics characteristics with respect to local & global stiffness is described in Section 3.3.2.3 and displayed in Table 4.1. Figure 4.2 illustrates which load case each compliance group represents and contains colour coding matched with the bar charts presented in Sections 4.2.1 & 4.2.2. In other words, these results present the relation between the local stiffness, lateral stiffness, torsional stiffness and bending stiffness of the BIW; and the vehicle dynamics behavior of the vehicle. A positive value in the percentage change means that the metric value is increasing for increased body stiffness, whilst a negative value means that the metric value is decreasing for increased body stiffness.

Table 4.1: Body stiffness groups and load cases

Compliance Group	**Load Case**	**Colours**
Toe Compliance Rear	Torque Z	Pink
Lateral Compliance Rear	Force Y	Yellow
Camber Compliance Rear	Torque X	Green
Toe Compliance Front	Torque Z	Light Blue
Lateral Compliance Front	Force Y	Grey
Camber Compliance Front	Torque X	Dark Blue
Torsional stiffness	Torsional kts	Blue
Bending stiffness	Three point bending test	Orange

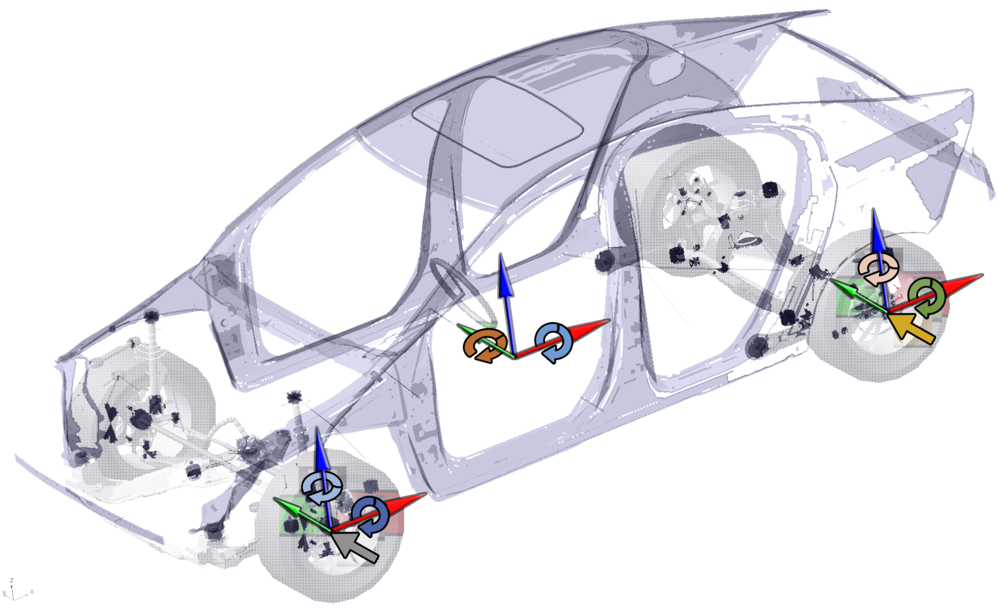

Figure 4.2: *CarMaker loadcases*

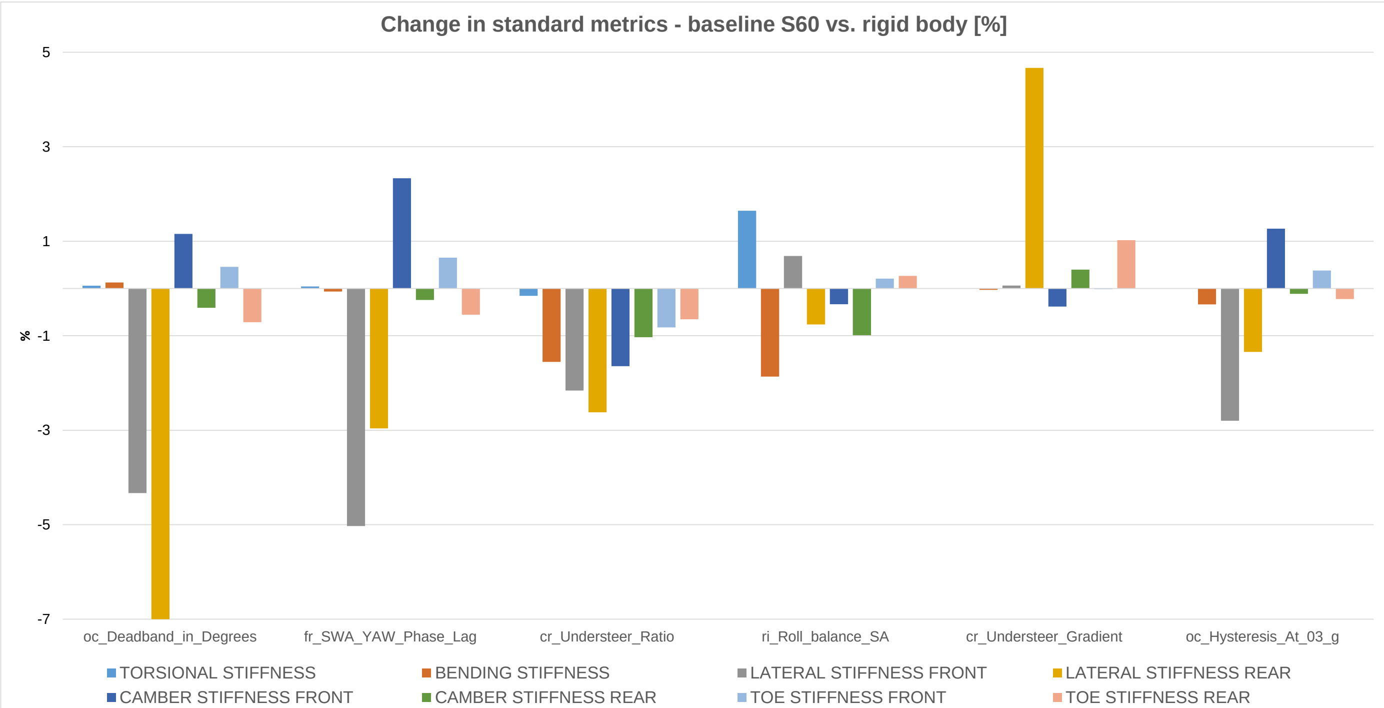

Figure 4.3: *Change in standard metrics - baseline vs rigid body*

CarMaker simulations are conducted with a rigid body, reinforced body and with the baseline Volvo S60 body as described in Section 3.1. The reinforced body configuration and the rigid body are compared with the baseline S60 body.

4.2.1 Rigid body

This section contains results from CarMaker comparing a rigid body with the baseline Volvo S60 body. Figures 4.3, 4.4 & 4.5 show the effect that the eight stiffness groups (seen in Table 4.1) have on vehicle dynamics characteristics. All bar charts in Sections 4.2.1 & 4.2.2 contains six out of all metrics calculated. These six metrics are the ones with the largest change for that certain case while modifying the body stiffness of the vehicle.

Figure 4.3 displays the percentage change of metric values with relation to the eight different body stiffness groups. As can be seen in Figure 4.3 metric values from On centre, Frequency response, Constant radius and Primary ride are represented. Meaning that it is in these maneuvers where the largest metric percentage difference is seen. Both the Lateral Front and Lateral Rear stiffness groups have a large effect in On centre, Constant radius and Frequency response (except for Lateral Front on Understeer gradient). Whilst global Torsional and Bending stiffness have a large effect on Primary ride. Camber Front is the third largest factor influencing On centre, Frequency response and Constant radius. Figure 4.3 is also showing that global Torsion and Bending stiffness has very limited effect on the overall metrics except for in Primary ride and the metric Understeer ratio.

Figure 4.4 displays the absolute metrics change normalized to a target range. The target range is used in order to gain a perspective on how much a metrics change is really perceived in a real situation in a real car. For example an equal percentage change between two different metrics might change the perceived vehicle dynamics characteristics very differently, whilst one might not affect it at all the other metric could have a drastic influence. Figure 4.4 contains metric values from On centre, Primary ride and Constant radius. The

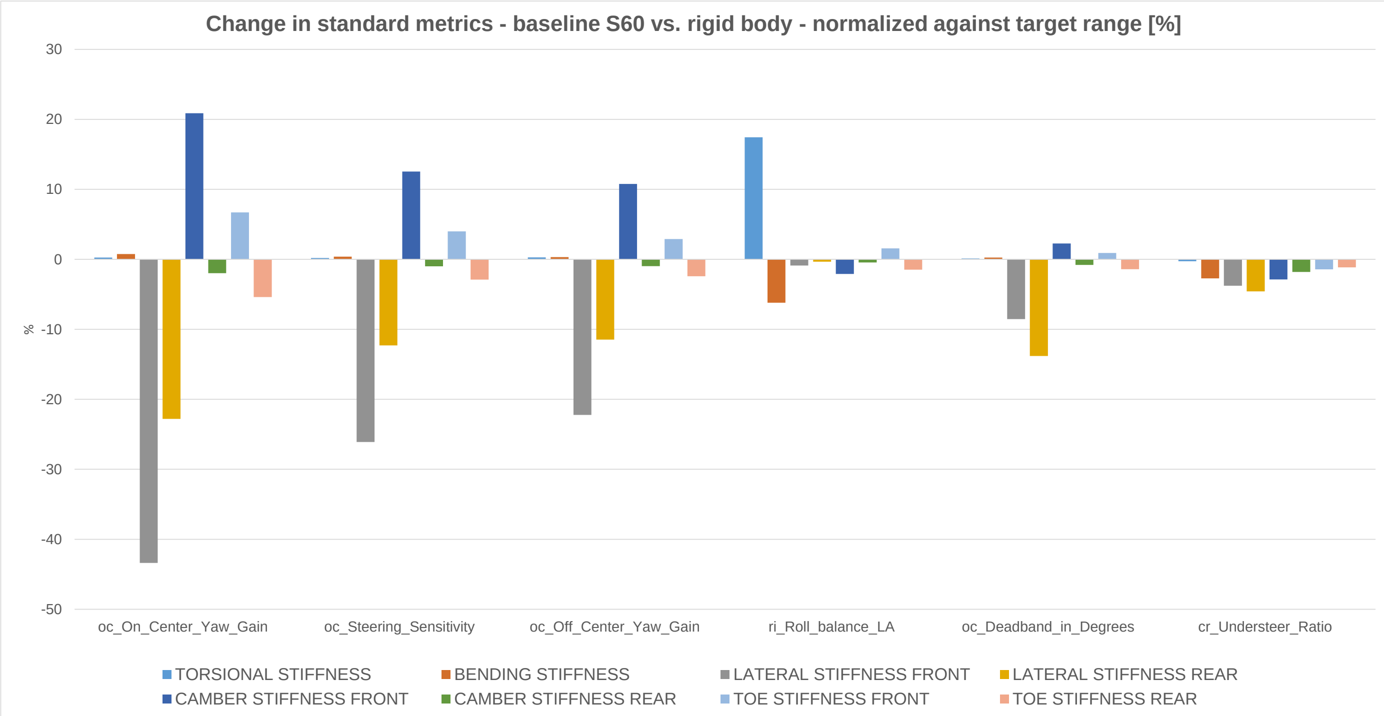

Figure 4.4: *Change in standard metrics, normalized against target range - baseline vs rigid body*

factors with the largest effect in On centre and Constant radius is Lateral stiffness front and Lateral stiffness rear, whilst global values for Torsional and Bending stiffness is the largest in Primary ride. Camber Front is also seen to have the third largest effect on On centre and Constant radius.

Figure 4.5 displays the percentage change in new metrics, calculated based on data from new load cases and maneuvers. The metrics showing the largest percentage change is from maneuver: Constant radius with bump and Constant radius with angled bump. Two of the largest factors influencing Constant radius with bump and Constant radius with angled bump is the global Torsional and Bending stiffness values. Further information about the motivation behind these maneuvers is explained in Section 5.3.1.1.

4.2.2 Reinforced body

This section contains results from CarMaker comparing a reinforced body with the baseline Volvo S60 body. The results presented in Figures 4.6, 4.7 & 4.8 is presented in the same way as in the previous section but with results comparing a reinforced body with the baseline.

Figure 4.6 contains results from the six metrics showing the largest percentage change; these six metrics are connected to maneuver: Primary ride, Frequency response, On centre and Constant radius. The results for Frequency response follows the previously seen trends in Section 4.2.1, with Lateral Front, Lateral Rear and Camber Front as the main factors; for On centre on the other hand Lateral Front and Camber Front are the largest factors. Constant radius is generally more influenced by Lateral Rear and Primary ride by Torsional, Bending, Camber Rear and Lateral Rear.

The results in Figure 4.7 illustrates that the four metrics showing the largest absolute metrics change normalized to the target range for a vehicle with a reinforced body compared to the baseline (On Center - Yaw Gain, On centre - Steering sensitivity, On centre - Off centre yaw gain & Primary ride - Roll balance) follow the same trends as the results displayed in Figure 4.4; Lateral Front, Lateral Rear & Camber Front are the major factors

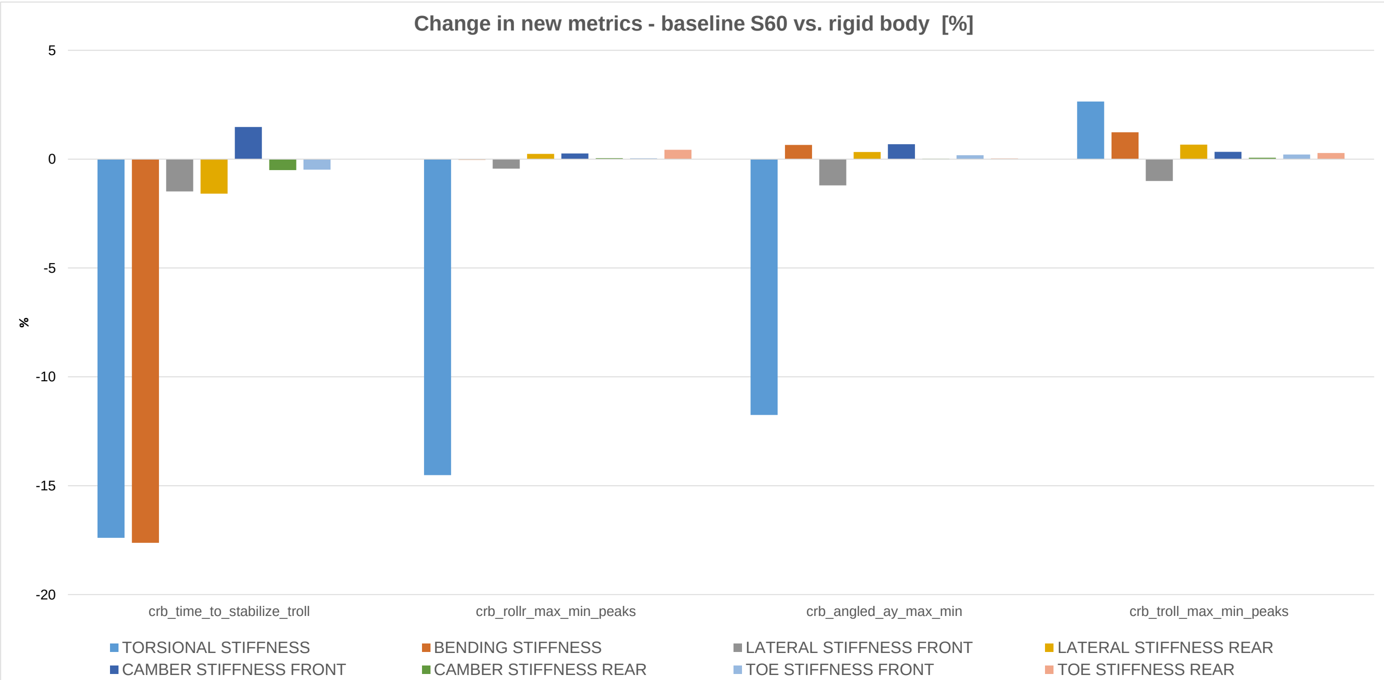

Figure 4.5: *Change in new metrics - baseline vs rigid body*

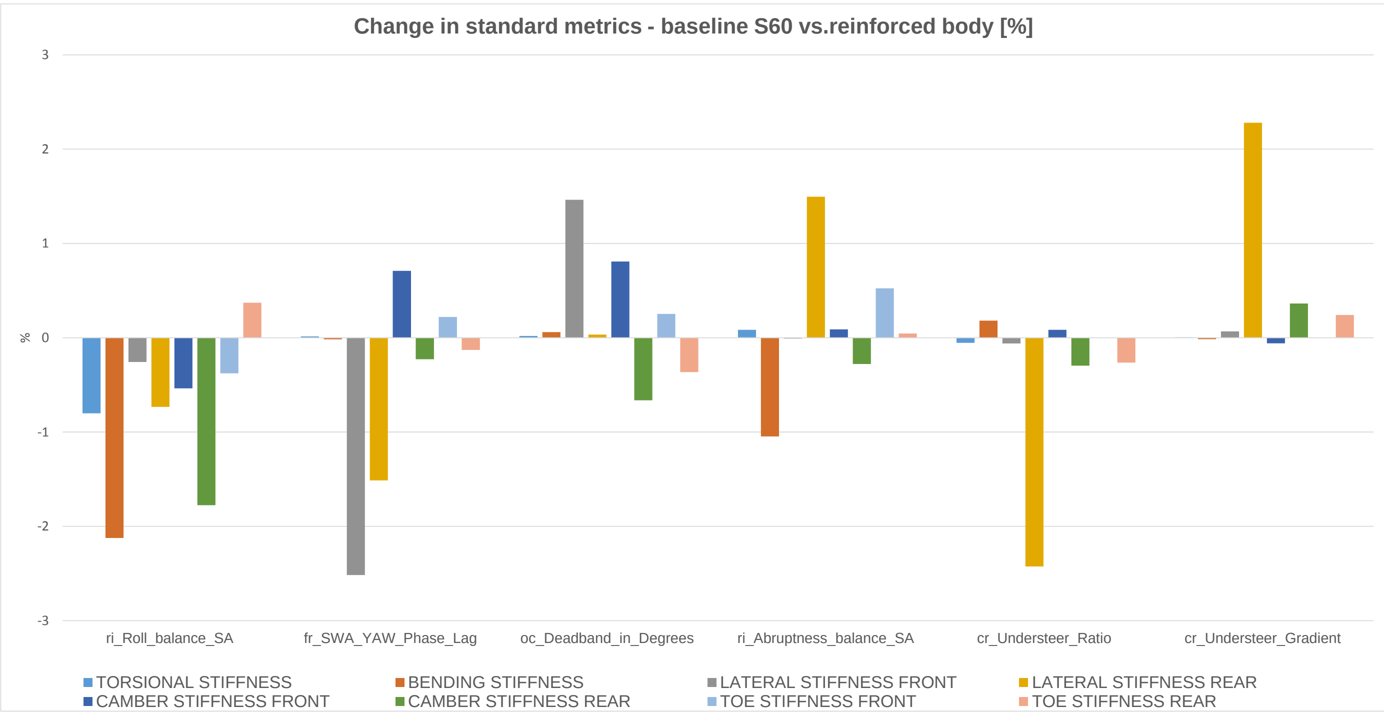

Figure 4.6: *Change in standard metrics - baseline vs reinforced body*

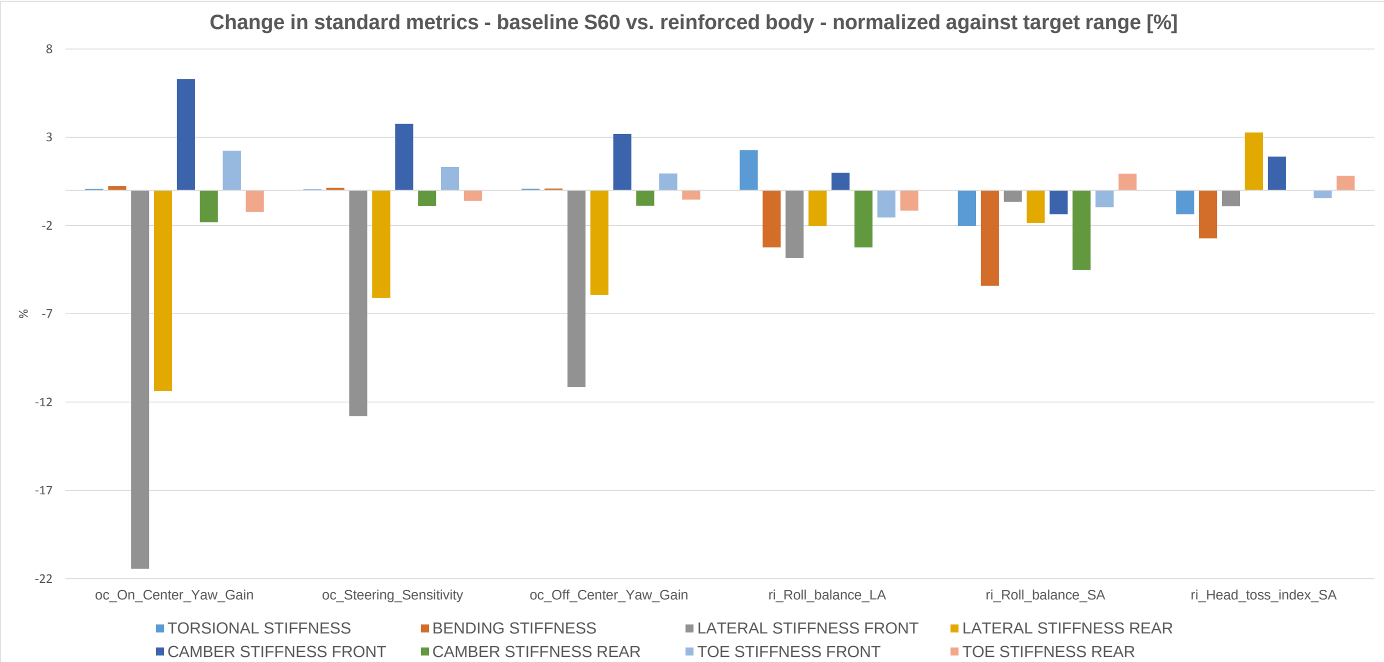

Figure 4.7: *Change in standard metrics, normalized against target range - baseline vs reinforced body*

in On centre and global values for Torsional & Bending stiffness together with Lateral Front, Lateral Rear, Camber Front & Camber Rear are major factors in Primary ride.

Figure 4.8 shows that the largest metric percentage change in new metrics calculated is in maneuvers: Constant radius with bump and Constant radius with angled bump. The largest factors are: global values for Torsional and Bending stiffness.

4.3 Correlation with Physical Testing

This chapter describes the correlation between the CAE analysis and the physical tests performed at HPG. The comparison has been done with two vehicle configurations: baseline body and reinforced body. The compared values in the following section are the difference in the metrics for these two configurations.

4.3.1 K&C

The Kinematics and Compliance values are calculated based on simulation results from Adams Car and from physical measurements taken at HPG as explained in the Method chapter of this report. The percentage difference in the K&C values between a baseline body and a reinforced body with all stiffeners mounted for both CAE and physical tests is presented in this section. This difference is thus expressing the compliance/stiffness of the body and as explained before, it is used in CarMaker for modeling lateral stiffness and local stiffness of the BIW.

Figure 4.9 shows the correlation for front compliance metrics: toe compliance, lateral camber compliance, lateral wheel center compliance, longitudinal spin compliance and longitudinal wheel center compliance. The blue columns represent the test data while the red columns represent the CAE simulations. The percentage value is comparing the baseline vehicle with the reinforced car. It can be seen that the trend of having less compliance

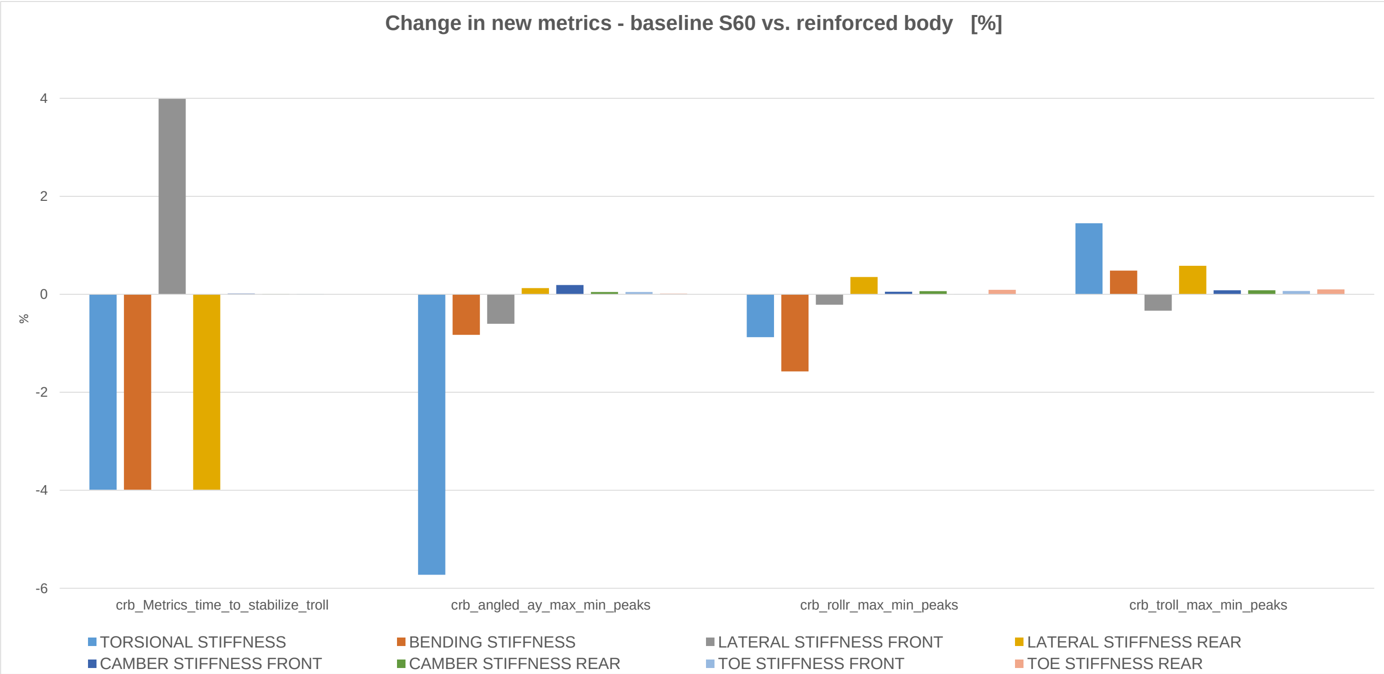

Figure 4.8: *Change in new metrics - baseline vs reinforced body*

with a stiffer configuration is the same for both physical tests and CAE analysis. The percentage difference between configurations is similar for all the measured metrics. However the compliance is overpredicted in toe front & longitudinal spin and under predicted in lateral camber, lateral wheel center & longitudinal wheel center.

Figure 4.10 presents the same metrics as the previous figure but for rear suspension. In this case it can be seen that the compliance is over predicted in CAE for toe, lateral camber & lateral wheel center. Whilst longitudinal spin & longitudinal wheel center are under predicted in CAE. The same trends are seen for the front suspension, for both CAE and physical testing.

Previously the compliance metrics from the K&C tests performed according to the method explained in Section 3.2.4 were presented. In Figure 4.11 and Figure 4.12 the kinematics metrics obtained from the wheel travel load cases are shown. The red columns correspond to CAE and blue correspond with physical test performed in the SPMM rig. The correlation in the delta value between the baseline body and the body with reinforcements show that for the front suspension (Figure 4.11) toe and camber measurements are following the same trend while the spin metric is slightly increasing in the CAE analysis but slightly decreasing for the Test Data.

The rear axle kinematic metrics results displayed in Figure 4.12 show that spin and toe are following the same trends for both CAE and Test Data. Camber presents a decreasing for CAE while it is slightly increasing for Test Data. It should be mentioned that the absolute toe variation between the two configurations is in the order of $0,01deg$ which makes the metric highly sensitive to changes in percentage.

Figure 4.13 shows the absolute lateral compliance for a reinforced Volvo S60 body. The blue bars represent the values for the front axle while the red bars represent the values for the rear axle. Columns to the left are SPMM rig measurements and columns to the right are CAE results. The absolute values of lateral stiffness has been removed due to confidentiality reasons but it can be seen that they are similar for both CAE and physical testing. It can be also seen that the car has higher compliance in the front than in the rear i.e. the vehicle has higher lateral stiffness in the rear.

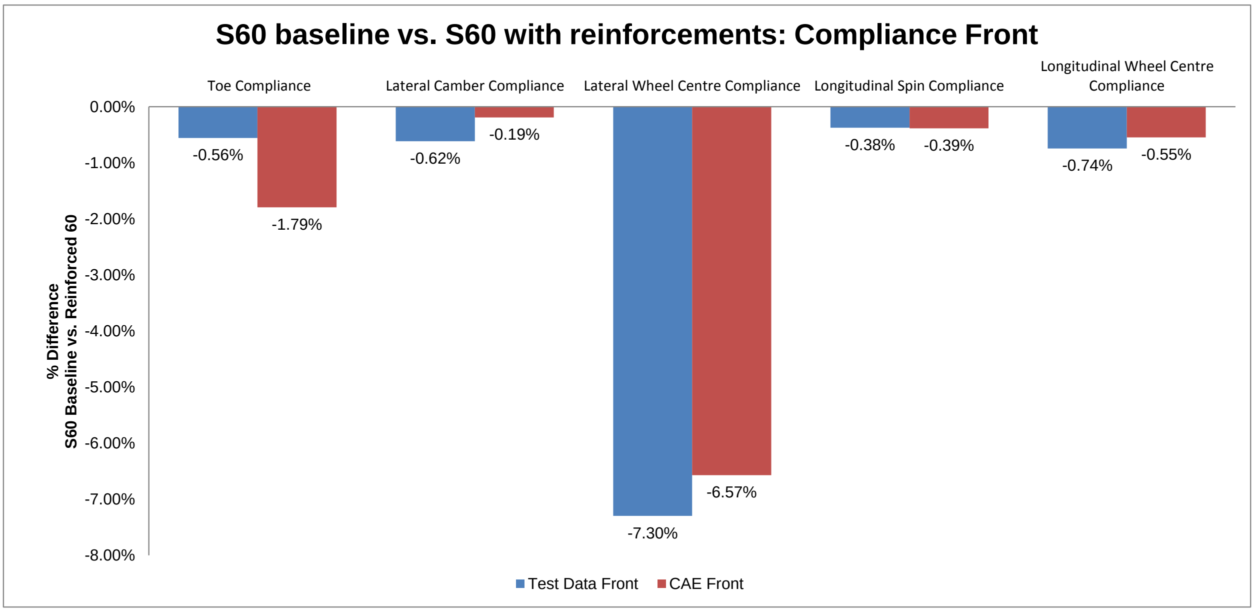

Figure 4.9: *Front Compliance Correlation*

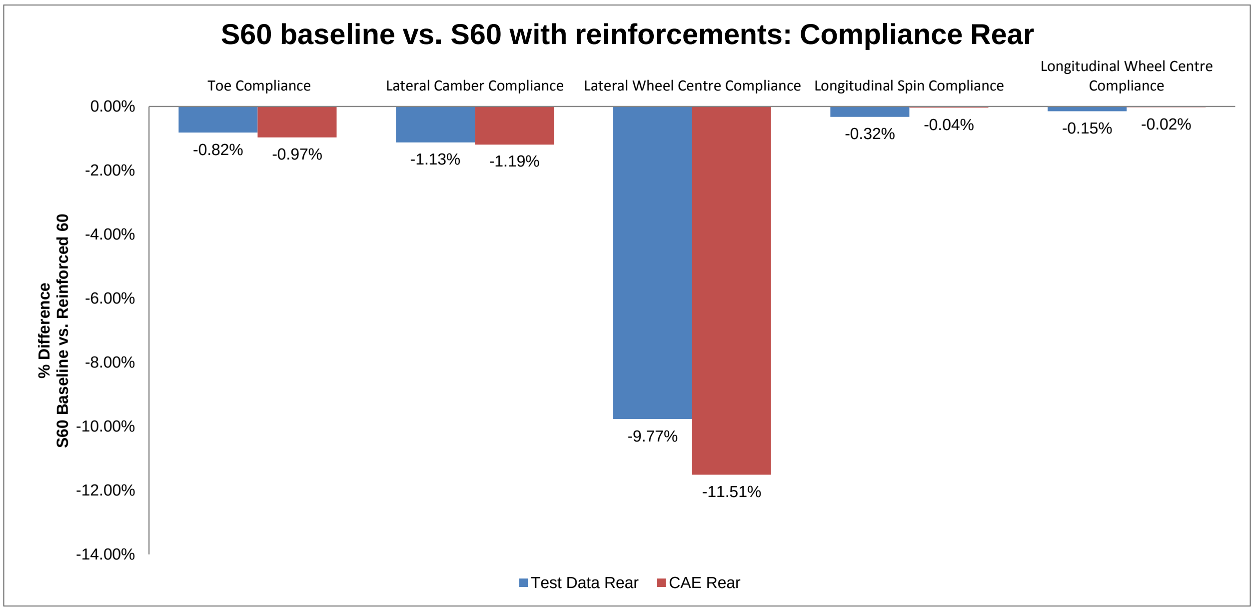

Figure 4.10: *Rear Compliance Correlation*

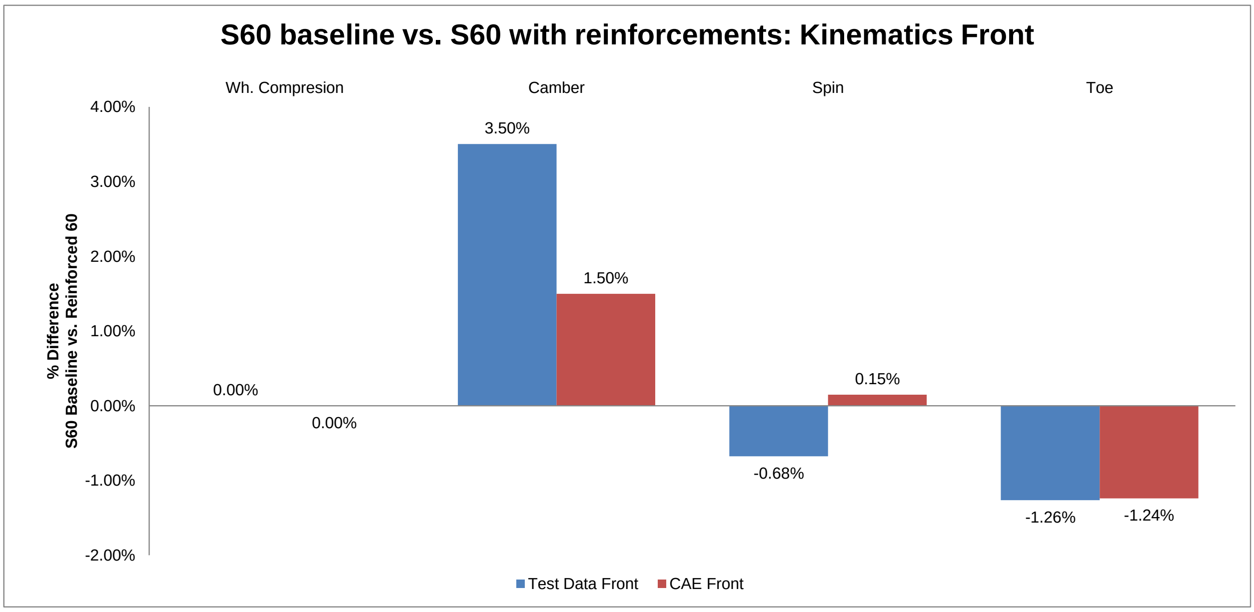

Figure 4.11: *Front Kinematics Correlation*

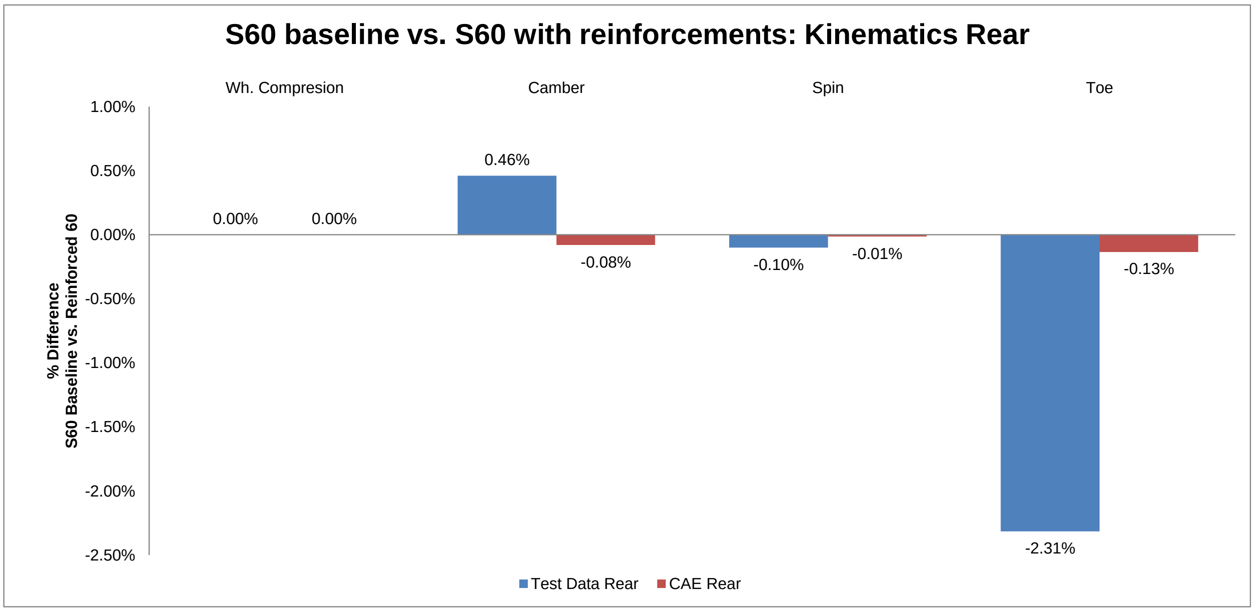

Figure 4.12: *Rear Kinematics Correlation*

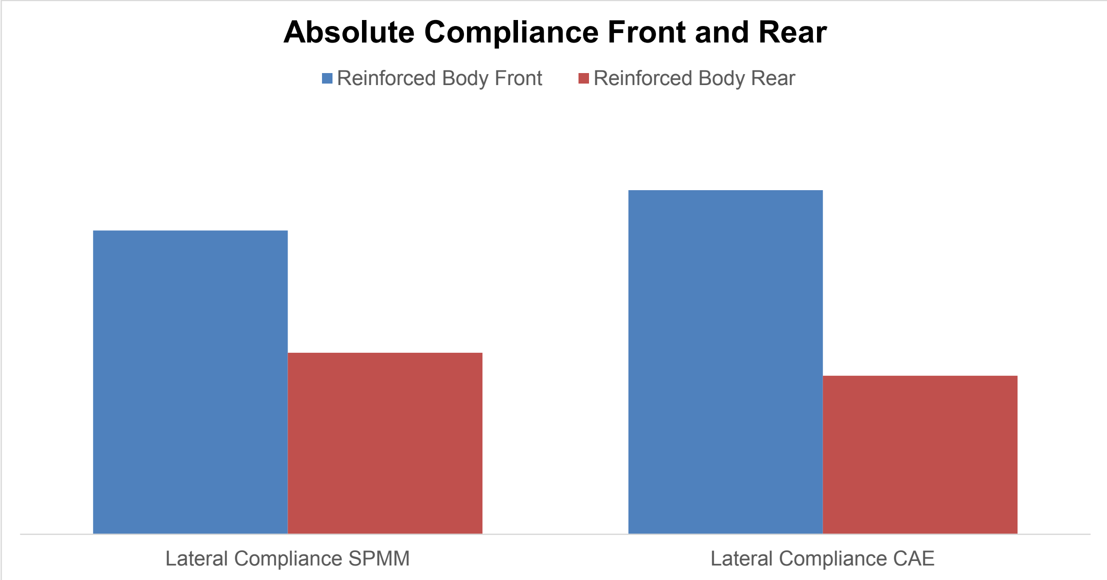

Figure 4.13: *Absolute Lateral Compliance*

4.3.2 Torsional stiffness

The torsional stiffness tests have been performed in CAE following the procedure explained in Section 3.2.4 and in the Test Lab following the method described in Section 3.4.2. The results presented in Figure 4.14 show the percentage change in body torsional stiffness between the baseline S60 body and the cases used for correlating, previously mentioned in Section 3.2.8. The results follow the same trends for three of the four configurations, giving as well a similar absolute value. For the correlation without front transversal, rear transversal, rear longitudinal & rear cross the value from CAE is moving towards a higher value compared to the baseline but towards a lower value for the test data. However the percentage variation from the original torsional stiffness is less than $2,0\%$ in both cases.

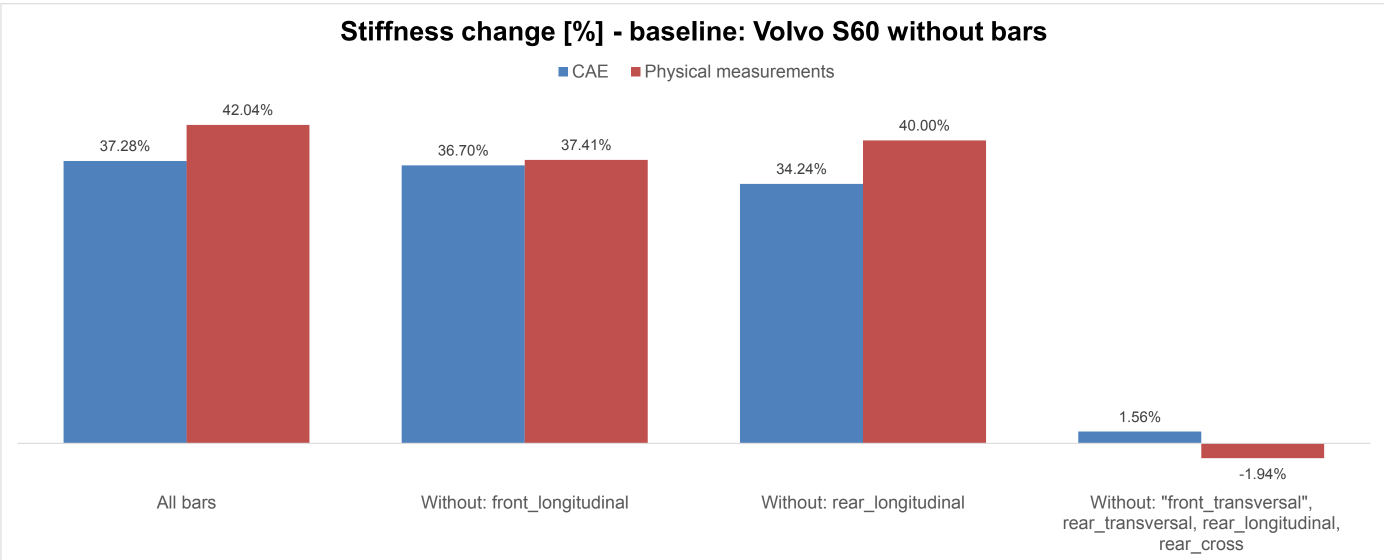

Figure 4.14: *Torsional Stiffness Correlation*

4.3.3 Full vehicle maneuvers

The correlation between CAE full vehicle simulations and Objective testing at HPG is presented in this section. The full subjective testing results are also presented in the following paragraphs. The CAE vs. objective testing correlation in the subsystem to vehicle relation implies the use of the model in CarMaker as explained in Section 3.3.1.

Figure 4.15 shows the correlation in the subsystem - vehicle level. The x-axis includes the twelve metrics that were showing a higher change between the baseline and reinforced body configuration. The blue bars represent the percentage change in the metrics measured in the test track using the method presented in Section 3.4.3 between baseline and reinforced vehicle configuration. The dark red bars represent the percentage change between the baseline vehicle and a vehicle fitted with a rigid BIW, the metrics are calculated in the simulations performed with the software CarMaker with the model and load cases explained in Section 3.3.1. The light red bars shows the results with the same model but compares the baseline vehicle to the vehicle fitted with body reinforcements. It can bee seen that the model is under predicting the influence of body stiffness in vehicle dynamics for all the metrics except Deadband in Degrees. However, the model in CarMaker is following the same trends for all the presented metrics.

From the full vehicle subjective testing it is seen that removing the rear cross from a full reinforced car gives a reduction in Phase lag and Dead Band. Furthermore it is seen that the car feels more unsafe at high g maneuvers. These results give information about the effect of the rear cross in the trunk to the vehicle dynamics behavior of the car. Other configurations could not been analyzed during subjective testing.

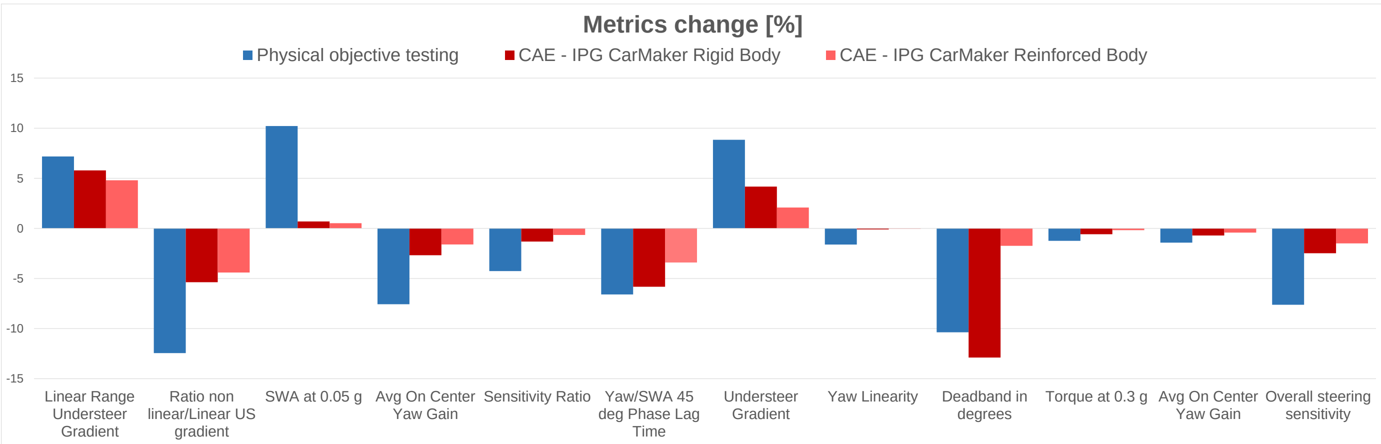

Figure 4.15: *Correlation CAE full vehicle (CarMaker) & Objective Testing*

5 Analysis and Discussion

This chapter analyzes the results presented in the previous section and tries to relate the different relation levels. An explanation of the possible causes and consequences of the different results is given in this section and it will further allow the conclusions of the study to be drawn. First the validation of the models comparing the CAE results with physical testing is discussed in Section 5.1 in order to ensure the reliability of the results. This analysis is performed for the three models used: Adams, Nastran and CarMaker. After that Section 5.2, 5.3 and 5.4 are presented. These chapters analyze the influence of body stiffness in the component to subsystem, subsystem to vehicle and component to vehicle relation levels.

5.1 Validation of models

The validation of the models can be analyzed in three levels:

- component to subsystem (Adams Car K&C simulations and Nastran static stiffness simulations),
- subsystem to vehicle (CarMaker full vehicle simulations) and
- component to vehicle (connecting the K&C and Nastran simulations together with the CarMaker full vehicle analysis).

The initial idea of the method developed for this project lays on the use of a simplified model in CarMaker to minimize the simulation time and to explore the design space. Thus the correlation in the subsystem-vehicle level is expected to show the correct trends but the absolute values are expected to show slight variations due to the compromises taken with the model. However, the component-subsystem relation, which is using a more detailed model in Adams Car, where the body stiffness is captured from a finite element model based on modal reduction, is expected to have better correlation in absolute terms.

5.1.1 Adams model: component to subsystem

The results presented in Section 4.3 follow the assumptions made for model validation in the component-subsystem level. The K&C analysis performed in Adams Car shows a good correlation with physical measurements for the comparison between the reinforced body with the baseline Volvo S60 body. The results from the rig tests are reflected in the CAE analysis and the same trends & approximately the same absolute values are seen. Furthermore the lateral wheel centre compliance metric, the compliance metric most affected by the increased body stiffness, has a difference between baseline and reinforced body of -7,30% in test data and -6,57% in CAE for front axle and -9,77% and -11,51% in the rear. This means that the reinforced body model is properly capturing the stiffness of the body while performing static analysis for estimating compliance metrics. However, the slightly difference in the metrics can be due to the limitations in the CAE simulation method used, where the suspension K&C metrics are measured independently for front and rear axles while in the SPMM rig they are measured at the same time. This means that the effect of a stiffness change in the rear area of the body would not be taken into account into the CAE K&C analysis of the front suspension but it may influence the real measurements in the SPMM rig and vice-versa for a change in stiffness for the front area of the BIW. It should also be mentioned that the rear axle is correlating worse for the mentioned lateral compliance metric than the front axle. While the CAE is under predicting the lateral compliance in the front, it is overpredicting it in the rear. This is connected with the limitation of the CAE method since, as presented in Figure 4.1, the reinforcements installed in the front have higher impact on the lateral stiffness than the rear ones. This yields that in the CAE analysis the influence of these front reinforcements is not captured in the rear axle measurements, whilst during the physical tests in the SPMM rig this influence is measured. So in the rear axle the compliance is over predicted in CAE because the stiffness of the front area of the body is not taken into account.

The kinematic metrics comparing the reinforced body with the baseline show a good correlation with physical measurements. The absolute variation between the baseline and reinforced body is in the order of $0,01$ deg and the percentage change is also smaller than for compliance metrics, even thought the smaller total difference will increase the sensitivity to any variation. This means that the kinematic metrics are less affected than the compliance measurements for changes in body stiffness. Ideally the kinematic metrics are only influenced by the suspension geometry, so the difference of having a less compliant body should not give any effect. However the local deformation of the hardpoints can slightly change these metrics. Either way the difference is proven to be small and it can be disregarded in favour for the compliance metrics to capture the local effects of body stiffness.

5.1.2 FEM model: component to subsystem

CAE analysis is under predicting the torsional stiffness change between the baseline and the reinforced Volvo S60 body. However, as seen in Figure 4.14, the CAE estimation for stiffness change has a similar value to the real tests. One of the cases analyzed, baseline with the underbody reinforcements added, shows a decreased value of torsional stiffness in the physical measurements while increased stiffness in the CAE analysis. Although the stiffness change that this case is showing is less than 2% it is believed that the reduction of body stiffness when adding a stiffener showed in the test data can be due to limitations in the test method used. As explained in Section 3.4.2, this method is measuring the body stiffness in a four post rig without isolating the body from the rest of the assembled parts of the vehicle.

5.1.3 CarMaker model: subsystem to vehicle

The second level of validation connects subsystem, K&C measurements and global stiffness values, with vehicle dynamics characteristics, metrics calculated from steady-state and transient maneuvers. The validation at this level explains the accuracy of the CarMaker model used in this study. In the results presented in Figure 4.15 metrics from Constant radius, On Center, Low G Swept Steer, Frequency Response and High G Swept Steer are presented. It can be seen that the results from the CarMaker S60 model are following the same trends as the results from the physical tests performed at HPG. However, in general the model is under predicting the effect of body stiffness. Even for a rigid body, modelled in CarMaker with the suspension compliance values from a rigid body and without the joint modelling global torsional and bending stiffness. Higher metric percentage difference can be seen for physical tests in comparison with the CAE analysis. This fact makes the model valid for finding and analyzing trends but not for targeting an absolute number in metrics. As stated in the explanation of the method, the results from the CarMaker model was not expected to show a good correlation with the absolute values from the physical tests since the vehicle is modelled in a simplified way to reduce the simulation time. However these results prove that there is a difference in vehicle dynamics characteristics for varying body stiffness in passenger cars and it can be estimated with a simple model. For a better correlation a more detailed model is required.

5.2 Component to Subsystem

The component to subsystem level relates the effect of each stiffener mounted in the car body to the local and global body stiffness values i.e. the load cases which are capturing the local stiffness (K&C) and torsional & bending stiffness. In other words this relation explains how each bar is increasing the local and global stiffness of the body.

The results show that the front stiffness has room for improvement: lateral, camber and toe K&C load cases are significantly affected when mounting the transversal bar to the vehicle. This yields to the fact that lateral, camber and toe compliance of the body can be reduced when stiffening up the chassis in the front area, mainly in the transversal direction. The longitudinal front bars, though, are not affecting local stiffness nor global values.

The underbody increases the stiffness of the floor of the vehicle. This structure does not show a big impact in local stiffness but it does have influence on bending stiffness. By increasing the floor stiffness the resistance of the body to bending increases more than 40%. One can think about the three point bending test used for estimating this value. When including the underbody reinforcement, the added rigidity leads to a reduction in the bending angle yielding a higher value of bending stiffness.

The cross section in the rear has a big impact on global torsional stiffness. Surprisingly this structure is the only one affecting the torsional stiffness of the body. Moreover this cross member is affecting the lateral compliance measurements in the rear axle more than any other reinforcement in the rear. And it can also be seen that lateral, camber and toe K&C load cases are not greatly influenced by the rest of the reinforcements added to the rear part of the body. Specially if we compare this fact with the results for the front axis, where the changes in body local stiffness where appreciable. This effect can be due to two main aspects. Firstly, one can think that the rear part of the body is already stiff enough so the reinforcements do not have a considerable effect. And secondly the effect of the suspension type and construction can be one of the reasons to the lack of improvement in local stiffness when adding bars to the rear section of the body: the fact that the rear subframe is mounted with bushing to the body may lead to a decreased effect of local stiffness in that area.

From these results it can be seen that torsional stiffness is not the only important parameter when talking about body stiffness. Other areas of the body can be modified in order to substantially increase the lateral, camber or toe stiffness, specially in the front, as it has been discussed. Notwithstanding this fact, one question arises: how these changes in compliance and global stiffness values affect vehicle dynamics behaviour? Is it the rear cross bar that is responsible of resulting in an improved driving experience? Are the transversal bars altering the vehicle performance? Connecting subsystem to vehicle characteristics will answer these questions.

5.3 Subsystem to Vehicle

The subsystem to vehicle dynamics characteristics relation i.e. relation between local & global stiffness values and handling, steering and ride characteristics relates how an increase in stiffness (added reinforcements) affects the performance of the vehicle. The study is performed with three vehicle configurations, the same base vehicle with a standard body, a reinforced body and a rigid body.

Results presented in Section 4.2 show that there is a large metrics percentage change in the following standard maneuvers: On centre, Frequency response, Constant radius and Primary ride. This trend can be seen for both a rigid body compared to the baseline and for a reinforced body compared to the baseline. When comparing the percentage metrics change for On centre, Frequency response and Constant radius it is seen that the factors with a large influence are: Lateral Stiffness Front and Lateral Stiffness Rear, though Toe Stiffness Rear is the second largest factor after Lateral Stiffness Rear for Constant radius - Understeer gradient for the comparison between a vehicle with rigid body with the baseline. Regarding the results from the new maneuvers presented in Section 4.2: Constant radius with bump and Constant radius with angled bump are seen to be influenced to a large extent by values for Global Torsional Stiffness and Global Bending Stiffness.

5.3.1 Rigid body compared to the baseline

It can be seen that increasing the local stiffness (Lateral & Toe Rear) at the rear part of the BIW increases the understeer gradient resulting in a more under steered vehicle, see Figure 4.3. This effect can be a result from the difference in yaw angles between front and rear axle, which is intuitively increasing with increased lateral acceleration and decreased stiffness leading to higher yaw rates and towards over steered vehicle behaviour. One can also say that the front and rear axle are more freely to move independent of each other when the stiffness is decreased. It can also be seen that increased stiffness at Toe Rear results in increased understeer gradient, due to the self aligning torque created around the rear wheel as a result from mechanical and pneumatic trail which tends to steer the rear wheel in the opposite way from the corner. Thus the angle generated from the self aligning torque will be reduced when stiffness is increased. Both increasing Camber Front and Camber Rear affects the understeer gradient, Camber Front reduces the understeer gradient due to the increased grip at the front axle whilst Camber Rear increases the understeer gradient due to the increased grip at the rear. Also, global stiffness values does not affect the understeer gradient to a large extant compared to local stiffness values.

The understeer ratio (non linear range understeer gradient/linear range understeer gradient) for a vehicle with rigid body compared to a flexible body decreases as seen in Figure 4.3 for increased stiffness in all areas of the BIW i.e. the vehicle under/over steer behaviour is more constant whilst moving between the linear and the non linear region of vehicle behaviour. As illustrated in Figure 4.3 phase lag between steering wheel angle and yaw rate is seen to decrease for increased lateral stiffness in front and rear for a vehicle with a rigid body compared to the baseline.

The On centre metrics; Deadband in degrees and Hysteresis are largely affected by Lateral Front, Lateral Rear and Camber Front, as seen in Figure 4.3 This is for a vehicle with a rigid body compared to the baseline. Hysteresis describes the torque required to change direction at a specified level of lateral acceleration. Deadband in degree represents the absolute difference in steering wheel angle at 0 steering wheel torque between left and right turning directions. The metric describes steering characteristics and especially torque feedback, it characterize returnability and delay between steering torque input and steering angle. The results show that this metric is affected in a significant way by the lateral stiffness at both front and rear of the car. One can think about the lateral stiffness load case presented in the theory section of this report. If this body parameter it is too low, the vehicle will laterally bend increasing the difference in yaw angles between front and rear axle. This will lead to a worse returnabilty when the car is trying to change direction from left to right and vice-versa. If the difference between the yaw angle at the front and at the rear axle would have a smaller value the deadband will decrease making the car more agile and responsive. This will happen if the lateral stiffness is high enough to avoid the lateral bending of the body thus keeping the yaw angles in front and rear axle to a similar value.

Primary ride - roll balance is affected by a change in global Bending and Torsional stiffness (see Figure 4.3), for a vehicle with a rigid body compared to the baseline. Roll balance is calculated as: Roll balance = Roll front / Roll rear. Increasing global Bending stiffness results in more roll of the rear axle in relation to the front axle whilst an increase in global Torsion results in increasing roll of the front axle compared to the rear axle.

The previous presented metrics are describing the absolute percentage change in the metric value. This number can be somewhat misleading due to that an equal percentage change between two different metrics might result in that one metric change is drastically changing the perceived vehicle characteristics, while the effect of the same percentage change for the other metric might not be felt by the driver. Figure 4.4 is instead of the absolute change, displaying the change normalized against a target range. Meaning that 100% represents a metric change as large as the complete target range. It can be seen from Figure 4.4 that there are large relative metrics changes for On centre: Yaw Gain, Steering Sensitivity and Deadband in degrees; Primary ride: Roll balance; Constant radius: Understeer ratio.

The three metrics from On centre seen in Figure 4.4 (On centre yaw gain, Steering sensitivity and off centre yaw gain) are showing the same trends regarding influencing factors. The largest factors in respective order are: Lateral Rear, Lateral Front and Camber Front. Steering sensitivity is calculated as the slope of lateral acceleration vs steering wheel angle, thus describing sensitivity to steering wheel input. On/off centre yaw gain describe how responsive the vehicle is to steering wheel inputs, both for small steering wheel angles (on centre) and for large steering wheel angles (off centre). It is seen that yaw gain, both for small steering wheel angles (on centre) and for large steering wheel angles (off centre) is decreasing with increased lateral stiffness, both front and rear. An increment in lateral stiffness will try to even out the difference between relative front and rear axle angles i.e. reducing steering angles on front and rear wheels. It can also be seen that the metrics are increasing in value for an increase in Camber Front; the increase in stiffness yields in better contact between tire and ground, which in turn lead to higher lateral force build up at the front axle. The same trends can also be seen for Steering sensitivity.

The percentage change in metric values between a rigid body and the baseline Volvo S60 body can be seen as a representation of the error from approximating the vehicle body with a rigid body instead of including a flexible body for full vehicle simulations. It was seen that the error is in the order of up to 13%.

5.3.1.1 New maneuvers

Figure 4.5 shows the four metrics showing the largest percentage change for the new maneuvers. Constant radius with bump and Constant radius with angled bump are seen to be affected to a large extent by values for Global Torsional Stiffness and Global Bending Stiffness. These maneuvers combine handling and ride characteristics and it can be seen that a stiffer body reduces the abruptness felt when passing a pump at speed; both peaks in roll rate and lateral acceleration is reduced together with a reduction in time for the vehicle to stabilize roll movement.

The motivation behind these new maneuvers, besides combining ride and handling effects in order to increase the effect of body stiffness on vehicle dynamics is to correlate subjective assessments and CAE simulations. Previously subjective assessments presented in Section 1.3 showed that a vehicle with a stiffer body was feeling more premium and solid while hitting a speed bump. The proposed new maneuvers and measured metrics are trying to capture that effect in order to quantify the influence of body stiffness on vehicle dynamics.

5.3.2 Reinforced body compared to the baseline

A reinforced body was also compared against the baseline Volvo S60 body, here a smaller metrics change can be noticed between the two vehicle configurations than for the results presented in Section 5.3.1 comparing a vehicle with a rigid BIW to the baseline vehicle. The reinforced body used in the simulation model to produce the results discussed in this section coincides with the reinforced body used for the physical tests.

It can be seen from Figure 4.6 that Primary ride - roll balance, Frequency response - steering wheel angle vs yaw phase lag, On centre - deadband in degrees and Constant radius - understeer gradient have almost the same relative importance comparing rigid vs baseline and for reinforced vs baseline. Steering wheel angle vs yaw phase lag and understeer gradient follow the exact same trends as for a vehicle with rigid body compared to the baseline.

The understeer ratio as seen in Figure 4.6 is decreasing for an increase in Lateral Rear. This result coincides with that seen from the comparison between rigid and baseline, but the other factors show less relative importance. This can be due to the fact that the body is not made fully rigid, but only reinforced with steel bars. Meaning that the total compliance is equal to the body compliance together with the suspension compliance. In the previous Section 5.3.1 only the suspension compliance is taken into account, due to that the body compliance is equal to zero for a rigid body. So the influence from the bars on different compliance groups i.e. where the bars increase stiffness, is a factor which affects the results. Total compliance for the case with a reinforced body might also act in the opposite direction to the suspension compliance and therefore change how the bars affect the vehicle behaviour.

There are two primary ride metrics among the six most affected metrics: roll balance and abruptness balance. Roll balance describes the relation between accumulated total roll for front and rear, whilst abruptness balance is representing the relation between accumulated body jerk for front and rear.

Figure 4.7 shows the metrics change normalized against the target range. It is clear that on/off centre yaw gain and steering sensitivity follow the same trends seen in Figure 4.4, which represents a vehicle with rigid body compared to the baseline vehicle. Meaning that Lateral Front has a large influence on the output metrics. Primary ride: roll balance can be seen to show slightly different relative importance of each factor. Another metric which is seen to have a large effect when comparing a vehicle with reinforced body with the baseline is Head toss, which describes abruptness and jerk in roll motion.

5.3.2.1 New maneuvers

Figure 4.8 shows the same trends as for a vehicle with a rigid body compared to the baseline, discussed in Section 5.3.1.1. The large relative percentage difference between these two cases show that there is room for improvement regarding ride characteristics with increased torsional stiffness. Lateral stiffness is also showing to affect the metrics when comparing a vehicle with a reinforced body with the baseline vehicle, this effect is not as large for the comparison between the vehicle fitted with a rigid body and the baseline vehicle.

5.3.3 Relation between how a reinforced or rigid body influence vehicle behaviour

The relative importance of each individual metric is changing based on if the comparison is done between a vehicle with a rigid or reinforced body to the baseline Volvo S60 body. This is due to that the reinforcement bars fitted to the reinforced body are not stiffening the body in the same way as if assuming that it is a rigid body i.e. the added bars is affecting the stiffness for a certain compliance groups to a greater extant than for other groups. Meaning that the compliance values between a reinforced and rigid body might differ significantly based on the position and properties of the bars in the reinforced body. Section 5.2 describes the effect from

Figure 5.1: *Change in standard metrics, normalized against target range - baseline vs reinforced body with overlapping results from baseline vs rigid*

each bar on local and global stiffness and it is seen that the groups where a larger change is seen is: Lateral Front, Camber Front, Toe Front, Global Torsion and Global Bending. Figure 5.1 contains the results from the comparison between a vehicle with a reinforced body compared with the baseline and the results from the comparison between a vehicle with rigid body compared with the baseline. It shows the effect the reinforcement bars have on vehicle behaviour compared to a if a rigid body was used, therefore it is a measure on how much it is possible to gain from further reinforcing the vehicle body.

5.3.4 Largest factors influencing handling, steering and ride characteristics

The results presented in Section 4.2 show that the largest factor affecting handling and steering characteristics is lateral stiffness for front and rear, whilst camber stiffness front is shown to be the third largest factor. Global values for torsional and bending stiffness is shown to have a large affect on Primary ride, but very limited affect on handling and steering characteristics in relation to the other factors.

5.4 Component to Vehicle

The component to vehicle dynamics characteristics study can be done by performing an analysis following each relation of the method connecting component to subsystem and subsystem to vehicle i.e. using the results from K&C simulations in Adams Car and FEM together with the full vehicle simulations in CarMaker. The results coming from CarMaker are used to give a more general answer and an overview to the question: how vehicle dynamics characteristics are affected by body stiffness.

This relation between component and vehicle dynamics characteristics can be done as well by using the previously described Adams model in full vehicle simulations for the most important body inputs and load cases. This simulations will allow the analysis to go deeper into some concrete characteristics of the car behaviour. However these simulations are not covered in this study.

From the CarMaker results it can be seen that even though the bending stiffness has room for improvement in the car, FEM simulations shows that this parameter can be increased, the vehicle dynamics analysis shows that bending stiffness has less effect in the car behaviour than, for instance, torsional stiffness and lateral stiffness. Torsional stiffness can also be improved significantly by increasing the stiffness in the trunk of the vehicle, and it has an influence in vehicle dynamics behaviour. However the simulations show that the lateral stiffness has a greater effect in vehicle dynamics than the rest of the body parameters. It can also be seen that the vehicle can be modified with bars so that the lateral front stiffness can be substantially increased but that the lateral rear stiffness can only be slightingly increased. However the lateral stiffness has still some impact in the vehicle dynamics behaviour in the on center maneuver. Overall this means that the vehicle has high sensitivity to rear lateral stiffness changes and that the front lateral stiffness is largely affecting the vehicle dynamics characteristics.

The simulations has shown as well that larger influence in vehicle dynamics can be achieved by adding a group of stiffeners to the car than by adding all the bars together or making the whole body rigid. This is because the effect of the different bars could counteract each other. For instance, an increment in lateral rear stiffness reduces the Deadband but an increment in camber front stiffness increases this metric. This can cause that changing from a flexible body to a rigid could have a limited effect on vehicle dynamics behaviour due to that the effects from stiffening up the vehicle in the whole BIW are counteracting each other.

Based on these results some design guidelines about body stiffness in relation with vehicle dynamics can be made. These design guidelines are summarized in Table 5.1 In order to decrease the deadband lateral stiffness should be increased both in front and rear of the car. A slightly change in the rear stiffness by reinforcing the trunk in the transversal direction or with a cross member will decrease this metric. A transversal reinforcement in the front part of the body will benefit the decrement in the deadband. Steering wheel angle and yaw phase lags can be reduced to have a more responsive car by increasing lateral stiffness specially in the rear par of the body. A transversal reinforcement in the front will cause an improvement in lateral stiffness but also in camber stiffness. Those effects will counteract resulting in less change in this metric. Regarding the understeer level of the car, an increment in body stiffness will cause in general a more understeer car, as it was seen in the Theory and Results section of this report. An increment in the lateral rear stiffness by a cross or transversal reinforcement will make a difference in this metric. Regarding the ride parameters the car will feel more balance by increasing the torsional stiffness as it was shown in the CarMaker results.

Table 5.1: Design Guidelines

Maneuver	**Vehicle Metric**	**Subsystem**	**Component**
On Center	Deadband reduction	Lateral Stiffness	Front transv. bar, rear cross
Frequency response	Phase Lag SWA-yaw reduction	Rear Lateral Stiffness	Rear cross and transv. bar
Constant radius	Understeer increment	Rear Lateral Stiffness	Rear cross and transv. bar
Primary ride	Roll Balance increment	Torsional stiffness	Transv. bar

6 Conclusions

- Full vehicle CAE simulations performed with the simulation tool IPG CarMaker show a significant difference in vehicle dynamic characteristics when comparing a passenger car with a reinforced body against a baseline Volvo S60 vehicle.
- On center, frequency response and primary ride are the most affected maneuvers while evaluating body stiffness vs. vehicle dynamics.
- Global torsional stiffness should be increased in order to improve roll balance in ride maneuvers. This influence is small in the standard studied maneuvers, but it can be captured using the new proposed maneuvers and metrics.
- Front and rear lateral stiffness should be raised in order to reduce Deadband and Steering Wheel Angle - Yaw phase lags.
- Physical measurements from objective testing follow the same trends as seen in CAE simulations in IPG CarMaker for full vehicle maneuvers including handling, steering and primary ride effects.
- Body stiffness can be captured to an acceptable level for handling, steering and ride maneuvers by using a model where global torsional and bending stiffness are taken into account by a joint between two rigid bodies and local stiffness effects are taking into account in the compliance values of the suspension. However a more detailed body model based on FEM and modal reduction is needed for a better correlation in absolute numbers and not only in trends when performing dynamic simulations.
- Global torsional stiffness is not only the main parameter when defining body stiffness targets and requirements for a better vehicle dynamics behaviour. Lateral stiffness shows to have a large effect on the dynamic behaviour and it should be considered when defining body stiffness goals.
- Maneuvers combining handling and ride effects are proven to be useful for defining body stiffness targets since they emphasize the influence of the body stiffness parameters in the vehicle dynamics behaviour.
- There is a significant error factor in full vehicle dynamics when the vehicle body is assumed to be rigid. This error can be estimated to up to 13% for certain metrics. The accuracy of the simulation results can be increased by using a flexible body instead of a rigid body for full vehicle simulations.
- Reinforcements fitted to a vehicle body can be seen to affect different aspects of vehicle performance with altering magnitude and relation dependent on where they are fitted i.e. different bars can counteract each others affect on vehicle dynamics characteristics. Resulting in that the vehicle can be tuned during development using body stiffness as a design variable.
- The CAE method used for this study based on first exploring the design space with a simple model and secondly perform a deeper analysis in the interesting areas with a more complex model can be translated to study other areas of the vehicle. Thus, this method can be useful to reduce the development time of a vehicle and to increase the understanding of design choices in a complex system.

7 Future work

- Further development of the presented method so it connects component and vehicle levels with a simple model in CarMaker.
- Refining the CarMaker model, so the correlation in absolute values with physical tests can be improved.
- Defining targets for body stiffness based on vehicle dynamics performance targets. The torsional stiffness, bending stiffness, and load cases presented to define lateral stiffness, camber stiffness, and toe stiffness can be used to define a target range of body characteristics according to the desired vehicle dynamics performance.
- Connecting component to vehicle characteristics with a validated model in Adams Car. The method presented in this report has used a simple model in order to explore the whole design space. The result of this study has concluded the areas of the BIW that can be improved to change the vehicle dynamics behavior of a passenger car. Furthermore this study has shown which maneuvers and metrics are useful for analyzing the influence of body stiffness on vehicle dynamics. However these results can not be used for targeting an actual value of BIW requirements. This could be done instead by using a validated model in Adams Car which connects directly component to full vehicle simulations. By using the design guidelines, areas of improvement, maneuvers and metrics shown in the conclusions section of this report, full car simulations could be performed in Adams Car to define body stiffness targets.
- Implementing the proposed new maneuvers in Adams Car and in Objective testing to further evaluate the influence of body stiffness on ride characteristics.
- Further confirm that the new maneuvers and metrics are also suitable for explaining and quantifying body stiffness influence on subjective vehicle assessments of vehicle dynamics characteristics.

References

[1] *Adams/Flex*. MSC Software. 2015.
[2] M.C.C. Bampton and R.R. Craig. Coupling of substructures for dynamic analyses. *AIAA Journal* **Vol. 6**.No. 7 (1968),
[3] Bhaskar Chaturvedi, Deepak Rana, and Mugundaram Ravindran. "Correlation of Vehicle Dynamics & NVH Performance with Body Static & Dynamic Stiffness through CAE and Experimental Analysis". *SAE Technical Paper*. SAE International, Apr. 2010. DOI: 10.4271/2010-01-1137. URL: http://dx.doi.org/10.4271/2010-01-1137.
[4] L. Coox et al. Numerical assessment of the impact of vehicle body stiffness on handling performance. *LMS International* (2012).
[5] *Correlation coefficient*. GraphPad Software, Inc. URL: http://www.graphpad.com/guides/prism/6/statistics/index.htm?stat_interpreting_results_correlati.htm.
[6] Andrew Deakin et al. "The Effect of Chassis Stiffness on Race Car Handling Balance". *SAE Technical Paper*. SAE International, Nov. 2000. DOI: 10.4271/2000-01-3554. URL: http://dx.doi.org/10.4271/2000-01-3554.
[7] John C. Dixon. *Tires, Suspension and Handling, Second Edition*. Society of Automotive Engineers, Inc., 1996.
[8] Esteco. *modeFrontier manual*. Version 4.6. 2014.
[9] Esteco. *modeFrontier tutorials*. 4.6. 2014.
[10] Stephanie Glen. *Statistics How To*. Andale Publishing, LLC. URL: http://www.statisticshowto.com/.
[11] J. Helsen et al. Global static and dynamic car body stiffness based on a Global static and dynamic car body stiffness based on a single experimental modal analysis test. *Modal testing: Methods and Case Studies. Proceedings of ISMA 2010 including USD 2010* (2010).
[12] *IPG CarMaker ReferenceManual*.
[13] *IPG CarMaker UsersGuide*.
[14] Hari Krishnan M et al. Establishing Correlation between Torsional and Lateral Stiffness Parameters of BIW and Vehicle Handling Performance. *SAE Int. J. Passeng. Cars – Mech. Syst.* **4** (Apr. 2011), 22–31. DOI: 10.4271/2011-01-0089. URL: http://dx.doi.org/10.4271/2011-01-0089.
[15] William F. Milliken and Douglas L. Milliken. *Race Car Vehicle Dynamics*. Society of Automotive Engineers, 1995.
[16] Enrico Sampo. "Modelling chassis flexibility in vehicle dynamics simulation". PhD thesis. University of Surrey, 2011.
[17] Enrico Sampo, Aldo Sorniotti, and Andrew Crocombe. "Chassis Torsional Stiffness: Analysis of the Influence on Vehicle Dynamics". *SAE Technical Paper*. SAE International, Apr. 2010. DOI: 10.4271/2010-01-0094. URL: http://dx.doi.org/10.4271/2010-01-0094.
[18] *SPMM 5000 Outline Specification*. SP20016 issue 2. AB Dynamics.
[19] *TameTire powered by Michelin*. IPG Automotive. URL: http://ipg.de/simulationsolutions/tametire/key-benefits/.
[20] Eric Weisstein. *Wolfram MathWorld*. Feb. 2015. URL: http://mathworld.wolfram.com/.
[21] Stijn Wolterink. *Torsional Stiffness Test Method Development*. Tech. rep. Volvo Cars, 2013.

Appendix

Appendix I

Table 7.1: Variables stored by CarMaker

Variable	**Unit**
ax	$\frac{m}{s^2}$
ay	$\frac{m}{s^2}$
heading (yaw)	rad
pitch rate (pitchr)	$\frac{rad}{s}$
position x (posx)	m
position y (posy)	m
roll rate (rollr)	$\frac{rad}{s}$
side slip at center of gravity (sscg)	rad
steering wheel angle (swa)	rad
steering wheel torque (swt)	Nm
total pitch (tpitch)	rad
total roll (troll)	rad
vx	$\frac{m}{s}$
vy	$\frac{m}{s}$
yaw rate (yaw)	$\frac{rad}{s}$
wheel travel lf (lfdef)	m
wheel travel lr (lrdef)	m
wheel travel rf (rfdef)	m
wheel travel rr (rrdef)	m
front wheel angle (fwa)	rad
steering wheel velocity (swv)	$\frac{rad}{s}$
Body accelerometer lf (lftm)	$\frac{m}{s^2}$
Body accelerometer rf (rftm)	$\frac{m}{s^2}$
Body accelerometer lr (lrtm)	$\frac{m}{s^2}$
Body accelerometer rr (rrtm)	$\frac{m}{s^2}$

Appendix II

S60-REAR SUSPENSION		Wh. Base	Wh. track	Wh. compr.	Camber	Spin	Toe	
Force x	*Compliance*	tx	ty	tz	rx	ry	rz	**Delta AVG**
Wheelbase C.	*Factor*	1.010	0.985	0.996	1.007	1.001	1.018	
	Delta	-0.99%	1.50%	0.38%	-0.66%	-0.06%	-1.75%	**0.89%**
	Delta max	0.06	0.00	0.00	0.00	0.00	0.01	*[mm] [deg]*
	Delta min	-0.12	0.00	0.00	-0.01	-0.01	-0.02	
Force y	*Compliance*	tx	ty	tz	rx	ry	rz	
Lateral	*Factor*	1.275	1.598	0.915	0.923	0.735	1.327	
	Delta	-21.59%	-37.43%	9.30%	8.31%	36.00%	-24.64%	**22.88%**
	Delta max	0.25	1.72	-0.01	-0.02	-0.04	0.08	*[mm] [deg]*
	Delta min	-0.15	-1.72	0.01	0.03	0.04	-0.08	
Torq x	*Compliance*	tx	ty	tz	rx	ry	rz	
Camber	*Factor*	0.910	0.925	1.005	1.015	1.025	0.996	
	Delta	9.95%	8.14%	-0.52%	-1.52%	-2.42%	0.44%	**3.83%**
	Delta max	0.00	-0.01	0.00	0.00	0.00	0.00	*[mm] [deg]*
	Delta min	0.00	0.01	0.00	0.00	0.00	0.00	
Torq y	*Compliance*	tx	ty	tz	rx	ry	rz	
Spin	*Factor*	0.981	0.996	0.996	1.006	1.009	1.038	
	Delta	1.91%	0.35%	0.41%	-0.59%	-0.89%	-3.69%	**1.31%**
	Delta max	-0.01	0.00	0.00	0.00	0.00	0.00	*[mm] [deg]*
	Delta min	0.02	0.00	0.00	0.00	-0.01	0.00	
Torq z	*Compliance*	tx	ty	tz	rx	ry	rz	
Toe	*Factor*	1.403	1.350	0.985	0.995	1.020	1.046	
	Delta	-28.74%	-25.94%	1.53%	0.51%	-1.94%	-4.39%	10.51%
	Delta max	0.03	0.04	0.00	0.00	0.00	0.02	*[mm] [deg]*
	Delta min	-0.05	-0.04	0.00	0.00	0.00	-0.02	
	Tot. AVG	**-7.89%**	**-10.68%**	**2.22%**	**1.21%**	**6.14%**	**-6.81%**	

S60-FRONT SUSPENSION		Wh. Base	Wh. track	Wh. compr.	Camber	Spin	Toe	
Force x	*Compliance*	tx	ty	tz	rx	ry	rz	**Delta AVG**
Wheelbase C.	*Factor*	1.018	1.006	0.939	0.940	0.991	0.994	
	Delta	-1.75%	-0.59%	6.54%	6.35%	0.86%	0.63%	**2.79%**
[mm] [deg]	*Delta max*	0.28	0.02	0.00	-0.01	-0.01	0.00	
	Delta min	-0.32	0.00	0.00	0.01	0.01	0.00	
Force y	*Compliance*	tx	ty	tz	rx	ry	rz	
Lateral	*Factor*	1.197	1.362	0.831	0.832	1.263	1.179	
	Delta	-16.42%	-26.57%	20.34%	20.18%	-20.81%	-15.18%	**19.92%**
[mm] [deg]	*Delta max*	0.82	1.42	0.00	-0.02482	0.06	0.12	
	Delta min	-0.89	-1.43	0.00	0.02696	-0.06	-0.12	
Torq x	*Compliance*	tx	ty	tz	rx	ry	rz	
Camber	*Factor*	0.981	0.862	1.138	1.140	1.014	1.367	
	Delta	1.98%	16.05%	-12.15%	-12.27%	-1.36%	-26.84%	**11.77%**
[mm] [deg]	*Delta max*	0.00	-0.01	0.00	0.01	0.00	0.01	
	Delta min	0.00	0.01	0.00	-0.01	0.00	-0.01	
Torq y	*Compliance*	tx	ty	tz	rx	ry	rz	
Spin	*Factor*	0.994	1.039	1.063	1.064	1.053	0.976	
	Delta	0.65%	-3.79%	-5.89%	-6.03%	-5.01%	2.41%	**3.96%**
[mm] [deg]	*Delta max*	-0.01	0.00	0.00	0.00	0.01	0.00	
	Delta min	0.01	0.00	0.00	0.00	-0.01	0.00	
Torq z	*Compliance*	tx	ty	tz	rx	ry	rz	
Toe	*Factor*	1.156	1.173	1.377	1.382	0.813	1.057	
	Delta	-13.50%	-14.75%	-27.40%	-27.62%	22.95%	-5.43%	**18.61%**
[mm] [deg]	*Delta max*	0.07	0.06	0.00	0.01	0.00	0.01	
	Delta min	-0.07	-0.06	0.00	-0.01	0.00	-0.01	
		-5.81%	**-5.93%**	**-3.71%**	**-3.88%**	**-0.67%**	**-8.88%**	

Color code
0%-10%
10%-20%
20%-max

Appendix III

S60-REAR SUSPENSION		Wh. Base	Wh. track	Wh. compr.	Camber	Spin	Toe	
Force x	*Compliance*	*tx*	*ty*	*tz*	*rx*	*ry*	*rz*	**Delta AVG**
Wheelbase C.	*Factor*	1.001	0.993	0.998	0.999	1.000	1.003	
	Delta	-0.09%	0.70%	0.17%	0.13%	0.03%	-0.29%	**0.23%**
	Delta max	0.01	0.00	0.00	0.00	0.00	0.00	*[mm] [deg]*
	Delta min	-0.01	0.00	0.00	0.00	0.00	0.00	
Force y	*Compliance*	tx	ty	tz	rx	ry	rz	
Lateral	*Factor*	1.112	1.070	0.971	0.971	0.924	1.138	
	Delta	-10.05%	-6.55%	2.99%	2.97%	8.27%	-12.09%	7.15%
	Delta max	0.12	0.30	0.00	-0.01	-0.01	0.04	*[mm] [deg]*
	Delta min	-0.07	-0.30	0.00	0.01	0.01	-0.04	
Torq x	*Compliance*	tx	ty	tz	rx	ry	rz	
Camber	*Factor*	0.993	0.973	1.007	1.007	1.009	0.996	
	Delta	0.68%	2.79%	-0.67%	-0.71%	-0.92%	0.42%	**1.03%**
	Delta max	0.00	0.00	0.00	0.00	0.00	0.00	*[mm] [deg]*
	Delta min	0.00	0.00	0.00	0.00	0.00	0.00	
Torq y	*Compliance*	tx	ty	tz	rx	ry	rz	
Spin	*Factor*	1.000	0.998	1.001	1.001	1.000	1.002	
	Delta	0.04%	0.22%	-0.08%	-0.12%	-0.05%	-0.20%	**0.12%**
	Delta max	0.00	0.00	0.00	0.00	0.00	0.00	*[mm] [deg]*
	Delta min	0.00	0.00	0.00	0.00	0.00	0.00	
Torq z	*Compliance*	tx	ty	tz	rx	ry	rz	
Toe	*Factor*	1.069	1.142	0.995	0.995	0.997	1.010	
	Delta	-6.49%	-12.42%	0.51%	0.47%	0.35%	-0.97%	**3.53%**
	Delta max	0.01	0.02	0.00	0.00	0.00	0.00	*[mm] [deg]*
	Delta min	-0.01	-0.02	0.00	0.00	0.00	0.00	
	Tot. AVG	**-3.18%**	**-3.05%**	**0.59%**	**0.55%**	**1.54%**	**-2.63%**	

S60-FRONT SUSPENSION		Wh. Base	Wh. track	Wh. compr.	Camber	Spin	Toe	
Force x	*Compliance*	*tx*	*ty*	*tz*	*rx*	*ry*	*rz*	**Delta AVG**
Wheelbase C.	*Factor*	1.005	1.004	0.990	0.972	1.002	1.005	
	Delta	-0.46%	-0.44%	1.00%	2.85%	-0.21%	-0.52%	**0.92%**
[mm] [deg]	*Delta max*	0.07	0.01	0.00	-0.01	0.00	0.00	
	Delta min	-0.09	0.00	0.00	0.01	0.00	0.00	
Force y	*Compliance*	tx	ty	tz	rx	ry	rz	
Lateral	*Factor*	1.069	1.093	0.895	0.878	1.196	1.079	
	Delta	-6.49%	-8.50%	11.77%	13.84%	-16.39%	-7.29%	**10.71%**
[mm] [deg]	*Delta max*	0.32	0.45	0.00	-0.02	0.05	0.06	
	Delta min	-0.35	-0.45	0.00	0.02	-0.05	-0.06	
Torq x	*Compliance*	tx	ty	tz	rx	ry	rz	
Camber	*Factor*	0.973	0.892	1.042	1.024	0.967	1.091	
	Delta	2.77%	12.13%	-4.05%	-2.30%	3.38%	-8.31%	**5.49%**
[mm] [deg]	*Delta max*	0.00	-0.01	0.00	0.00	0.00	0.00	
	Delta min	0.01	0.01	0.00	0.00	0.00	0.00	
Torq y	*Compliance*	tx	ty	tz	rx	ry	rz	
Spin	*Factor*	1.004	1.032	1.009	0.991	1.003	0.995	
	Delta	-0.37%	-3.11%	-0.88%	0.89%	-0.26%	0.47%	**1.00%**
[mm] [deg]	*Delta max*	0.00	0.00	0.00	0.00	0.00	0.00	
	Delta min	0.00	0.00	0.00	0.00	0.00	0.00	
Torq z	*Compliance*	tx	ty	tz	rx	ry	rz	
Toe	*Factor*	1.051	1.078	1.106	1.091	0.828	1.018	
	Delta	-4.85%	-7.24%	-9.58%	-8.33%	20.85%	-1.79%	**8.77%**
[mm] [deg]	*Delta max*	0.02	0.03	0.00	0.00	0.00	0.00	
	Delta min	-0.02	-0.03	0.00	0.00	0.00	0.00	
		-1.88%	**-1.43%**	**-0.35%**	**1.39%**	**1.47%**	**-3.49%**	

Color code
0%-10%
10%-20%
20%-max

Appendix IV

Table 7.2: Effect of stiffening bar - groups on compliance values

Load case interpretation	Front Longitudinal	Front Transversal	Rear Cross	Rear Longitudinal	Rear Transversal	Underbody	Load_case
Axis Bending [Fx] - Front	0.27	0.80	0.01	0.00	0.00	0.34	Fx_Front
Axis Bending [Fx] - Rear	0.00	0.00	0.06	0.04	0.13	0.04	Fx_Rear
Lateral - Front	0.86	11.63	0.07	0.02	0.09	2.17	Fy_Front
Lateral - Rear	0.02	0.03	3.49	1.09	2.48	0.37	Fy_Rear
Camber - Front	0.66	6.63	0.16	0.04	0.07	0.99	Tx_Front
Camber - Rear	0.01	0.00	0.63	0.13	0.28	0.05	Tx_Rear
Axis torsion [Ty] - Front	0.26	0.57	0.01	0.00	0.01	0.20	Ty_Front
Axis torsion [Ty] - Rear	0.00	0.00	0.06	0.02	0.05	0.01	Ty_Rear
Toe - Front	0.37	8.39	0.04	0.01	0.03	0.25	Tz_Front
Toe - Rear	0.02	0.02	1.58	0.61	1.56	0.02	Tz_Rear
Global Torsion	0.48	0.87	30.41	2.51	0.63	2.93	kts
Global Bending	0.08	1.10	1.10	16.01	1.01	42.72	three point bending

Appendix V

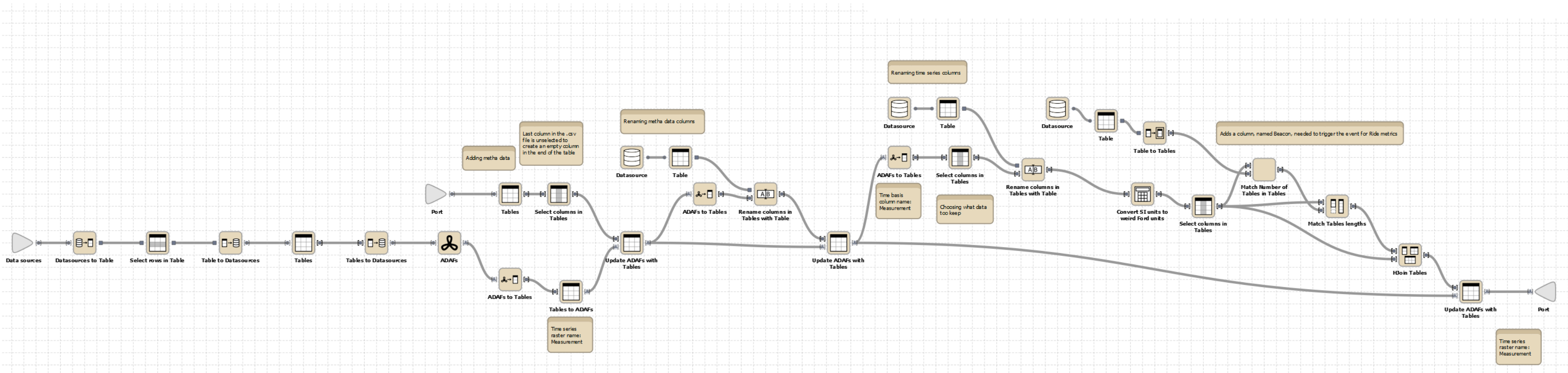

Figure 7.1: *Sympathy for Data - CM read and unit/coordinate system conversion flow*

Appendix VI

Simplified bicycle model equations:

$$m \cdot \frac{{v_x}^2}{R} = F_{yF} + F_{yR} \tag{7.1}$$

$$F_{yF} \cdot l_F - F_{yR} \cdot l_R = 0 \tag{7.2}$$

$$F_{yF} = -C_F \cdot S_{yF} \tag{7.3}$$

$$F_{yR} = -C_R \cdot S_{yR} \tag{7.4}$$

$$\beta_F = a_F + \alpha_F \tag{7.5}$$

$$\beta_R = a_R + \alpha_R \tag{7.6}$$

$$a_R = lcs_R + rs_R \tag{7.7}$$

$$a_F = \delta_F + lcs_F + rs_F \tag{7.8}$$

$$\omega_z = \frac{v_x}{R} \tag{7.9}$$

$$\alpha_F = S_{yF} \tag{7.10}$$

$$\alpha_R = S_{yR} \tag{7.11}$$

$$\beta_F = \frac{v_y + l_F \cdot \omega_z}{v_x} \tag{7.12}$$

$$\beta_R = \frac{v_y - l_R \cdot \omega_z}{v_x} \tag{7.13}$$